American Mineralogist, Volume 100, pages 1668–1707, 2015

THE SECOND CONFERENCE ON THE LUNAR HIGHLANDS CRUST AND NEW DIRECTIONS

REVIEW

Magmatic volatiles (H, C, N, F, S, Cl) in the lunar mantle, crust, and regolith: Abundances, distributions, processes, and reservoirs† 🔓

FRANCIS M. MCCUBBIN[1,2,*], KATHLEEN E. VANDER KAADEN[1,2], ROMAIN TARTÈSE[3], RACHEL L. KLIMA[4], YANG LIU[5], JAMES MORTIMER[3], JESSICA J. BARNES[3,6], CHARLES K. SHEARER[1,2], ALLAN H. TREIMAN[7], DAVID J. LAWRENCE[3], STEPHEN M. ELARDO[1,2,8], DANA M. HURLEY[3], JEREMY W. BOYCE[9] AND MAHESH ANAND[3,6]

[1]Institute of Meteoritics, University of New Mexico, 200 Yale Blvd SE, Albuquerque, New Mexico 87131, U.S.A.
[2]Department of Earth and Planetary Sciences, University of New Mexico, 200 Yale Blvd SE, Albuquerque, New Mexico 87131, U.S.A.
[3]Planetary and Space Sciences, The Open University, Walton Hall, Milton Keynes, MK7 6AA, U.K.
[4]Planetary Exploration Group, Space Department, Johns Hopkins University Applied Physics Lab, Laurel, Maryland 20723, U.S.A.
[5]Jet Propulsion Laboratory, California Institute of Technology, Pasadena, California 91109, U.S.A.
[6]Department of Earth Sciences, The Natural History Museum, Cromwell Road, London, SW7 5BD, U.K.
[7]Lunar and Planetary Institute, USRA, 3600 Bay Area Boulevard, Houston, Texas 77058, U.S.A.
[8]Geophysical Laboratory, Carnegie Institution of Washington, 5251 Broad Branch Road NW, Washington, D.C. 20015, U.S.A.
[9]Department of Earth and Space Sciences, University of California, Los Angeles, California 90095-1567, U.S.A.

ABSTRACT

Many studies exist on magmatic volatiles (H, C, N, F, S, Cl) in and on the Moon, within the last several years, that have cast into question the post-Apollo view of lunar formation, the distribution and sources of volatiles in the Earth-Moon system, and the thermal and magmatic evolution of the Moon. However, these recent observations are not the first data on lunar volatiles. When Apollo samples were first returned, substantial efforts were made to understand volatile elements, and a wealth of data regarding volatile elements exists in this older literature. In this review paper, we approach volatiles in and on the Moon using new and old data derived from lunar samples and remote sensing. From combining these data sets, we identified many points of convergence, although numerous questions remain unanswered.

The abundances of volatiles in the bulk silicate Moon (BSM), lunar mantle, and urKREEP [last ~1% of the lunar magma ocean (LMO)] were estimated and placed within the context of the LMO model. The lunar mantle is likely heterogeneous with respect to volatiles, and the relative abundances of F, Cl, and H_2O in the lunar mantle (H_2O > F >> Cl) do not directly reflect those of BSM or urKREEP (Cl > H_2O ≈ F). In fact, the abundances of volatiles in the cumulate lunar mantle were likely controlled by partitioning of volatiles between LMO liquid and nominally anhydrous minerals instead of residual liquid trapped in the cumulate pile. An internally consistent model for lunar volatiles in BSM should reproduce the absolute and relative abundances of volatiles in urKREEP, the anorthositic primary crust, and the lunar mantle within the context of processes that occurred during the thermal and magmatic evolution of the Moon. Using this mass-balance constraint, we conducted LMO crystallization calculations with a specific focus on the distributions and abundances of F, Cl, and H_2O to determine whether or not estimates of F, Cl, and H_2O in urKREEP are consistent with those of the lunar mantle, estimated independently from the analysis of volatiles in mare volcanic materials. Our estimate of volatiles in the bulk lunar mantle are 0.54–4.5 ppm F, 0.15–5.3 ppm H_2O, 0.26–2.9 ppm Cl, 0.014–0.57 ppm C, and 78.9 ppm S. Our estimates of H_2O are depleted compared to independent estimates of H_2O in the lunar mantle, which are largely biased toward the "wettest" samples. Although the lunar mantle is depleted in volatiles relative to Earth, unlike the Earth, the mantle is not the primary host for volatiles. The primary host of the Moon's incompatible lithophile volatiles (F, Cl, H_2O) is urKREEP, which we estimate to have 660 ppm F, 300–1250 ppm H_2O, and 1100–1350 ppm Cl. This urKREEP composition implies a BSM with 7.1 ppm F, 3–13 ppm H_2O, and 11–14 ppm Cl. An upper bound on the abundances of F, Cl, and H_2O in urKREEP and the BSM, based on F abundances in CI carbonaceous chondrites, are reported to be 5500 ppm F, 0.26–1.09 wt% H_2O, and 0.98–1.2 wt% Cl and 60 ppm F, 27–114 ppm H_2O, and 100–123 ppm Cl, respectively.

The role of volatiles in many lunar geologic processes was also determined and discussed. Specifically, analyses of volatiles from lunar glass beads as well as the phase assemblages present in coatings on those beads were used to infer that H_2 is likely the primary vapor component responsible for propelling the fire-fountain eruptions that produced the pyroclastic glass beads (as opposed to CO). The textural occurrences of some volatile-bearing minerals

* E-mail: fmccubbi@unm.edu † 🔓 Open access: Article available to all readers online. Special collection papers can be found on GSW at http://ammin.geoscienceworld.org/site/misc/specialissuelist.xhtml.

0003-004X/15/0809–1668$05.00/DOI: http://dx.doi.org/10.2138/am-2015-4934CCBYNCND

are used to identify hydrothermal alteration, which is manifested by sulfide veining and sulfide-replacement textures in silicates. Metasomatic alteration in lunar systems differs substantially from terrestrial alteration due to differences in oxygen fugacity between the two bodies that result in H_2O as the primary solvent for alteration fluids on Earth and H_2 as the primary solvent for alteration fluids on the Moon (and other reduced planetary bodies). Additionally, volatile abundances in volatile-bearing materials are combined with isotopic data to determine possible secondary processes that have affected the primary magmatic volatile signatures of lunar rocks including degassing, assimilation, and terrestrial contamination; however, these processes prove difficult to untangle within individual data sets. Data from remote sensing and lunar soils are combined to understand the distribution, origin, and abundances of volatiles on the lunar surface, which can be explained largely by solar wind implantation and spallogenic processes, although some of the volatiles in the soils may also be either indigenous to the Moon or terrestrial contamination. We have also provided a complete inventory of volatile-bearing mineral phases indigenous to lunar samples and discuss some of the "unconfirmed" volatile-bearing minerals that have been reported. Finally, a compilation of unanswered questions and future avenues of research on the topic of lunar volatiles are presented, along with a critical analysis of approaches for answering these questions.

Keywords: Water, apatite, hydrogen, space weathering, Moon, magma ocean, isotopes, remote sensing, Review

Introduction

Highly volatile magmatic species (H_2O, H_2, CO_2, CO, CH_4, HCl, HF, H_2S, SO_3, N_2, NH_3, noble gases, etc.) affect a wide range of important physical properties of geologic materials including the stability and rheological characteristics of minerals and melts. The *P-T* space over which volatiles are important in geologic systems is nearly unlimited, as they affect the physicochemical processes of magmas in which they are dissolved, play a fundamental role in mass transport within the crusts and mantles of planetary bodies when present as supercritical fluids, and are important for chemical and physical weathering on planetary surfaces. Therefore, characterization of volatile budgets as well as their associated geochemical processes is a key step in developing models for the formation and subsequent evolution of planetary bodies (e.g., Albarède 2009; Dasgupta and Dixon 2009; Dasgupta et al. 2007; Holloway 1998; Holloway and Jakobsson 1986; Jambon 1994; Liebscher and Heinrich 2007; Rossman 1996; Webster and Mandeville 2007).

Magmatic volatiles participate in a large number of processes in geologic systems on the Earth, and they have been shown to play at least some role in geologic systems on Mercury, Venus, the Moon, Mars, and asteroids, although we certainly know much less information regarding these bodies (Alexander et al. 2012; Fogel and Rutherford 1995; Hirschmann and Withers 2008; Kerber et al. 2009; McCubbin et al. 2010a, 2010b, 2010c, 2012b; Righter et al. 2008; Rutherford and Papale 2009; Saal et al. 2008; Sarafian et al. 2013). Of these planetary bodies, the Moon is the most depleted in volatile elements (Day and Moynier 2014; Humayun and Clayton 1995; Paniello et al. 2012; Taylor 2001; Taylor et al. 2006b), and it is the primary subject of this work.

With respect to the Moon, magmatic volatiles are poorly understood, and the magmatic volatile inventory of the lunar mantle, crust, and surface, aside from being low, is largely unconstrained. Although the Moon is volatile-depleted, there is evidence indicating that magmatic volatiles have played a role in several geologic processes within and on the Moon. Specifically, magmatic volatiles have been implicated as the propellants that drove fire-fountain eruptions, which produced the pyroclastic glass beads encountered at each of the Apollo landing sites and the LUNA 20 and 24 landing sites (Colson 1992; Delano et al. 1994; Elkins-Tanton et al. 2003b; Fogel and Rutherford 1995; Rutherford and Papale 2009; Sato 1979; Shearer et al. 2006; Weitz et al. 1999). Furthermore, vesicular basalts, analogous to those produced during crystallization of volatile-bearing terrestrial lavas, have been found on the Moon during several of the Apollo missions. In fact, Apollo sample 15556 (mare basalt) has been reported to contain up to 50% vesicles by volume (i.e., Butler 1971; Ryder and Schuraytz 2001). Last, the lunar regolith has served as an important reservoir for exogenic hydrogen, likely from the solar wind, spallation, and meteorites, that has been analyzed in return samples and also detected remotely through spectroscopic investigations (Clark 2009; Colaprete et al. 2010; Epstein and Taylor 1970a, 1970b, 1971, 1972, 1973; Friedman et al. 1970a, 1970b, 1971; Merlivat et al. 1972, 1974, 1976; Pieters et al. 2009; Sunshine et al. 2009).

In recent years, there has been a focused effort to determine the abundances and distributions of magmatic volatiles in lunar materials both through laboratory studies and through orbital spacecraft-based investigations. These modern efforts were largely sparked by substantial advances in detection sensitivity for several analytical/remote observation techniques, which led to a renaissance in the study of lunar volatiles that largely started in 2007 when two groups independently began reassessing the hydrogen inventory of lunar samples (as summarized by Anand 2010). In addition to all of these recent analyses of volatiles, there were substantial efforts in the 1970s and to a lesser extent the 1980s and 1990s to understand the abundances, distribution, and origin of volatiles in lunar materials. Little effort has been made to bridge the initial studies of lunar volatiles to more recent ones. Furthermore, many of the results from sample analysis and remote sensing are highly complementary in nature, and little has been done to merge these data sets into a clear picture of volatiles in and on the Moon. The primary goal of the present review is to compile information and data on the elements H, C, N, F, S, and Cl in lunar materials and from lunar remote sensing to determine what we know about volatiles and their respective isotopes on the Moon and where the outstanding questions remain.

Analytical techniques

A wide range of techniques have been used to analyze volatile elements and volatile-bearing minerals in lunar samples. In fact, many analytical techniques and protocols have been developed and enhanced specifically for the study of lunar

samples. We provide a summary of techniques that were used and how they were implemented and/or improved upon for the study of lunar volatiles in the online supporting material. We do not cover every technique used to analyze volatiles on the Moon, but we cover those techniques that required specific development to overcome the challenges inherent to the analysis of volatiles in lunar samples.

Data review

Volatile-bearing mineralogy

Volatile-bearing minerals on the Moon may actually span a wide range of mineral types including phosphates, silicates, sulfides, native elements, oxy-hydroxides, halides, and carbonates. Below, we summarize the volatile-bearing minerals that have been verified to occur in lunar samples, although we include a list of "unconfirmed" reports of volatile-bearing minerals from lunar samples in the online supplement[1].

Apatite. Apatite, ideally $Ca_5(PO_4)_3(F,Cl,OH)$, is the most common volatile-bearing mineral in lunar rocks and along with merrillite, makes up the primary reservoir for phosphorus and rare earth elements on the Moon (Hughes et al. 2006; Jolliff et al. 1993, 2006). Apatite occurs in nearly all lunar rock types (apatite has not been reported in ferroan anorthosites or volcanic glass beads), but the ubiquity of apatite in lunar samples should not be misconstrued as apatite being abundant because it is always a trace mineral and can be somewhat elusive in many samples. Apatite has been a popular target for estimating the abundances of volatiles in the Moon because it has F, Cl, and OH as essential structural constituents, and the abundances of volatiles in apatite commonly occur in much greater abundances than in whole rocks or glasses (Anand et al. 2014; Barnes et al. 2013, 2014; Boyce et al. 2010, 2014; McCubbin et al. 2010b, 2010c, 2011; Patino-Douce and Roden 2006; Patino-Douce et al. 2011; Tartèse et al. 2013, 2014b). Consequently, a substantial amount of new data on lunar apatite have recently emerged from both electron probe microanalysis (EPMA) and secondary ion mass spectrometry (SIMS) instruments, in part due to the recent development of high quality apatite standards (Table 1). One can now begin to assess the variability of apatite occurrences and compositions among the various lunar rocks types.

Apatites in lunar samples range in crystal habit from anhedral to euhedral and range in size from sub-micrometer to 2 mm (McCubbin et al. 2011; Treiman et al. 2014). Many of the anhedral apatites are clearly late-crystallizing phases that are filling the available space interstitial to the earlier formed phases (Fig. 1a). The smallest apatites typically occur in mare basalts, and the larger apatites occur in plutonic rocks and impactites (e.g., troctolite 76535 and granulite 79215; Fig. 1b). Although there has been one report of a chlorapatite in sample 14161, 7062b (McCubbin et al. 2011), and hydroxylapatite has been reported in the brecciated matrix of Northwest Africa (NWA) 773 (Tartèse et al. 2014a), nearly all of the apatites that have been analyzed in lunar samples are fluorapatite (McCubbin et al. 2011) (i.e., the mol% F exceeds the mol% of Cl and the mol% of OH in the apatite). However, within the fluorapatite field there is substantial compositional variability in the volatile abundances of apatite that correlates with lunar rock type. Specifically, apatite grains in mare basalts typically contain little chlorine (typically less than 0.1 sfu; McCubbin et al. 2011), and many of the grains have elevated hydroxyl abundances [from less than 100 ppm H_2O in 12040 to 7000 ppm H_2O in 12039, Miller Range (MIL) 05035, and LaPaz Icefield (LAP) 04841; Greenwood et al. 2011; Tartèse et al. 2013; Table 2], whereas apatite grains in the magnesian suite, alkali suite, and KREEP-rich impact melts are enriched in chlorine compared to mare basalts (typically greater than 0.1 sfu; McCubbin et al. 2011), and they typically have much lower water contents (from less than 100 ppm H_2O in troctolite 76535 and up to 1600 ppm H_2O in norite 77215; Barnes et al. 2014; Table 2). Apatites from KREEP basalts span across the mare basalt field and highland crust field with maximum abundances of H_2O that are intermediate between the mare basalts and highlands rocks (from ~40 ppm H_2O in the driest apatite of 72275 to ~2500 ppm H_2O in the wettest apatite in the olivine gabbro lithology of Northwest Africa (NWA) 773; McCubbin et al. 2010b; Tartèse et al. 2014b; Table 2). A compilation of published apatite F-Cl-OH components from both SIMS and EPMA analyses are presented in Figure 2 to illustrate the variation in apatite volatile chemistry from various rock types in the

[1] Deposit item AM-15-84934, Supplementary Material and Supplemental Tables 1–5. Deposit items are free to all readers and found on the MSA web site, via the specific issue's Table of Contents (go to http://www.minsocam.org/MSA/AmMin/TOC/).

Table 1. Apatite standards used for SIMS analysis of volatiles and δD in lunar apatites

References	Name	Locality	H_2O (ppm)	F (wt%)	S (ppm)	Cl (ppm)	δD (‰)
Boyce et al. (2010)	Mud Tank	Northwest Territory, Australia	8300 ± 300		35 ± 3		
	Durango[a]	Mexico	1170 ± 117		1480 ± 148		
	F-apatite	Synthetic	192 ± 19			42 ± 1	
	Cl-apatite	Synthetic	42 ± 4			68000 ± 2500	
McCubbin et al. (2010b)	Durango[a]	Mexico	900 ± 200	3.53 ± 0.35		4500 ± 600	
	Colorado[b]	USA	3600 ± 200	2.6 ± 0.1		9500 ± 300	
	Morocco[c]	Morocco	3800 ± 200	2.5 ± 0.1		4100 ± 200	
Greenwood et al. (2011)	Durango[a]	Mexico	478 ± 48				−120 ± 5
	Linopolis	Brazil	15700 ± 1570				−125 ± 5
Barnes et al. (2013)	Morocco[c]	Morocco	4560 ± 340				−80 ± 5
	Imaichi	Japan	400 ± 80				
Tartèse et al. (2013)[d]	Ap003[a]	Durango, Mexico	600 ± 400	3.44 ± 0.22	1280 ± 200	4500 ± 1200	
	Ap004[c]	Atlas Mountains, Morocco	5500 ± 500	2.39 ± 0.24	1000 ± 120	4100 ± 400	−45 ± 5
	Ap005[b]	Crystal Lode pegmatite, Colorado, U.S.A.	3700 ± 300	2.45 ± 0.22	400 ± 120	9500 ± 600	−73 ± 4
	Ap018	Lake Baikal, Sludyanka, Russia	2000 ± 400	3.28 ± 0.38	3640 ± 520	1300 ± 400	−90 ± 14

[a] Denotes apatites from the same locality in Durango, Mexico.
[b] Denotes apatites from the same locality in Eagle County, Colorado, U.S.A.
[c] Denotes apatites from the same locality in the High Atlas Mountains, Morocco.
[d] Standards originally described in McCubbin et al. (2012a).

lunar crust. The ranges of volatile abundances of apatites from various lithologic types are compiled in Table 2.

Sulfides and sulfur. The most common S-bearing mineral on the Moon is troilite (FeS). Troilite in the lunar environment is typically stoichiometric FeS with less than 1 wt% of other components such as Ni, Co, Cr, Zn, and Ti (e.g., Colson 1992; Papike et al. 1991, 1998; Shearer et al. 2012; Skinner 1970). Other sulfides have been identified in minor or trace amounts in a limited number of samples from the highlands or mare basalts. These trace sulfides include chalcopyrite ($CuFeS_2$), cubanite ($CuFe_2S_3$), bornite (Cu_5FeS_4), sphalerite ([Zn,Fe]S), pentlandite ([Fe,Ni]S), and mackinawite ($Fe_{1+x}S$) (Carter et al. 1975; Carter and Padovani 1973; El Goresy et al. 1973b; Papike et al. 1991, 1998; Ramdohr 1972; Taylor and Williams 1973). Elemental sulfur and sulfides that contain Pb and Zn have been reported on the surfaces of pyroclastic volcanic glass beads (Butler 1978; McKay et al. 1972; McKay and Wentworth 1992, 1993; Wasson et al. 1976), but require further examination to determine their mineralogical identity.

In lunar crustal rocks, sulfides (dominantly troilite) occur as either primary magmatic crystallization products (Fig. 1d) or as products of vapor/fluid interaction with existing crustal rocks (Figs. 1e–1f and see below). Magmatic troilite is typically found as discrete grains or in late-stage mesostasis pockets, sometimes intergrown with Fe-metal (e.g., Skinner 1970). Vapor or fluid deposited troilite is often found to fill cracks or as intergrowths

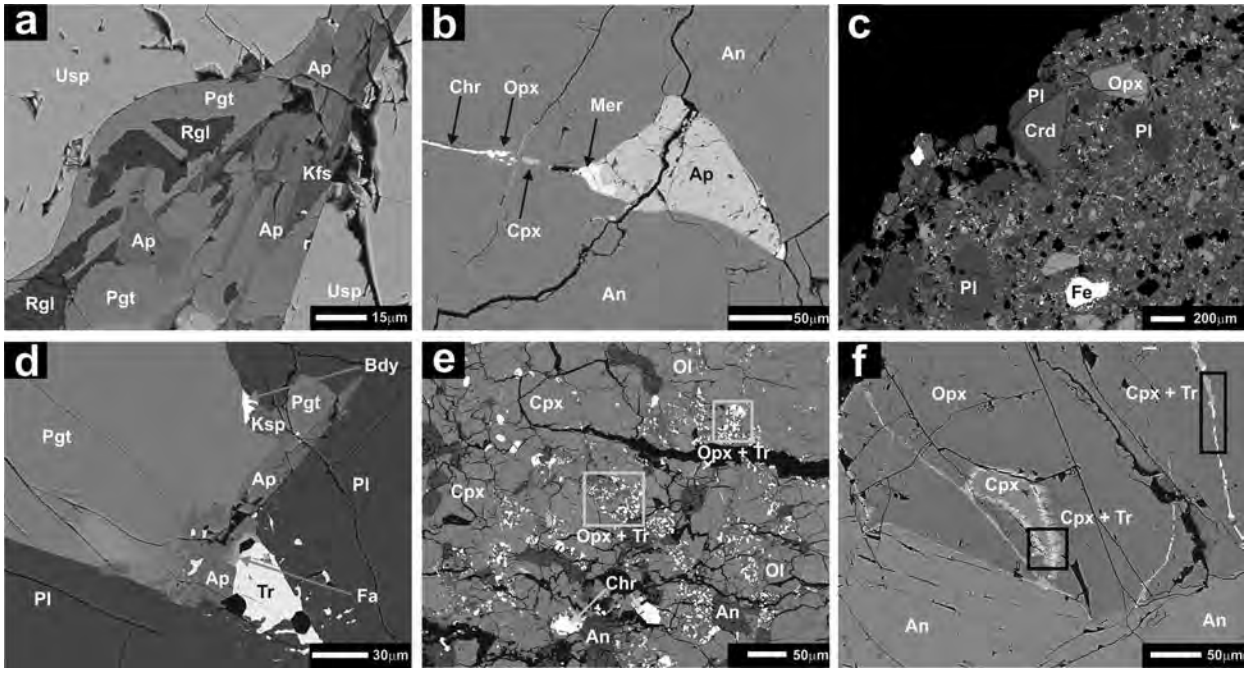

Figure 1. BSE images of regions within lunar samples containing volatile-bearing minerals. (**a**) Low-Ti mare basalt 15058, (**b**) Troctolite 76535, (**c**) Spinel troctolite 72435, (**d**) Low-Ti mare basalt 15058, (**e**) Gabbronorite clast in 67915, and (**f**) Troctolite 76535. Phase abbreviations are as follows: An = anorthitic plagioclase, Ap = apatite, Bdy = baddeleyite, Chr = chromite, Cpx = clinopyroxene, Crd = cordierite, Fa = fayalite, Fe = iron metal, Kfs = potassium-rich alkali feldspar, Mer = merrillite, Opx = orthopyroxene, Pgt = pigeonite, Pl = plagioclase, Rgl = residual glass, Tr = troilite, Usp = ulvöspinel. Inset boxes both highlight examples of secondary alteration of silicates to sulfides.

Table 2. Abundance of volatiles in lunar apatites, basalts, glasses, and regolith

Volatile (ppm[a])	H_2O	C	N	F	S	Cl
Interior of orange glass	5–13	–	–	9–17	282–490	0.02–0.14
Interior of green glass	0.4–30	–	–	2–10	114–270	0.03–0.50
Interior of yellow glass	17–46	–	–	29–40	518–576	1.3–2.0
Mare basalts	9–98	3–70	0.3–20	18–78	300–3300	0.3–28
Olivine hosted melt inclusions in orange glass	270–1200	–	–	37–72	450–880	1.5–2.4
Apatites in mare basalts	Up to 7600	–	–	18600–37900	Up to 463	Up to 15700
Apatites in Mg- and alkali-suite rocks	Up to 530	–	–	27000–36300	–	2400–17800
Apatites in breccias and impact melt rocks	Up to 16744	–	–	19900–36800	–	1500–36200
Mineralized coatings on lunar glasses	–	–	–	Up to 3000	Up to 650	~100
Agglutinates	13–488	–	–	–	–	–
Lunar soil and regolith breccias	4	Up to 280 (average 100–150)	4–209	9–520	60–600	0.6–270

Notes: Data compiled from a number of previously published studies (Boyce et al. 2010; Butler and Meyer 1976; Duncan et al. 1973; Fegley and Swindle 1993; Gibson and Moore 1974; Goldberg et al. 1976; Haskin and Warren 1991; Hauri et al. 2011; Jovanovic et al. 1976; Jovanovic and Reed 1973, 1975; Liu et al. 2012a; Mathew and Marti 2001; McCubbin et al. 2011, 2010b; Mortimer et al. 2015; Muller 1974; Reed and Jovanovic 1973a, 1973b; Reed et al. 1977; Saal et al. 2008; Tartèse et al. 2013, 2014a; Taylor et al. 2004; Wang et al. 2012; Wänke et al. 1976).

[a] When only an upper value is given, the lower bound value reported is below analytical detection, otherwise a range is reported.

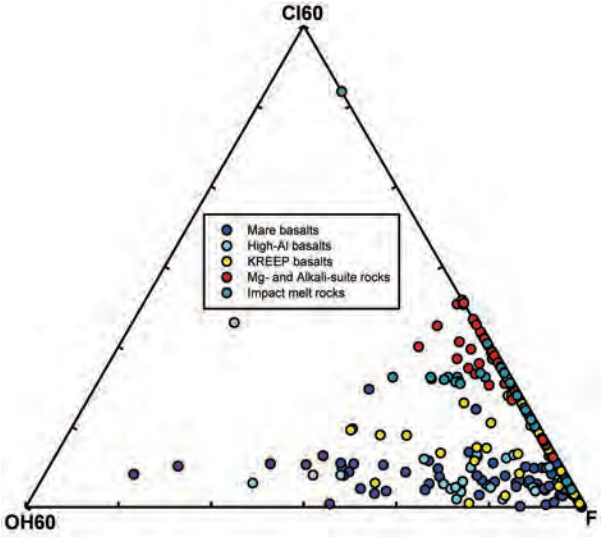

Figure 2. Truncated ternary plots of apatite X-site occupancy (mol%) from mare basalts high-Al basalts, KREEP basalts, magnesian and alkali suite rocks, and impact melt rocks. Data yielding (F+Cl) > 1 atom are plotted along the OH^- free join assuming 1 – Cl = F. Data used for plot are from literature (Boyce et al. 2010; Elardo et al. 2014; McCubbin et al. 2011, 2010b, 2010c; Tartèse et al. 2014b; Taylor et al. 2004) with the exception of apatite from high-Al basalt 14321,1842 where the EPMA data are available in a supplementary data table[1] available online.

with olivine and/or pyroxene. These textures have been observed in clasts within Apollo 16 fragmental breccias 67915, 67016, and 66095 (known as the "Rusty Rock") (Colson 1992; El Goresy et al. 1973b; Lindstrom and Salpas 1983; Norman 1982; Norman et al. 1995; Papike et al. 1991; Shearer et al. 2012; Taylor et al. 1973; Taylor and Williams 1973), in Mg-suite troctolite 76535 (Elardo et al. 2012), and in Mg-suite gabbronorite 76255 (Shearer et al. 2015). Sphalerite with 28 mol% troilite in solution has also been documented in 66095 (El Goresy et al. 1973b; Taylor et al. 1973). Chalcopyrite in association with pentlandite and troilite has been observed in vugs within Apollo 17 breccias 76016 and 76215 (Carter et al. 1975), and pentlandite has also been reported in Apollo 14 breccia 14315 (Ramdohr 1972).

Oxy-hydroxides. Oxy-hydroxides are exceedingly rare in lunar rocks, but their presence has been confirmed (Agrell et al. 1971, 1972; Butler 1972; El Goresy et al. 1973b; Shearer et al. 2014; Taylor et al. 1973, 1974). Rusty alteration in lunar rocks was first reported in Apollo 14 breccias and became more widely recognized in Apollo 16 breccias. The alteration is typically found in association with metal grains, and the best-studied sample is "Rusty Rock" 66095. In a thin section from 66095, the iron metal grains are associated with thin gray margins and brown stains that extend into the adjacent silicates and have been interpreted as rusting in situ (Taylor et al. 1973). Although numerous Apollo 16 breccias exhibit some rust around metallic iron grains, not all contain the significant enrichment of volatile elements observed in 66095. Goethite with variable amounts of Cl (0.8–5.2 wt%) was reported surrounding metal grains (Butler 1972; El Goresy et al. 1973b; Taylor et al. 1973). During the original examination of 66095 (Butler 1972), an extraordinary amount of yellow colored staining was reported on its surface and interior. Taylor et al. (1973, 1974) determined that some of the "rust" in 66095 was the hydrous iron oxide akaganeite (βFeOOH), with 1–3 wt% Cl. Using both Raman spectroscopy and transmission electron microscopy (TEM), Shearer et al. (2014) confirmed the observation of Taylor et al. (1973, 1974) that akaganéite was an important phase making up this alteration. The *d*-spacings measured from the TEM electron backscatter diffraction patterns were consistent with akaganéite. Shearer et al. (2014) identified an alteration stratigraphy from body-centered cubic Fe-Ni alloy (kamacite) → paramagnetic face-centered cubic Fe-Ni alloy → lawrencite → akaganéite. Further, they identified goethite and hematite intergrown with the akaganéite and lawrencite. Importantly, a lunar origin for the akaganéite is still debated.

Chlorides. Chlorides in lunar samples are rare and occur in unique lunar environments. Some of the rarity may be partially tied to their fragility (e.g., surface coatings) and their reactivity with the terrestrial environment during sample return, curation, and analysis. Two chlorides have been identified in lunar samples: halite (NaCl) and lawrencite ($FeCl_2$).

Halite has been observed as minute euhedral crystals associated with surface coatings on Apollo 17 orange volcanic glass beads (McKay et al. 1972; McKay and Wentworth 1992, 1993). The surface coatings are typically 20–150 nm thick and exhibit geochemical stratigraphy (McKay and Wentworth 1992, 1993). Lawrencite ($FeCl_2$) is the other chloride initially inferred from the composition of rust in 66095 and experimental results of lawrencite alteration (Taylor et al. 1973, 1974). It was concluded that lawrencite was present in these samples and was totally consumed by rapid reaction with moisture in the air. Reexamining the alteration in 66095 using TEM, Shearer et al. (2014) identified a very thin layer of lawrencite ($FeCl_2$) adjacent to the fcc Fe-Ni alloy. The ring pattern in the electron diffraction pattern indicates that the lawrencite is polycrystalline and presumable very fine-grained. The energy-dispersive X-ray spectra showed that either some O is incorporated into the lawrencite or that given the very fine-grained character of the lawrencite, some Fe oxide may be present along grain boundaries as a result of oxidation.

Graphite, carbides, and organics. The presence of primary graphite in lunar magmas has been an ongoing topic of substantial debate tied to the volatile propellant of the fire-fountain eruptions that produced the pyroclastic glass beads (Fogel and Rutherford 1995; Nicholis and Rutherford 2009; Rutherford and Papale 2009; Sato 1979). The studies that suggest the existence of graphite in the lunar interior focus mainly on the lunar pyroclastic glasses. Sato (1979), based on experimental results on Apollo 17 orange glass (74220), suggested that graphite exists in the source region of the orange glass magma and was responsible for reducing the melt as partial melting began. Similarly, Nicholis and Rutherford (2009), through a series of experiments on the same composition, concluded a CO-rich gas phase, present due to the oxidation of graphite, would be generated during magma ascent at ~8.5 km beneath the lunar surface. Fogel and Rutherford (1995) examined the green and yellow pyroclastic glasses and yellow impact glasses and did not detect any dissolved carbon species by FTIR, however they

still suggested graphite was present at depth and the oxidation of this graphite is capable of producing the pyroclastic eruption of the lunar fire-fountains. Despite all of the claims for the requirement of graphite in the lunar interior, graphite has not been found in any lunar samples as a primary igneous phase. In fact, lunar graphite has only been discovered in a single sample, 72255, which is an Apollo 17 impact melt breccia (Steele et al. 2010). Steele et al. (2010) concluded the graphite in 72255 was present as both rolled graphene sheets and graphite whiskers and was produced either by an impactor that struck the lunar surface or by condensation from the carbon-rich gas released during an impact event involving carbonaceous material. Because both formation mechanisms have the graphite forming on the Moon, the graphite is considered lunar in origin, even if its formation is tied to impact processes.

Several occurrences of carbides have been reported from lunar samples including cohenite $(Fe,Ni)_3C$, moissanite (SiC), and aluminum carbide (Al_4C_3). Cohenite has been identified in several lunar soils and regolith breccias including 10046, 14003, 68501, and 66095,78 (El Goresy et al. 1973a; Frondel et al. 1970; Goldstein and Axon 1973; Goldstein et al. 1972, 1976). Moissanite has only been tentatively identified in lunar breccia 12013,10 (Gay et al. 1970), and in lunar soils 65901,5 and 65501,1 (Jadweb 1973). A single occurrence of aluminum carbide was reported in thin section 863 from Luna 20 in a troctolitic rock (Tarasov et al. 1973). The reports of cohenite and moissanite have been largely interpreted to come from the infall of meteoritic material to the Moon (Frondel 1975). Further details on the chemistry and structure are required to confirm the presence of aluminum carbide in Luna 20,863, but Tarasov et al. (1973) reports that the grain is texturally associated with olivine and feldspar in the troctolitic sample, and therefore appears to be indigenous to the sample.

Organics, in the form of amorphous macromolecular carbon, have been recently reported as coatings on lunar volcanic glass beads in sample 74220 (Thomas-Keprta et al. 2014). The organic carbon is similar to that which was recently found in martian meteorites (Steele et al. 2012). This carbon has been shown to form inorganic compounds under reducing conditions at elevated hydrogen fugacity (Eck et al. 1966), and these conditions would be consistent with those of the vapor plume surrounding a lunar pyroclastic fire-fountain eruption. Importantly, although a terrestrial source for this organic carbon was ruled out, Thomas-Keprta et al. (2014) did not rule out an extraselenian source of the carbon from meteorites.

Nominally anhydrous minerals. Minerals without volatile elements as essential structural constituents are typically referred to as nominally anhydrous minerals (NAM) or nominally volatile-free minerals. These phases can store volatiles within crystallographic defects typically at trace abundances (Bell and Rossman 1992; Libowitzky and Beran 2006; Smyth 2006; Wright 2006). The most commonly studied nominally anhydrous minerals include olivine $(Fe,Mg)_2SiO_4$, pyroxenes $(Fe,Mg,Ca)_2Si_2O_6$, garnets $(Fe,Mg,Ca)_3Al_2(SiO_4)_3$, and feldspars $Ca_x(Na,K)_{1-x}Al_{1+x}Si_{3-x}O_8$. Experimental studies have shown that F, Cl, and H can be stored in the above NAM phases; however the mineral-melt partition coefficients for Cl are typically much smaller than for F and H, likely due to the large ionic radius of Cl^- (Beyer et al. 2012; Hauri et al. 2006; McCubbin et al. 2012c; O'Leary et al. 2010; Tenner et al. 2009).

Lunar samples commonly have olivines, pyroxenes, and feldspars, but the only NAM for which H_2O abundances have been quantified in lunar samples is feldspar (Hui et al. 2013; Mills et al. 2014). Hui et al. (2013) used polarized micro-FTIR to measure the abundances of H_2O in anorthitic plagioclases from troctolite 76535,164 and ferroan anorthosites 15414,238 and 60015,787. They demonstrated that the plagioclase in the FAN's had up to 6 ppm H_2O, and the plagioclase in the Mg-suite troctolite had 2.7 ppm H_2O. Mills et al. (2014) used SIMS to measure the H_2O abundances of alkali feldspar in a granitoid clast in breccia 15405,78, reporting up to 1000 ppm H_2O. McCubbin et al. (2010b) analyzed nominally anhydrous phases in NWA 2977, 15404,51, and 14053,16 as part of their study of volatile abundances in apatite by SIMS, but the H_2O contents were indistinguishable from analyses of the "blank" synthetic forsterite mounted in indium. Liu et al. (2012b) polished rock chips of 12056, 12063, and 74255 and mounted them in indium for SIMS analysis. Using terrestrial olivine and pyroxenes as standards (Mosenfelder et al. 2011; Mosenfelder and Rossman 2013a, 2013b), Liu et al. (2012b) reported that the Fe-rich olivines and pyroxenes may contain several parts per million H_2O above the background values.

Although not a volatile-bearing mineral, sensu stricto, cordierite $(Mg,Fe)_2Al_4Si_5O_8$ is of potential importance for lunar volatiles because its open structural channels can trap neutral molecules, including H_2O, CO_2, and CO (Fig. 3). Abundances of these species can be analyzed by vibrational spectroscopy and/or SIMS and used to retrieve the fluid compositions with which the cordierite last equilibrated (e.g., Bul'Bak and Shvedenkov 2005; Harley and Carrington 2001; Harley et al. 2002; Rigby and Droop 2008; Rigby et al. 2008; Vry et al. 1990).

Cordierite is known only from two lunar samples. The spinel-troctolite 15295,101 contains ~8% cordierite associated with plagioclase, olivine, Mg-Al spinel, ilmenite, rutile, troilite, and-Fe metal (Marvin et al. 1989); the other lunar cordierite is in lunar spinel troctolite 72435a and consists of a single 30 μm grain in a pink spinel grain (Dymek et al. 1976; Shearer et al. 2015) as well as a grain that is >100 μm that is partially encased by anorthitic plagioclase (Fig. 1c). None of these lunar cordierites have been analyzed for volatiles with high precision and high detection sensitivity. Treiman and Gross (2012) analyzed the cordierite in 15295,101 for volatile content with EPMA and FTIR. The EPMA analysis is consistent with a low abundance of volatiles, ~<1% by mass, based on analytical totals. The FTIR transmission spectra showed no H_2O absorption bands, and a possible detection (<0.1%) of CO (but equally possibly an artifact). The 72435 cordierites have not been analyzed for volatiles.

The occurrence of cordierite in a lunar rock requires unusual conditions. The rock's bulk composition must be highly aluminous, such as might form by partial melting of a spinel troctolite (Marvin et al. 1989; Treiman 1991) but could not form by normal igneous processes from a chondritic or peridotitic source. On the Moon, spinel-rich rocks themselves are rare and of uncertain origins (Gross et al. 2014; Gross and Treiman 2011; Herzberg 1983; Herzberg and Baker 1980; Prissel et al. 2012; Vaughan et al. 2013), so that one might expect partial melts from them to be

rarer still. Confining pressure must be less than ~0.3 GPa (Marvin et al. 1989; McCallum and Schwartz 2001; Treiman 1991), but that limit only excludes the deepest portions of the lunar crust. It would be extremely important to find additional samples of cordierite-bearing rock and to analyze their volatile abundances using methods with high detection sensitivity.

Volatiles within volcanic rocks

The volcanic rocks that will be discussed here include mare basalts as well as the eruptive products of volatile-assisted pyroclastic fire-fountains. Bulk rock data for the volatiles are compiled for the mare basalts, whereas we investigate both the interior and exterior volatile inventories of the pyroclastic glass beads.

Mare basalts. A few measurements of H abundances have been carried out on bulk samples of Apollo mare basalts and they range from 1–11 ppm H, and much of this H has been attributed to either spallation reactions or solar wind implantation (Haskin and Warren 1991). Although there are not many analyses, mare basalts have 18–78 ppm F (Table 2). Samples from Apollo 11 are reported to have anomalously elevated F abundances ranging from 190–260 ppm F (Haskin and Warren 1991), but given the paucity of data and the inexplicably high values, additional analyses of F in mare basalts would be worth pursuing. Cl abundances in mare basalts range from approximately 300 ppb to 28 ppm, although Cl abundances are typically <10 ppm (Haskin and Warren 1991). S abundances of mare basalts range from approximately 300 to 3200 ppm (Gibson et al. 1977; Haskin and Warren 1991; Table 2). Mare basalts typically contain less than 1 ppm of indigenous N (Becker et al. 1976; Des Marais 1978, 1983; Mathew and Marti 2001; Mortimer et al. 2015; Muller 1974), which has hampered measurement efforts to date, but N abundances have been measured as high as 20 ppm N (Haskin and Warren 1991). Similar to N and H, there is much debate over the indigenous inventory of C in lunar basalts vs. the fraction that can be attributed to secondary processes. Of the mare basalts that have been measured, their carbon contents range from 3–70 ppm C (Haskin and Warren 1991; Mortimer et al. 2015; Table 2), with reports of 3.3–7.0 ppm indigenous C in mare basalts (Mortimer et al. 2015).

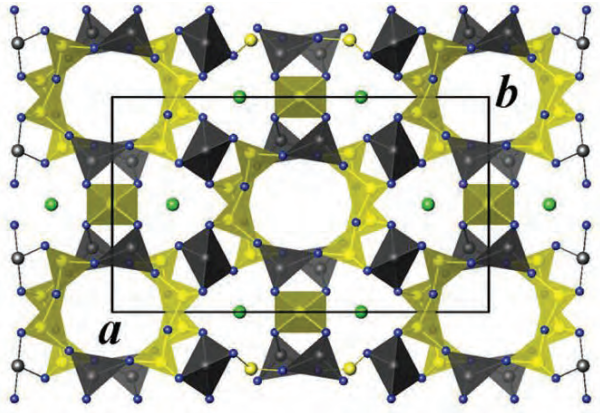

Figure 3. Projection of cordierite structure, looking down *c*. *a* = 1.71 nm. Channels that can hold volatiles are at corners and center of black rectangle. Green = magnesium atoms, blue = oxygen atoms, yellow = silicon atoms. The image is in the public domain and available for download from http://commons.wikimedia.org/wiki/File:Cordierite_structure.png.

Pyroclastic glasses. Although volatiles have been implicated in the origin of many volcanic glass beads that were recovered from the lunar surface during the Apollo missions, the assisting volatile has never been positively identified. Speculations of the assisting volatile have included sulfide-rich vapor (Butler and Meyer 1976; Meyer et al. 1975), C-rich vapor (Fogel and Rutherford 1995; Nicholis and Rutherford 2009; Rutherford and Papale 2009; Sato 1979), F- and Cl-bearing vapor (Elkins-Tanton et al. 2003b; Goldberg et al. 1976), and H_2-rich vapor (Sharp et al. 2013a; Vander Kaaden et al. 2015). These speculations have been largely derived from analysis of volatiles in the glass beads and volatile-rich coatings that occur on glass beads as well as inferred physicochemical conditions of eruption (e.g., low oxygen fugacity). The volatile-abundances associated with the beads and coatings are presented below.

Interior volatiles in volcanic glasses. The presence of pyroclastic deposits on the surface of the Moon, formed by fire-fountain style eruptions, is commonly used as strong evidence that at least some lunar magmas were not completely devoid of magmatic volatiles. Our approach and understanding of volatile abundances in the pyroclastic glasses changed dramatically in 2008 with the publication of Saal et al. (2008). Consequently, we will discuss pre-2008 and post-2008 studies separately.

Before 2008, substantial efforts were devoted to measuring volatile contents in lunar samples, and particular attention was given to the volcanic glass beads. The beads were measured for H_2O and CO_2 using bulk techniques (Epstein and Taylor 1973; Friedman et al. 1972; Gibson 1977; Gibson and Moore 1973a; Kaplan and Petrowski 1971), but it was concluded that H, and in part C, were produced by solar wind implantation on the lunar surface and that the molecular H_2O analyzed likely represented terrestrial contamination (see for example Epstein and Taylor 1973). The low abundances of C that were measured were used to infer low C contents in the lunar mantle, low C solubility in magmas at reducing conditions, and CO loss during degassing (Fogel and Rutherford 1995; Sato 1979). Many studies have also measured F, S, and Cl abundances in the glasses both by bulk and in situ techniques, and it has been largely reported that abundances of these volatiles are often close to or even below detection limits in the interiors of the glass beads (Butler and Meyer 1976; Chou et al. 1975; Elkins-Tanton et al. 2003a, 2003b; Fogel and Rutherford 1995; Gibson and Andrawes 1978a; Gibson et al. 1975; Goldberg et al. 1975; Jovanovic et al. 1976; Jovanovic and Reed 1975; Klein and Rutherford 1998; Meyer et al. 1975; Wieler et al. 1999). All these studies pointed to the fact that volatiles, including magmatic volatiles, were highly depleted in the volcanic glasses, and only extraselenian surface implanted volatiles or terrestrial contaminants were present.

Unambiguous detection and quantification of water and other volatile abundances in lunar pyroclastic glasses by Saal et al. (2008) heralded a new era in lunar volatiles research. Their SIMS analyses showed that the high-Ti orange glasses contain ~5–13 ppm H_2O, 9–17 ppm F, 0.02–0.14 ppm Cl, and 282–490 ppm S. The very-low-Ti green glasses displayed an even larger range of volatile contents. They contain ~0.4–30 ppm H_2O, 2–10 ppm F, 0.03–0.50 ppm Cl, and 114–270 ppm S (Table 2). Importantly, the

relative abundances of these volatiles remained nearly constant in each of the analyses (Saal et al. 2008). Finally, two analyses were carried out on low-Ti yellow glasses and they had the highest abundances of volatiles with 17–46 ppm H_2O, 29–40 ppm F, 1.3–2.0 ppm Cl, and 518–576 ppm S. Saal et al. (2008) also measured the radial concentration profiles of H_2O, F, Cl, and S, within a single very-low-Ti glass bead, which showed a decrease of volatile contents from core to rim from ~30 to ~14 ppm for H_2O, ~8.5 to 5 ppm for F, ~0.27 to 0.14 ppm for Cl, and ~260 to 220 ppm S. These profiles provided substantial support for the volatiles being indigenous to the quenched lava as opposed to products of terrestrial contamination or solar wind implantation as previously suggested. The shapes of the profiles for each of the volatiles were also consistent with magmatic degassing. Saal et al. (2008) argued that the initial, pre-degassing, abundances of volatiles in these glasses had to be much higher. Hauri et al. (2011) followed up on this initial study by reporting the volatile contents of olivine-hosted melt inclusions within some of the high-Ti orange pyroclastic glass beads. They measured 270–1200 ppm H_2O, 37–72 ppm F, 1.5–2.4 ppm Cl, and 450–880 ppm S in these melt inclusions (Table 2), with the relative abundances of the volatiles again being nearly constant. Wetzel et al. (2014) reported carbon contents in the olivine-hosted melt inclusions to range from 0.47–5.65 ppm. As these melt inclusions are trapped in olivine crystals contained within primitive lunar volcanic glasses, which quenched within minutes after eruption, post-eruptive H diffusion in or out of the inclusions likely occurred (Bucholz et al. 2013) but is expected to be minor.

Mineralized coatings on volcanic glasses. Two types of glasses have been found on the Moon: impact glasses and volcanic glasses. Delano and Livi (1981) constructed a specific set of criteria to differentiate between the two. Among the criteria for the pristine volcanic glasses are surface correlated volatiles, found as volatile coatings on the lunar glasses. Analysis of these coatings has been conducted using numerous techniques including radiochemical neutron-activation analysis, instrumental neutron-activation analysis, scanning electron microscopy, electron probe microanalysis, resonant nuclear reaction techniques, energy-dispersive spectrometry, Raman spectroscopy, and secondary ion mass spectrometry (Chou et al. 1975; Clanton et al. 1978a, 1978b; Elkins-Tanton et al. 2003b; Goldberg et al. 1976; Krahenbuhl et al. 1977; McKay and Wentworth 1992, 1993; Meyer et al. 1975; Morgan and Wandless 1984; Thomas-Keprta et al. 2014). The elements Ag, Au, Bi, Br, C, Cd, Cl, Cu, F, Ga, Ge, Hg, I, In, K, Na, Ni, P, Pb, S, Sb, Se, Te, Tl, and Zn have been detected in the coatings via direct analysis, leaching experiments, and selective volatilization (Butler 1978; Butler and Meyer 1976; Chou et al. 1975; Cirlin et al. 1978; Clanton et al. 1978b; Colson 1992; Elkins-Tanton et al. 2003b; Fogel and Rutherford 1995; Gibson and Moore 1974; Goldberg et al. 1976; Krahenbuhl et al. 1977; McKay and Wentworth 1992, 1993; Meyer 1990; Meyer et al. 1975; Morgan and Wandless 1984; Reed et al. 1977; Silver 1975; Tatsumoto et al. 1987; Wasson et al. 1976). Micromound coatings (i.e., vapor-deposited coatings) have also been found on the surfaces of the Apollo 17 orange and black glasses as well as Apollo 15 green glass (Clanton et al. 1978a; Heiken and McKay 1974; McKay et al. 1973a; 1973b; McKay and Wentworth 1992, 1993). These coatings range in thickness from 0.002 to 0.03 μm (McKay et al. 1973a, 1973b), and they vary from dense and continuous to coatings containing cracks, scrapes, gouges, and vesicles presumably from post crystallization events (McKay and Wentworth 1992, 1993). Volatile-rich grains and small euhedral crystals were found in these micromound structures and contained NaCl and sulfur-rich phases (McKay and Wentworth 1992).

Although there have been numerous elements detected in the coatings of lunar glass beads, S, Zn, Cl, and F are the most abundant elements found in most of the samples. Detected in almost 95% of all lunar glass beads, sulfur is the most ubiquitous element found in these coatings (Butler 1978; Butler and Meyer 1976; Clanton et al. 1978b; Colson 1992; Elkins-Tanton et al. 2003b; Gibson and Moore 1974; McKay and Wentworth 1992; Meyer et al. 1975; Wasson et al. 1976). Gibson and Moore (1974) detected up to 650 ppm S in an orange glass sample, making sulfur slightly more abundant than Zn and more abundant than Cl and F. Sulfur in the coatings of the glass beads is present as ZnS (Colson 1992; McKay and Wentworth 1992; Wasson et al. 1976), FeS that has exsolved from the interior of the glass droplets, Cu sulfides (Wasson et al. 1976), and/or as elemental sulfur (McKay and Wentworth 1992). Sulfur has also been shown to be associated with oxygen as well as carbon (McKay and Wentworth 1992).

Zn has been detected in 84% of lunar glass coatings up to ~300 ppm (Butler and Meyer 1976). Butler (1978) showed the proportions of Zn to S are constant on the surface of an individual droplet, although this ratio varies from droplet to droplet. Although Reed et al. (1977) suggested Zn is too soluble to be present as a sulfide, Colson (1992) showed through thermodynamic calculations of vapor-sulfide equilibria that the presence of H (even in small amounts) in the vapor is required to explain ZnS precipitation. McKay and Wentworth (1992) suggested zinc may be present as zinc carbonate or zinc oxide. Another abundant element, although less abundant than both S and Zn in lunar coatings, is Cl. Under lunar conditions, Zn could form highly volatile chlorides as well (Wasson et al. 1976).

Chlorine has been found at the ~100 ppm level in volcanic glass bead coatings (Butler and Meyer 1976) and is usually shown to be present mainly as NaCl (Clanton et al. 1978b; McKay and Wentworth 1992, 1993). Cirlin et al. (1977) also suggested Cl may be present in the form of $PbCl_2$ and other chlorides. Fluorine, on the other hand, has been detected up to 3000 ppm in a tenth of a micrometer thick surface layer of an Apollo 15 green glass sample (Goldberg et al. 1976). Calculations by Naughton et al. (1972) predict CaF to be the most abundant gaseous fluoride molecule. Goldberg et al. (1976) have ruled out many simple water-soluble fluoride salts in the lunar coatings because the F deposits on both orange and green glass beads was not removed after being exposed to hot water for 10 min. However, it is difficult to rule out oxyfluorides and various sulfur-fluorine compounds (Goldberg et al. 1976).

Volatiles in the lunar megaregolith

We use the term lunar megaregolith to refer to secondary or primary crustal materials that have been re-processed, broken down, re-melted, and/or redistributed by impact and space weathering processes. The material we include as part of the

lunar megaregolith includes crystalline and partially crystalline impact melts and impact melt sheets, agglutinates, lunar soil, and regolith breccia matrix. We adopt the term lunar megaregolith and use it instead of regolith because it is a broader term that encompasses more than lunar sediments and includes both large- and small-scale products of secondary processing like the lithologic products of impact melt sheets, impact melts, and agglutinates.

Apatite from impact melts. Apatite occurs in many impact melts and impact melt breccias, and the volatile abundances of these apatites are typically very similar to apatites found in the lunar highlands Mg-suite and alkali-suite rocks (Fig. 2). Apatites from lunar impact melts typically have low OH abundances with minimal detectable missing component from EPMA analyses (McCubbin et al. 2011) and ≤100 ppm H_2O indicated by direct analysis by SIMS (Barnes et al. 2014). Many of the impact melts in which apatite has been analyzed on the Moon are KREEP-rich, and it has been suggested that the volatile-abundances of apatites in KREEP-rich impact melts may be providing information about the volatile abundances of KREEP, especially given the similarity in volatile abundances of apatites among the KREEP-rich impact melts and the highlands Mg- and alkali-suite rocks (McCubbin et al. 2011). However, no study has been designed to investigate the effects of shock on the OH systematics of pre-existing apatite, making these results difficult to interpret at present.

Agglutinates. Physical and chemical changes in lunar soil occur through constant bombardment by meteorite, micrometeorite, and energetic particles (e.g., solar wind, solar flares, and galactic rays; Lucey et al. 2006; Papike et al. 1991). Lunar soils decrease in FeO and MgO abundance and increase in CaO, Al_2O_3, Na_2O, and K_2O abundance with decreasing grain size (from 90 to <10 μm). This trend reflects preferable comminution of feldspar and friable mesostasis by impact (e.g., Papike et al. 1981, 1982; Taylor et al. 2001, 2010). Agglutinates are unique alteration products on the surface of airless bodies such as the Moon. They are essentially conglomerates of mineral, rock, and glass fragments cemented by impact melts of lunar soils (Fig. 4). Papike et al. (1981) suggested that composition of agglutinates can be modeled by fusion of the finest fraction (F^3) of soils. This model applies to agglutinitic glasses from mare soils because their compositions are broadly similar in composition to the <10 μm fraction of soils. However, agglutinitic glasses in Apollo 16 highland soils do not fit this model; their compositions are more mafic than the coarser fraction (45–20 μm) of lunar fines (Liu and Taylor 2011; Papike et al. 1981; Taylor et al. 2010). Papike et al. (1981) suggested that the mafic minerals in highland rocks are of smaller size and thus easier to be concentrated in the fine fraction and taken up by agglutinitic glass. However, the compositional variations observed in highlands soils follow similar trends with grain size as the mare soils. The more mafic composition of highland agglutinitic glasses indicates that large-scale mixing was operative between mare and highlands (Pieters and Taylor 2003; Taylor et al. 2010).

The agglutinitic glasses are filled with vesicles and metal iron globules. Housley et al. (1973) proposed that nanophase-Fe^0 was generated through reduction of FeO in the agglutinitic melts by implanted solar-wind hydrogen. A few studies measured different soil components and reported high H abundances in lunar agglutinates (Des Marais et al. 1974; Gibson and Andrawes 1978b). However, several agglutinitic glasses were examined previously using FTIR spectroscopy yielding OH contents <50 ppm, which was the detection limit at that time (Taylor et al. 1995). With the discovery of surface OH/H_2O by remote sensing (Clark 2009; Pieters et al. 2009; Sunshine et al. 2009), Liu et al. (2013, 2012a) re-examined agglutinates using both FTIR spectroscopy and SIMS because recent technological advancements in both techniques allowed for much higher detection sensitivities.

A few agglutinate grains from lunar soil 10084 and 70051 were doubly polished to self-supporting slabs with 50–200 μm thickness for FTIR analysis, and SIMS analyses were conducted at a high spatial resolution of 10 μm^2, which allows for the measurement of small patches of glass between minerals and vesicles. Liu et al. (2012a) measured 12 grains of Apollo 11 soil 10084, 3 grains of Apollo 17 soil 70051, and 1 grain of Apollo 16 soil 64501. SIMS results of 13 agglutinates indicate that agglutinitic glasses contain H equivalent to 27 ± 14 to 470 ± 18 ppm H_2O (Liu et al. 2012a). The low value, 27 ppm, was obtained on a plagioclase grain in 10084agg2. These abundances were adjusted to roughly half of the reported values, after MPI-DING standards were recalibrated using transmission micro-FTIR (Liu et al. 2013).

Lunar soils and regolith breccias. Shortly after each Apollo mission and up to 1991, lunar soils were analyzed for hydrogen and other volatiles using bulk analysis methods, including step heating, mechanical crushing, or chemical dissolution, in association with mass spectrometry. A few studies investigated individual components (e.g., Gibson and Andrawes 1978b). Between 1991–2008, there was a hiatus in analyzing volatile abundances in lunar samples, although isotope compositions of hydrogen, oxygen, nitrogen, and noble gases of lunar soil grains have been studied to understand the composition of the Sun (Benkert et al. 1993; Hashizume and Chaussidon 2005; Hashizume et al. 2000; Heber et al. 2003; Ireland et al. 2006; Nier and Schlutter 1994; Wieler et al. 1999). Although recent interests

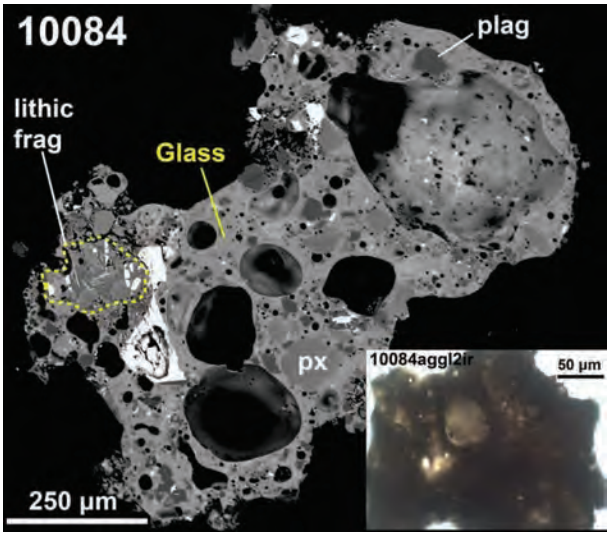

Figure 4. Backscattered electron image of a polished agglutinate from Apollo 11 10084. The inset shows a polished agglutinate under transmitted light. Glass, lithic fragments (lithic frag), plagioclase (plag), and pyroxene (px) are labeled accordingly.

peaked again after discoveries of OH/H_2O on the surface of the Moon (Clark 2009; Pieters et al. 2009; Sunshine et al. 2009), only a few studies re-analyzed lunar soils for their volatile contents (Furi et al. 2012; Liu et al. 2012a, 2013; Mortimer et al. 2015; Sharp et al. 2010b). Thus, pre-1991 data still forms the basis of our understanding of volatiles in lunar soils. There are many excellent reviews on these topics, including Lunar Chemistry and Lunar Regolith chapters in the Lunar Sourcebook (Haskin and Warren 1991; McKay et al. 1991; and references for pre-1991 data are listed in these chapters). Correlations between H, N, and noble gases were also assessed in Fegley and Swindle (1993). Here, we present a synthesis of bulk H, C, N, S, F, and Cl in lieu of recent discoveries.

Lunar soils and regolith breccias generally contain more H_2 (45 ppb, equivalent of 405 ppb H_2O; Fegley and Swindle 1993) than crystalline rocks (<10 ppb H_2, equivalent of <90 ppb H_2O; Friedman et al. 1971, 1972; Stievenard et al. 1990). The carbon contents in lunar soils and regolith breccias can reach up to 280 ppm C, with an average of ~100 to 150 ppm among soils from different missions (summary table A8.6 in Haskin and Warren 1991). The nitrogen contents among lunar soils and regolith breccias range from 4 to 209 ppm, generally higher than in lunar rocks by one to two orders of magnitude (Haskin and Warren 1991; Mathew and Marti 2001; Muller 1974). Early studies of lunar regolith observed coupled increases in carbon and nitrogen abundances, suggesting a common source.

Compared to H, C, and N, there are limited studies of fluorine and chlorine in lunar regolith. The concentrations of F in soils range from 9 to 520 ppm, whereas Cl contents range from 0.6 to 270 ppm (Jovanovic et al. 1976; Jovanovic and Reed 1973, 1975; Reed et al. 1971, 1977; Reed and Jovanovic 1973a, 1973b). Similar to other volatile elements, soils and breccias are more enriched in F and Cl than rocks, although the soils exhibit substantial variations in Cl concentration. Importantly, no clear differences in Cl contents among soil maturity have been observed (Sharp et al. 2010b). There have been a limited number of studies on Cl in lunar breccias, which have largely focused on the "Rusty Rock" 66095. Apollo 16 breccia 66095 (better known as "Rusty Rock") has been of great interest since its arrival on Earth due to its rusty alteration. 66095 is classified as an impact melt breccia consisting of ~78% fine-grained subophitic to ophitic impact melt (Garrison and Taylor 1980). Shearer et al. (2014) demonstrated that Cl is heterogeneously distributed in 66095 but is closely associated with both goethite and phosphates. They also showed that in the goethite itself, the Cl content is lowest directly adjacent to the metal and increases outward. Akaganéite found on the rims of metal Fe grains that are <10 μm in size were irregularly dispersed throughout the matrix and associated with sulfides (e.g., troilite) and as intergrowths with goethite (Provencio et al. 2013; Taylor et al. 1973). Akaganéite occurs mostly as elongate, somatoidal crystals (Provencio et al. 2013). Individual akaganéite grains display relatively homogenous Cl contents (Burger et al. 2013) containing between 1–4 wt% Cl (Provencio et al. 2013). Lawrencite grains up to 1 μm in size were also identified adjacent to Fe-Ni metal (El Goresy et al. 1973b; Provencio et al. 2013). El Gorsey et al. (1973b) identified troilite and sphalerite surrounded by goethite in 66095, where the goethite Cl content ranges from 0.90 to 4.18 wt% and S content ranges from 0.06 to 0.47 wt%. Other volatile elements that appear to be particularly enriched in 66095 include Tl, Ge, Sb, Zn, Pb, and Cd (Ebihara et al. 1981; Krahenbuhl et al. 1973; Nunes and Tatsumot 1973).

Lunar soils and breccia matrix contain 60–600 ppm S (Duncan et al. 1973; Wänke et al. 1976), which is similar to the S abundances of mare basalts (300–3300 ppm S; Gibson et al. 1977; Haskin and Warren 1991). Sulfur-mineralized clasts in some lunar breccias contain bulk S ranging from 0.4 to 1.24 wt% (Norman et al. 1995; Shearer et al. 2012). Samples 67016,294 and 67016,297 are feldspathic fragmental breccias and 67915,150 is a feldspathic polymict breccia (Shearer et al. 2012). There have been numerous reports of sulfide replacement textures in these rocks, including troilite veining and sulfide-pyroxene intergrowths, which are wormy or vermicular in texture (Lindstrom and Salpas 1983; Norman 1982; Norman et al. 1995; Shearer et al. 2012). In sample 67016,294, intergrowths of pyroxene and troilite have been observed ranging in widths between 4 and 10 μm and in lengths between 100 and 1000 μm. Veining in sample 67915 is much less pervasive and generally occurs in segments of approximately 10 μm. The breccia matrix of sample 67016 contains between 0.006 and 0.019 bulk wt% S (Duncan et al. 1973; Wänke et al. 1976), whereas sulfur-mineralized clasts in the breccia contain bulk S ranging from 0.84 to 1.24 wt% (Norman et al. 1995; Shearer et al. 2012). There is a similar trend observed in sample 67915, in which the bulk S content of the breccia matrix is ~0.06 wt% (Wänke et al. 1976), and the sulfur-mineralized clasts are richer in S, containing between 0.40 and 0.9 wt% S (Shearer et al. 2012).

Volatiles in surface features from remote sensing

Broadly distributed hydroxyl and water. In 2009, three instruments recorded detections of hydroxyl and potentially water on the lunar surface. The Moon Mineralogy Mapper (M^3) detected an absorption band attributed to the 2.8 μm O-H stretching across much of the Moon, with a negligible signature of OH^- in the lunar maria near the equator (Pieters et al. 2009). Because of the low spectral sampling near 3 μm, the precise shape and position of this absorption could not be characterized by M^3. This absorption was also measured by the Cassini Visual and Infrared Mapping Spectrometer (VIMS) and EPOXI High Resolution Instrument Infrared (HRI-IR) instruments (Clark 2009; Sunshine et al. 2009). Though the VIMS observations were made in 1999, calibration challenges in the 3 μm region initially prevented a unique identification of water on the Moon until a decade later. Both VIMS and HRI-IR extend to longer wavelength than M^3, enabling a more complete characterization of hydroxyl/water absorption features. Although measurements from both spacecraft had far lower spatial resolution than M^3, the VIMS and HRI-IR data both showed that the absorption bands exhibit a clear minimum near 2.8 μm, attributable to O-H stretching. The regional absorptions were shown by both instruments to be broad, with full-widths at half maximum ranging from about 200 nm in equatorial highland soils through about 400 nm pole-wards of ~45°N and S latitude (Clark 2009). There was also evidence that over the course of the lunar day, even equatorial latitudes became hydrated, with hydration features waning as the surface heated up (Sunshine et al. 2009). Because of the uncertainties in the scattering properties of the upper regolith, the

amount of water was estimated to range between 10–1000 ppm over the majority of the surface, with localized enhancements being higher (Clark 2009).

In general, all instruments observed that the band depth of the 2.8 μm absorption strengthens toward the poles, with the apparent absorption band minimum also shifting to slightly longer wavelengths (Clark 2009; Pieters et al. 2009; Sunshine et al. 2009). The regional enhancements at high latitudes do not show a positive correlation with previously measured neutron spectrometer measurements of hydrogen (Pieters et al. 2009). Instead, they appear to correlate primarily with lithologic type (Fig. 5), with feldspathic materials exhibiting stronger OH^- absorptions than more mafic regions (Cheek et al. 2011; Pieters et al. 2009). When the absorptions near 3 μm in M^3 data are modeled as two separate bands, one centered near 2.8 μm and one near 3.0 μm, the 2.8 μm hydroxyl absorption is seen to vary smoothly from a minimum near the equator to a maximum at the poles, while the 3.0 μm absorption does not appear until approximately 45° latitude, and then strengthens sharply with proximity to the poles (McCord et al. 2011).

The Lyman Alpha Mapping Project (LAMP) instrument onboard the Lunar Reconnaissance Orbiter (LRO) was used to search for the surface hydroxyl/water by comparing the slope of the UV spectrum in the wavelength range containing the 165 nm absorption edge and at a neighboring higher wavelength range. A redder slope spanning 165 nm is indicative of higher hydration. The LAMP data were binned by local time and latitude to examine the putative diurnal signature. They corroborated both the latitudinal effect and the diurnal effect at low latitude (Hendrix et al. 2012).

Poles and permanently shadowed regions. Despite the general depletion in volatiles observed in early measurements of the Apollo samples, it was anticipated that enhanced concentrations of water might be present within permanently shadowed regions (PSR), most of which are located at the lunar poles, due to billions of years of cometary impacts, solar wind interactions, and retention by cold traps within the PSRs (Arnold 1979; Watson et al. 1961). Initial indications of enhanced ice concentrations at the lunar poles were reported using data from a bistatic radar experiment on the Clementine spacecraft (Nozette et al. 1996). These results were disputed, however, as the radar signature could not be uniquely attributed to water ice (Simpson and Tyler 1999). Recent radar data remains consistent with, but not definitively diagnostic of water ice. Specifically, data from the LRO and Chandraayan-1 missions show results that are consistent with enhanced water ice in some, but not all, of the permanently shadowed polar craters at the north and south poles (Spudis et al. 2010, 2013).

The first definitive evidence for enhanced hydrogen concentrations at the lunar poles came from epithermal neutron data acquired with the Lunar Prospector Neutron Spectrometer (LP-NS) (Feldman et al. 1998). This initial report plus additional studies (Feldman et al. 2000, 2001; Lawrence et al. 2006) showed that both lunar poles contain average hydrogen concentrations of 100–150 ppm hydrogen over large-area footprints (~100–200 km). The LP-NS neutron data are consistent with the presence of 1–3 wt% water equivalent hydrogen (WEH) within PSRs (Eke et al. 2009; Elphic et al. 2007; Feldman et al. 2000, 1998, 2001; Lawrence et al. 2006; Teodoro et al. 2010). Neutron-derived average equatorial H concentrations are roughly 50 ppm (Lawrence et al. 2006), which is very close to the lunar sample average of 50 ppm H (Haskin and Warren 1991).

Heterogeneously distributed hydrogen at the lunar poles was also later detected from orbit by the Lunar Exploration Neutron Detector (LEND) instrument on the LRO spacecraft (Miller et al. 2012; Mitrofanov et al. 2010, 2012). These data, coupled with LP-NS hydrogen maps, were used to help select the Lunar Crater Observation and Sensing Satellite (LCROSS) impact site (Mitrofanov et al. 2010). The LCROSS mission shepherding spacecraft observed the impact of a spent upper stage of an Atlas V rocket into the permanent shadows of the south polar crater Cabeus in October of 2009 (Schultz et al. 2010). The spectral range of the near-infrared spectrometer on the LCROSS shepherding spacecraft ranged from 1.3–2.4 μm; thus, it was unable to measure the fundamental hydroxyl absorption at 2.8 μm that was observed by the Cassini VIMS, EPOXI HRI-IR, and M^3 instruments. Based on the spectral signature of the ejecta and crater, the concentration of water ice in the regolith at the impact site was estimated to be on the order of 5% by mass (Colaprete et al. 2010). The positions of the modeled absorptions, near 1.4, 1.9, and 2.2 μm suggested that the regolith and vapor plume included not only water ice, but also mineral-bound hydroxyl. Simultaneously, the UV/Vis instrument detected the hydroxyl radical between 308.5 and 309.5 nm. Its light curve peaked 30 s after impact, which is interpreted to indicate desorption of mineral bound hydroxyl. A second rise in the OH^- signature may have stemmed from the photodissociation of water vapor in sunlight.

The LAMP ultraviolet spectrograph onboard LRO also observed the ejecta plume created by the LCROSS impact (Gladstone et al. 2010). Based on the far-ultraviolet light curve from a field of view that swept across the impact site at an altitude of ~7 to 38 km as the vapor plume expanded in sunlight, they estimated that the plume contained ~120 kg of molecular hydrogen, as well as ~40 kg of carbon monoxide and ~12 kg of mercury (Hurley et al. 2012), suggesting that other volatile species might be trapped in the permanently shadowed craters. Additionally, Killen et al. (2010) detected sodium in the plume from a ground-based telescope. In fact the near-infrared (NIR) data from the LCROSS SSC are also consistent with the presence of a suite of volatile molecules released from the permanently shadowed region within Cabeus (Colaprete et al. 2010).

Igneous provinces. On the basis of near-infrared data, the volcanic lunar basalts are generally less enriched in hydroxyl than the highlands (Clark 2009; Pieters et al. 2009; Sunshine et al. 2009). The hydroxyl signature that is present in the maria also appears to weaken significantly with time of day (Sunshine et al. 2009). In contrast to the basalts, several of the pyroclastic deposits on the lunar surface appear to contain enhanced amounts of water (>500 ppm) based on mapping by Li and Milliken (2013). The highest modeled water abundances (>1500 ppm) were found in the Aristarchus, Montes Harbinger, Sulpicius Gallus, Rima Bode, and Humorum pyroclastic deposits (Li and Milliken 2014). All of these deposits are located within the Procellarum KREEP (potassium, rare earth elements, and phosphorus) Terrane (PKT), a region on the nearside of the Moon that is highly enriched in incompatible elements (Jolliff et al. 2000). Not all

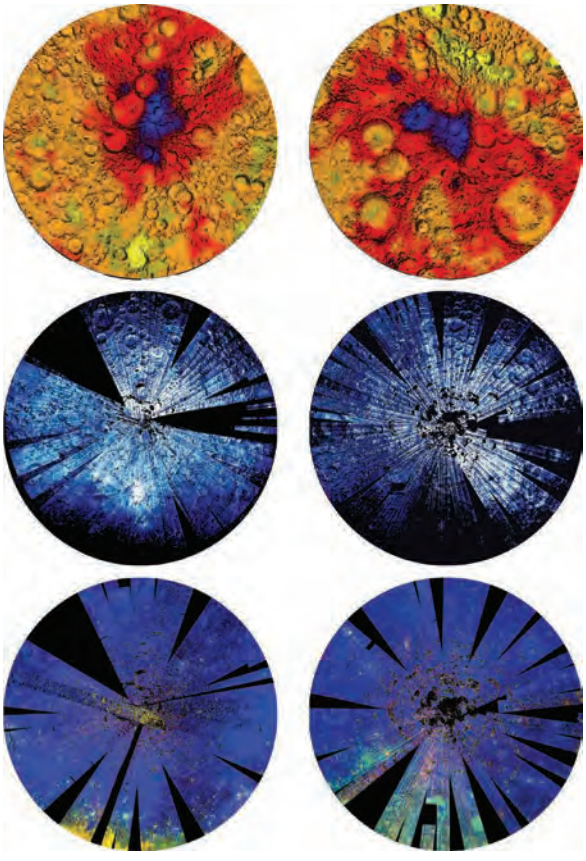

FIGURE 5. Distribution of epithermal neutrons (**top**) and 3000 nm water absorption (**middle**) at the lunar poles (from 70–90° for the neutrons; 60–90° north and south for reflectance). For reference, a map using the standard M^3 color composite for the same regions is shown in the **bottom** row. In this case, the red channel depicts the integrated 1000 nm mafic absorption band depth, the green channel depicts the integrated 2000 nm mafic absorption band strength, and the blue channel depicts the reflected light at 1500 nm. In this composite, mare basalts appear yellow, noritic material appears cyan, and anorthositic material appears blue. The north pole is on the left, with the nearside at the bottom, and the south pole is on the right, with the far side on the bottom. The yellow region on the bottom left is the northern portion of Mare Frigoris, and the cyan region on the right is part of South Pole-Aitken basin. For the neutron maps, dark colors represent low epithermal neutron counts, which indicate locations of hydrogen enhancements. Neutron data modified from Lawrence et al. (2006). M^3 maps created using mosaics produced by Joseph Boardman for M^3 data validation purposes (Boardman et al. 2011; Green et al. 2011).

pyroclastics within the PKT were found to contain as much water. Li and Milliken (2014) report that the deposits at Sinus Aestuum contain no detectable hydration and the water content of others throughout the PKT range from 500–800 ppm water. Pyroclastics within Mare Moscoviense, outside of the PKT, are modeled to have ~800 ppm water (Li and Milliken 2014).

The 61 km diameter Bullialdus crater, centered at 20.7°S, 337.8°E in Mare Nubium, lies along the southern edge of the PKT. Though the mare basalts surrounding Bullialdus crater do not exhibit a hydroxyl signature, the central peak, which excavated noritic material, exhibits an enhanced hydroxyl absorption relative to its surroundings. To explore the cause of this anomaly, Klima et al. (2013) investigated M^3 coverage of the crater during three different times of the lunar day. In all cases, the central peak remains hydrated while the surroundings are essentially hydroxyl-free. The hydroxyl signature is associated with the crests of the central peak, where the largest boulders and freshest (least space-weathered) material are exposed.

The Compton Belkovich volcanic complex, located at 61.1°N, 99.5°E, is also enriched in hydroxyl (and potentially water) relative to its surroundings (Bhattacharya et al. 2013; Petro et al. 2013). Compton Belkovich is also the location of enhanced thorium, as measured by the Lunar Prospector Gamma Ray Spectrometer (Lawrence et al. 1999, 2003, 2007) and has been interpreted as a location of non-mare silicic volcanism (Jolliff et al. 2011). Bhattacharya et al. (2013) estimate an average water content of 0.3 wt% within the complex; however, because of the high latitude of this feature, it is also overprinted by a regional hydroxyl/water signature. Nevertheless, the maximum water content calculated by Li and Milliken (2013) for the polar latitudes is ~1000 ppm, still significantly lower than was interpreted for Compton Belkovich.

Isotopic data for volatile elements

Isotopic compositions are traditionally expressed in δ notation according to the following equation

$$\delta\,{}^{M}X = \left[\frac{{}_{\text{Heavy}}{}^{M}X_{\text{Measured}} \times {}_{\text{Light}}{}^{M}X_{\text{Standard}}}{{}_{\text{Light}}{}^{M}X_{\text{Measured}} \times {}_{\text{Heavy}}{}^{M}X_{\text{Standard}}} - 1\right] \times 1000 \quad (1)$$

where $({}_{\text{Heavy}}{}^{M}X_{\text{Measured}}/{}_{\text{Light}}{}^{M}X_{\text{Measured}})$ is the isotopic ratio of the measured sample, $({}_{\text{Light}}{}^{M}X_{\text{Standard}}/{}_{\text{Heavy}}{}^{M}X_{\text{Standard}})$ is the isotopic ratio of the standard, and $\delta^{M}X$ is the δ value of the isotope expressed in per mil. The standard for D/H is Vienna Standard Mean Ocean Water with D/H of 1.5576×10^{-4} (Coplen 1994). The reference standard used for $^{13}C/^{12}C$ is the Pee Dee Belemnite carbonate (PDB), which has $^{13}C/^{12}C$ ratio of 1.123×10^{-2} (Irwin et al. 1977), although more modern studies utilize the Vienna Pee Dee Belemnite (VPDB) (Coplen 1994). The $^{15}N/^{14}N$ reference standard used is the terrestrial atmosphere (AIR), where $^{15}N/^{14}N(AIR) = 3.678 \times 10^{-3}$ (Marty 2012). The $^{34}S/^{32}S$ reference standard used is troilite from the Canyon Diablo iron meteorite (CDT), which has $^{34}S/^{32}S$ ratio of 4.41626×10^{-2} (Ding et al. 2001). The reference standard for $^{37}Cl/^{35}Cl$ is standard mean ocean chloride (SMOC), which has a $^{37}Cl/^{35}Cl$ ratio of 0.324 (Kaufmann et al. 1984).

Hydrogen. *Bulk-sample measurements of soils and regolith breccias.* In the early 1970s, numerous workers measured H isotopic compositions in lunar soils and regolith breccias using step-wise heating (Epstein and Taylor 1970a, 1970b, 1971, 1972, 1973; Friedman et al. 1970a, 1970b, 1971; Merlivat et al. 1972, 1974, 1976). The δD value of H_2 and H_2O extracted from soils and regolith breccias ranged from –1000 to –400‰ for H_2 and –900 to –120‰ for H_2O. The δD of H_2 decreased with increasing H_2 content in soils and breccias, while the δD of H_2O increased with increasing molar H_2O/H_2 ratio.

Minerals and agglutinates in soils and regolith breccias. A couple of studies have investigated the water content and H isotopic composition of minerals and agglutinates from lunar soils and regolith breccias. Hashizume et al. (2000) carried out analyses of H and N contents and their isotopic compositions in 500 to 1000 μm sized olivine, pyroxene, and ilmenite grains

from regolith breccia 79035 and soil 71501. They selected these samples to study the effect of solar wind (SW) implantation on the H and N isotope systematics of lunar surface materials. These samples had very different SW exposure histories, with regolith breccia 79035 having been exposed to SW for 1 to 2 Ga, whereas the soil 71051 had been irradiated for about 100 Ma (Hashizume et al. 2000). Analysis of an ilmenite grain from soil 71501 yielded fairly constant H_2O content 20–100 ppm with depth, with δD decreasing from elevated values of +500‰ down to 0‰. In a silicate grain from regolith breccia 79035, H_2O content decreased with depth from ~1000 to ~200 ppm over about 400 nm while δD remained at –280‰. Analyses of several grains in regolith breccia 79035 yielded δD values as low as –916‰, indicating the presence of almost pure SW hydrogen (i.e., ~–1000‰). In contrast, D enrichment up to +450‰ (after correction for spallation production of D) highlights the contribution of a non-solar H component in soils recently exposed to SW.

Liu et al. (2012a) reported the water content and H isotopic composition of mineral fragments and glasses in agglutinates from three different soil samples. In the agglutinates, the D/H values were determined on the same spots where the H contents were obtained in 8 agglutinates. The samples ranged from –844 ±40‰ to +5500 ± 134‰ (2σSD) (Fig. 6). The majority of that data (6 agglutinates) was below δD values of –550‰. Glasses in two agglutinates (10084agg2; 10084agg8ir) displayed large positive δD values (+191 ± 99‰ to +4206 ± 134‰). The terrestrial contamination was deemed to be negligible because the visible contaminants in vesicles and cracks contain δD values of about –50 to –200‰, significantly different from δD values of agglutinitic glass. Furthermore, if terrestrial contamination produced the observed OH, one would expect that D/H values and $1/H_2O$ would follow a mixing line between the Earth and solar wind, and such a trend is not evident in Figure 6.

Bulk-sample measurements of mare basalts. A few measurements of H_2 and H_2O abundances and H isotopic compositions have been carried out on bulk samples of Apollo mare basalts (Friedman et al. 1971; Merlivat et al. 1974). Low-Ti basalt 12051 contained 6 ppm H_2 with a δD of +340‰; high-Ti basalts 70215 and 75035 contained 1.5 ppm H_2 with a δD of +200‰ and 0.5–2 ppm H_2 with δD values ranging from approximately +250‰ down to –100‰, respectively. The low δD split of 75035 was interpreted as resulting from more implantation of solar wind H. In the three other bulk analyses conducted on mare basalts, hydrogen is characterized by a δD of about +200–300‰, which is higher than known terrestrial materials. These elevated δD values have been ascribed to cosmic-ray spallation processes (e.g., Friedman et al. 1971).

Pyroclastic volcanic glasses. Recently, Saal et al. (2013) reported the isotopic composition of hydrogen dissolved in the lunar pyroclastic glasses and in their olivine-hosted melt inclusions to gain insights into the source of lunar magmatic water. Their data show that all glass beads and melt inclusions are D-enriched compared to terrestrial ocean water, with δD values ranging from +200 to +5000‰. However, as pointed out by Saal et al. (2013), secondary processes that can affect D/H ratios, among which include cosmic-ray spallation and magmatic degassing (solar wind implantation was negligible in these samples; Saal et al. 2013), must be accounted for to establish the actual H isotopic composition of lunar indigenous water. Data from Saal et al. (2013) displayed a negative correlation between δD values and H_2O content for different glass types, pointing to a set of processes that have modified the original magmatic water present in these lunar magmas during and/or after their eruption. Once corrected for spallogenic production of H and D, the total range of δD values of the pyroclastic glasses was substantially lowered (–700 to +2200‰, excluding one outlier with δD around +4000‰). Excluding glasses with H_2O below 10 ppm, due to large uncertainties, the data displayed a slight negative trend of δD with H_2O content. Saal et al. (2013) interpreted this trend for high-Ti glasses as reflecting kinetic degassing of H_2 followed by OH-dominated diffusion at later stages. The low- to very-low-Ti glasses glasses with more than 10 ppm H_2O, displayed higher D/H ratios than high-Ti glasses. This difference could indicate that degassing of H_2 was more important in the low- to very-low Ti glasses than in high-Ti glasses. The fraction of total hydrogen present as H_2 depends on several system parameters (T, P, f_{O_2}, amount of H-bearing species; Hirschmann et al. 2012), so it would be difficult to glean additional information regarding initial magmatic abundances of H from the H isotopic compositions and present day H abundances of the glasses without additional information. Given the elevated Habundances of the olivine-hosted melt inclusion glasses, spallation did not have any significant effect on the D/H ratios, although H exchange either out of or into the inclusions could have occurred (i.e., Gaetani et al. 2012). Regardless, these glasses are the best samples (potentially least altered by degassing or spallation) to estimate an upper limit for the primitive H isotope composition of lunar water, which Saal et al. (2013) determined was approximately +190‰. This value is within the range of carbonaceous chondrite δD values (e.g., Alexander et al. 2012). Also, the striking similarity of both pre-eruptive H_2O content (Hauri et al. 2011) and D/H ratios (Saal et al. 2013) of lunar pyroclastic glasses and terrestrial MORB-type magmas supports the idea of a common origin, similar in composition to carbonaceous chondrites (Sarafian et al. 2014), for at least some terrestrial and lunar water.

Apatite in mare basalts. The H isotopic composition of water in lunar samples has also been investigated through analyses of the mineral apatite. Greenwood et al. (2011) were the first to report δD values for lunar apatites. They measured water contents and H isotopic compositions of apatite in several samples, mostly mare basalts. For apatite in the high-Al basalt 14053 they reported H_2O abundances of 570–930 ppm with δD values clustering around –200‰. Greenwood et al. (2011) also carried out several apatite analyses in low-Ti mare basalt 12039 that yielded a sixfold variation in apatite H_2O contents between 1000 and 6000 ppm, with elevated δD values ranging from +400 to +1000‰. Additional measurements of apatite D/H in mare basalts were published by Barnes et al. (2013) and Tartèse et al. (2013). In low-Ti mare basalts, apatite analyses yielded large ranges in H_2O content within individual samples, similar to what Greenwood et al. (2011) reported for apatites in sample 12039. In Apollo 12 samples 12064 and 12039, H_2O contents of apatite ranged from 700 to 2400 ppm and 1500 to 3800 ppm, respectively. Apatites in these two samples were characterized by narrow ranges in D/H ratios and yielded similar average δD values of +896 ± 76‰ and +873 ± 65‰, respectively (Barnes

et al. 2013; Tartèse et al. 2013). In Apollo 15 samples 15058 and 15555, apatite H_2O contents ranged from 200 to 750 ppm and 1200 to 3600 ppm, respectively, with very similar average δD values of +581 ± 62‰ and +597 ± 99‰, respectively (Tartèse et al. 2013). Apatite H_2O contents and H isotopic composition has also been measured in high-Ti mare basalts (Barnes et al. 2013; Greenwood et al. 2011; Tartèse et al. 2013). In mare basalt 10044, Greenwood et al. (2011) and Barnes et al. (2013) reported very consistent ranges in H_2O abundances of 850–1250 ppm (average = 1023 ± 169 ppm) and 856–1735 ppm (average = 1271 ± 224 ppm), respectively and δD values of ~ +570 to +640‰ and ~ +530 to +1010‰, respectively. The large data set obtained by Barnes et al. (2013) showed that the D/H ratios of water in apatites in basalt 10044 are highly variable, while the H_2O contents display much less variation. Tartèse et al. (2013) analyzed apatites in sample 10058, which are characterized by H_2O contents of 1100–1600 ppm (average = 1350 ± 200 ppm) and variable δD values of ~ +620 to +1100‰, very similar to apatites in 10044. Additionally, one analysis in apatite in mare basalt 75055 yielded 1070 ± 180 ppm H_2O with a δD value of +735 ± 36‰ (Greenwood et al. 2011), which is in good agreement with data reported for two other high-Ti basalts 10044 and 10058. Finally, Tartèse et al. (2013) reported OH-δD systematics for apatites from two basaltic meteorites, LAP 04841 and MIL 05035. In LAP 04841, analyses carried out on 5 apatite grains yielded elevated H_2O contents of 3500–7600 ppm, with δD values ranging from +280 to +560‰. In MIL 05035, the H_2O contents and δD values measured on 4 apatite grains ranged from 2000 to 7500 ppm and +100 to +570‰, respectively. These results are consistent with apatite H_2O contents of 2000–5500 ppm and an average δD value of +400 ± 80‰, reported for another piece of MIL 05035 by Wang et al. (2012). All of the H_2O and δD data from apatites in mare basalts are summarized in Figure 6.

Apatite in samples from lunar highlands. Apatites in samples from the lunar highlands are characterized by lower H_2O contents than apatites in mare basalts. As highlighted by Saal et al. (2013), care needs to be taken when interpreting the δD signatures associated with low OH contents (typically <100 ppm OH), where spallation processes can contribute significant amounts of D resulting in elevated δD values. All values given below have been corrected for spallogenic-produced D and H using the spallation production rates of Merlivat et al. (1976) and available cosmic-ray exposure ages compiled in the lunar sample compendium (http://curator.jsc.nasa.gov/lunar/lsc/index.cfm). The highlands samples containing apatite can be divided into two groups. The first group includes felsic rocks, which encompasses lunar granites and rocks from the alkali suite and the second group includes mafic to ultramafic cumulates that make up the magnesian suite.

From the felsic group, apatites from alkali anorthosites, felsites, quartz monzodiorites (QMDs), and granites have been analyzed for H_2O and δD. Greenwood et al. (2011) reported that

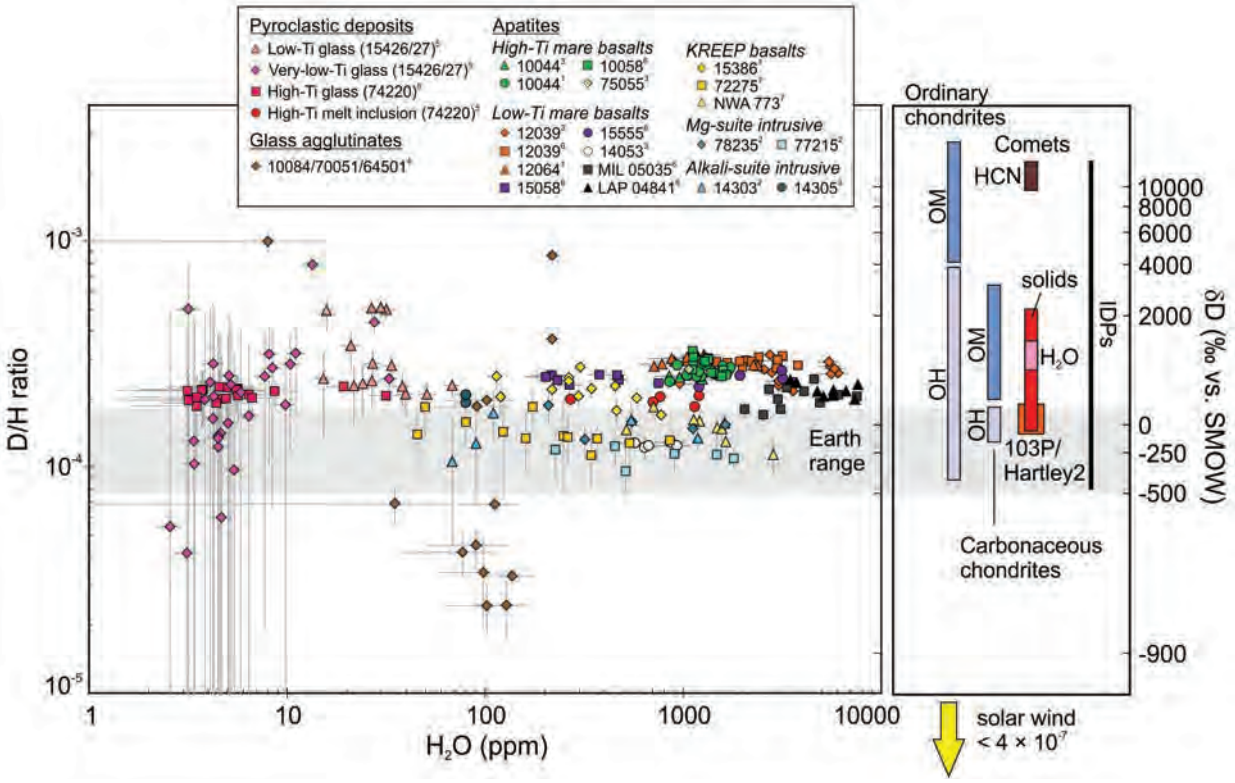

FIGURE 6. D/H values vs. H_2O contents (in ppmw H_2O) from a wide array of lunar materials including pyroclastic lunar glasses, apatites from various lunar rocks types, and agglutinitic glasses (Barnes et al. 2013, 2014; Greenwood et al. 2011; Liu et al. 2012a, 2013; Saal et al. 2013; Tartèse et al. 2013, 2014b). Reference values for Earth, chondrites, comets, IDPs, and solar wind are also provided (Alexander et al. 2012; Robert et al. 2000).

an apatite grain in an alkali anorthosite clast (14305,303) contained 80 ± 20 ppm H_2O with an average δD of +280 ± 120‰. Robinson et al. (2013) analyzed apatites in samples from two felsites (12013 and 77538) and two quartz monzodiorites (both from 14161), reporting a range of 175–190 ± 55 ppm H_2O and δD of +335 to +410 ± 75‰ in the felsites, and +160 to +190 ± 55 ppm H_2O and δD of +120 to +340 ± 90‰ in the QMDs. Barnes et al. (2014) measured apatite in a granite clast in sample 14303 finding 70–1200 ppm H_2O and average δD of +105 ± 130‰.

From the magnesian suite, apatites from troctolites and norites have been analyzed. Several studies have reported analyses of apatite in the Mg-suite troctolite 76535 and reported from 28–100 ppm H_2O with corresponding δD values between +40 and +640‰ (Barnes et al. 2014; Boyce et al. 2013; Robinson et al. 2013). Barnes et al. (2014) measured the H_2O content and D/H ratio in apatites from two norites (78235 and 77215), reporting that apatite from these samples has 200–1650 ppm H_2O and 450–1800 ppm H_2O, respectively. Furthermore, the apatites in the norite samples had weighted average δD values of –27 ± 98‰ for 78235 and –281 ± 49‰ for 77215.

Carbon. To measure the $\delta^{13}C$ values in lunar samples, both pyrolysis and combustion techniques have been employed as well as stepwise heating and single temperature release techniques. As stated previously, various authors compared the two techniques and found they yield similar results (i.e., Friedman et al. 1971, 1974; Kaplan and Petrowski 1971; Kerridge et al. 1975b). Gases released during carbon isotopic analyses using these techniques include CO, CO_2, and CH_4.

Initial analyses of the carbon isotopic composition of lunar samples began in the early 1970s after the return of the Apollo 11 samples (Epstein and Taylor 1970b; Kaplan and Smith 1970; Moore et al. 1970). Samples from subsequent Apollo missions were also analyzed for carbon isotopes, increasing the lunar data set (Becker 1980; Cadogan et al. 1971; Chang et al. 1971, 1974; Des Marais 1978, 1983; Des Marais et al. 1975; Epstein and Taylor 1971, 1972, 1973, 1975; Friedman et al. 1970a, 1971, 1974; Gardiner et al. 1978; Grady and Pillinger 1990; Kaplan et al. 1976; Kaplan and Petrowski 1971; Kaplan and Smith 1970; Kerridge et al. 1974, 1975b, 1978; Norris et al. 1983; Petrowski et al. 1974; Pillinger 1979; Smith et al. 1973). Figure 7 is a compilation of the carbon concentration (parts per million) and the $\delta^{13}C$ (‰) composition of lunar samples and illustrates the difference in isotopic composition of carbon relative to sample type (rocks vs. soils). Carbon concentrations in returned lunar samples are typically less than 260 ppm. $\delta^{13}C$ values of lunar samples range from approximately –40 to +24‰. Taking only Apollo sample data into account, one can recognize a weak positive correlation between increasing carbon concentration and increasing $\delta^{13}C$ values (inset in Fig. 7), the opposite trend is seen in drill-core samples. The higher total carbon content of many lunar soils is characteristic of a mixed mare and highland origin of mature regolith samples (Petrowski et al. 1974). With few exceptions, lunar rocks exhibit a depleted $\delta^{13}C$ signature when compared to the lunar soil components, indicating they contain more of the light isotope (^{12}C) compared to lunar soil components. Moore et al. (1970) showed that the finest sized materials (<53 μm size fraction) contain the highest concentration of carbon (500 ± 20 ppm), suggesting that carbon in lunar soil is dominated by surface-correlated carbon components (Des Marais et al. 1975; Kerridge et al. 1974). These authors suggested the difference in total C from their analyzed samples could be the result of different proportions of coarse- and fine-grained fragments within individual samples. This suggestion is similar to the interpretation of Kaplan and Petrowski (1971) who proposed that the spread in their isotopic values could be due to carbon compounds from multiple sources being present within a single sample.

Using the whole range of Apollo data included in Figure 7, the average $\delta^{13}C$ value of lunar basaltic rocks is around –25‰, whereas lunar soils/fines have a more ^{13}C-enriched signature (on average, around +10‰). Kaplan and Smith (1970) suggested the isotopically heavier carbon may have escaped from the basaltic samples during crushing and sample preparation or the basalts only contained a small amount of indigenous lunar carbon and are more susceptible to terrestrial contamination. Additionally, although their $\delta^{13}C$ values are quite distinct, lunar rocks and lunar soil components both show a variation in $\delta^{13}C$ on the order of ~+50‰. Analyses of two lunar meteorites (Allan Hills 81005 and Yamato 86032) by Grady and Pillinger (1990), while displaying vastly different carbon concentrations (479 and 320 ppm, respectively), also showed a tight grouping of $\delta^{13}C$ values (–21.9 and –25.2‰, respectively), similar to the range recorded in Apollo basalt samples (Fig. 7).

Nitrogen. The abundance and isotopic composition of nitrogen in lunar samples has been studied in detail by several groups since the return of the Apollo and Luna samples in the 1970s and has continued to the present day. Nitrogen concentrations have been measured using techniques such as pyrolysis/evolved gas analysis, SIMS, and neutron activation analysis. Isotopic data for N in lunar samples were mainly acquired through stepped combustion/pyrolysis experiments and, more recently, from SIMS measurements and laser extraction techniques.

N in lunar soils. Using stepped heating techniques, common patterns of N isotopic variations are observed across different lunar soil samples; low-temperature (<600 °C) N releases are typically ^{15}N-enriched, followed by a higher temperature ^{15}N-depleted signature (between 600–900 °C). At the very highest temperatures (above ~1000 °C), N releases are also enriched in ^{15}N (Becker and Clayton 1975, 1978; Kerridge 1993), due to contributions from cosmogenic ^{15}N (Assonov et al. 2002; Becker et al. 1976; Pillinger 1979). This "V-shaped" pattern (e.g., Becker and Clayton 1975; Brilliant et al. 1994; Thiemens and Clayton 1980) of isotopic variation with temperature indicates the presence of three distinct N components in lunar soil samples (Assonov et al. 2002; Becker et al. 1976; Thiemens and Clayton 1980).

N in mare basalts and pyroclastic glasses. Lunar rocks contain much less N than soils, typically less than 1 ppm of indigenous N (Becker et al. 1976; Des Marais 1978, 1983; Mathew and Marti 2001; Mortimer et al. 2015; Muller 1974), which has hampered measurement efforts to date. At such low abundances, indigenous lunar isotopic signatures are masked by those of cosmogenic components (Mathew and Marti 2001). In several instances, N abundances in rocks were below the detection limit of the instruments used, and isotopic data could not be measured (e.g., Kaplan et al. 1976). However, a recent study by Mortimer et al. (2015) was able to measure abundances of 0.13–0.83 ppm indigenous N in mare basalts and reported the $\delta^{15}N$ value of this nitrogen to be

+0.4 ± 9‰. From stepped heating analyses of bulk rock samples, it appears most of the N present in lunar rocks is released below 500 °C, and this N has been attributed to terrestrial contamination (Des Marais 1978; Grady and Pillinger 1990). As with N in lunar soils, N isotopic signatures at the highest temperature releases (>1000–1100 °C) are dominated by cosmogenic N (Becker and Clayton 1975; Becker et al. 1976; Des Marais 1978; Mathew and Marti 2001), present at roughly the same abundance as procedural blank levels (Des Marais 1983) and enriched in $\delta^{15}N$. Because the main target element for the spallogenic production of N is ^{16}O (Reedy 1981), which is present in both relatively high and uniform abundances across different lunar rock samples (Des Marais 1983), cosmogenic N (as identified by high temperature heavy $\delta^{15}N$ values) is a good measure of cosmic ray exposure (CRE) age for samples, its production rate being largely unaltered by differences in rock mineralogy (Des Marais 1983).

Nitrogen that is interpreted as being indigenous to the Moon has been analyzed using stepped combustion/pyrolysis (e.g., Becker et al. 1976; Kerridge et al. 1991; Mathew and Marti 2001; Murty and Goswami 1992) and crushing (e.g., Barry et al. 2013). The types of samples chosen for analysis of indigenous N include lunar meteorites MacAlpine Hills (MAC) 88104 and MAC 88105, glassy spherules taken from the Apollo 17 double drive core soils 74001/74002, and bulk rock (anorthosite, anorthositic breccia, and basalt) samples (Kerridge et al. 1991; Mathew and Marti 2001; Murty and Goswami 1992). Despite the diversity in sample selection, the observed range of $\delta^{15}N$ values (Table 3) is relatively small, supporting the idea that these values are possibly indigenous lunar N signatures (Murty and Goswami 1992).

Sulfur. Most studies of lunar samples indicate that there are three distinct S-isotope reservoirs on the Moon. Indigenous lunar S, as determined from analyses of numerous lunar igneous rocks, has nearly the same isotopic composition as does S from primitive meteorites. In a compilation of S isotope data from Haskin and Warren (1991), the $^{34}S/^{32}S$ ratio in lunar igneous rocks is only 0.05% different from the ratio in troilite from the Canyon Diablo iron meteorite. Lunar igneous rocks presented in this compilation have a $\delta^{34}S$ of –0.5 to +2.0‰. More recently, Farquhar and Wing (2005) and Wing and Farquhar (2015) presented a new set of high precision measurements of relative $^{34}S/^{32}S$, $^{34}S/^{32}S$, and $^{36}S/^{32}S$ values in mare basalts. Their data confirms that lunar mare basalts are characterized by a high degree of sulfur isotopic homogeneity, with $\delta^{34}S = +0.58 \pm 0.05$‰, $\Delta^{33}S = +0.008 \pm 0.006$‰, and $\Delta^{36}S = +0.2 \pm 0.2$‰. Subtle variations within this population in $\Delta^{33}S$ and $\delta^{34}S$ were attributed to cosmic-ray induced spallation reactions and S loss prior to eruption, respectively (Wing and Farquhar 2015). The isotopic composition of sulfur in lunar soils is distinctly different from lunar igneous rocks. The soils are enriched in heavy sulfur (^{34}S) with $\delta^{34}S$ values between +4 to +17‰. The $\delta^{34}S$ of mature lunar soils is generally more enriched in heavy sulfur than the more immature soils (i.e., maturity index is the ratio of ferromagnetic resonance intensity to total iron content). Kerridge et al. (1975a, 1975b) suggested that the enrichment of the soils in heavy S and its correlation to maturity indices was a result of S loss and isotopic fractionation through vaporization or ion sputtering. In an attempt to model this process, McEwing et al. (1980) illustrated in a series of heating experiments (at 1196 °C) that residual troilite would become increasing enriched in ^{34}S as the extent of the reaction increased. Evaporated troilite would be enriched in ^{32}S. With 0 to 12.5% of the reaction completed, the evaporated troilite would have a $\delta^{34}S$ of –3.87 to –5.36‰ relative to the starting material. The S composition of the dissociated troilite was even more enriched in ^{32}S with $\delta^{34}S$ ranging from –14.13 to –8.12‰ as the extent of the reaction increased.

Although rare, lunar materials with negative $\delta^{34}S$ values have been documented in a few studies. Ding et al. (1983) observed that the condensation coatings on the smaller size fraction of orange glass from the Apollo 17 pyroclastic deposit had a negative $\delta^{34}S$ that reached values of –2.62‰. In a brecciated olivine-bearing, anorthositic gabbro in sample 77017, Petrowski et al. (1974) reported a bulk $\delta^{34}S$ value of –5.2‰. Kerridge et al. (1975b) reported bulk $\delta^{34}S$ values of 0.02 to –2.2‰ on different splits of sample 67015. Shearer et al. (2012) determined that the sulfur isotopic composition of the vein and replacement troilite associated with lunar highlands clasts (FANs and Mg-suite) ranges from approximately –1.0 to –3.3‰. As samples that are enriched in light S relative to most other lunar samples are seemingly rare, the origin of this light S reservoir has not been explored in detail. Petrowski et al. (1974) suggested that this light S signature reflected either the incorporation of fractionated S of extra-selenian origin or that indigenous S on the Moon is much more heterogeneous than was apparent from most other analyses. Ding et al. (1983) suggested that the negative $\delta^{34}S$ observed in the Apollo 17 volcanic glasses is a product of the fire-fountaining process that produced these volcanic glasses. They suggested that the high-Ti basaltic magma represented by the orange glass had a $\delta^{34}S$ value of approximately 0‰, but lunar fire-fountaining resulted in light S being enriched in the associated vapor cloud and this S condensed on the surface of the orange glass droplets. The most negative $\delta^{34}S$ value occurred on the smallest size fraction of the glass as a result of its larger surface/mass ratio (and thus a high proportion of vapor condensates that are enriched in light S relative to the glass). Shearer et al. (2012) and Bell et al. (2015) suggested that the replacement and vein troilite were derived from the interaction of a vapor phase with plutonic rock lithologies in the shallow lunar crust. The enrichment of ^{32}S in the vapor phase may be attributed to the extensive degassing of a crustal magma or the high-temperature partial breakdown of troilite in the shallow crust.

Chlorine. There is a fairly limited amount of data on Cl-isotopes from lunar materials, with much of the data coming from a single study that combined gas source mass spectrometry with SIMS analyses (Sharp et al. 2010b). This study indicated that the Moon had the most extreme range in $\delta^{37}Cl$ values observed for any Solar System materials to date, with a range that exceeds that observed on the Earth (–1 to +25‰ for the Moon and ~0‰ for Earth). Furthermore, the extreme end of these values has since been pushed further with reports of an apatite grain in an impact melt sample (lunar meteorite Dhofar 458) that yielded a $\delta^{37}Cl$ value of up to +81‰ (Wang et al. 2012).

Lunar soils and regolith breccias. Sharp et al. (2010b) analyzed a mature soil (64501,232), an immature trench soil (61220,39), and two regolith breccias (12034,116 and "Rusty Rock" 66095). There was no clear correlation between Cl contents or $\delta^{37}Cl$ values with soil maturity as both mature and

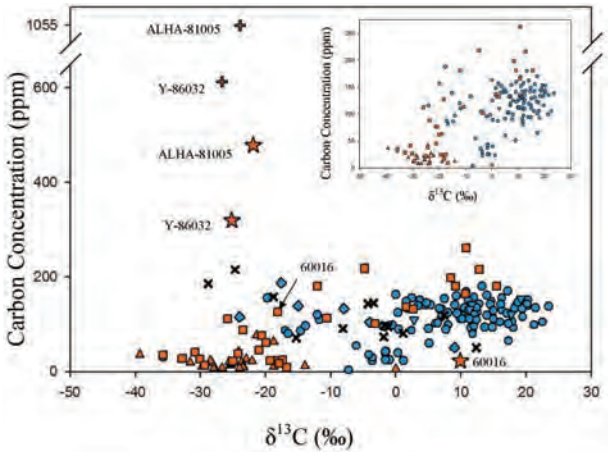

Figure 7. Carbon concentration and isotopic composition in lunar samples (Cadogan et al. 1971; Chang et al. 1971, 1974; Des Marais 1978; Des Marais et al. 1975; Epstein and Taylor 1970b, 1971, 1972, 1973, 1975; Friedman et al. 1970a, 1971, 1974; Grady and Pillinger 1990; Kaplan et al. 1976, 1970; Kaplan and Petrowski 1971; Kaplan and Smith 1970; Kerridge et al. 1975b, 1978; Moore et al. 1970; Petrowski et al. 1974; Smith et al. 1973). The orange and blue symbols separate lunar rocks from lunar soil components, respectively. Circles represent soils/fines, downward facing triangles represent agglutinates, diamonds represent dust, "X" represent drill-core samples, upward facing triangles represent basalts, squares represent breccias, plus signs represent meteorites, and the stars represent the samples from which Grady and Pillinger (1990) removed terrestrial contamination from the analyses of ALHA-81005, Y-86032, and 60016 (see text for details). The inset shows only Apollo rocks and soils.

immature soils yielded similar isotopic values in the leachable and non-leachable sample portions. A large fraction of Cl in the soil samples was soluble in water, and the chlorine isotopic values of leachates were always lighter than those of the residue, but both are heavier than terrestrial and planetary samples (Fig. 8). Both of the regolith breccias analyzed by Sharp et al. (2010) yielded similar δ^{37}Cl values in the non-leachable components in the soils (+14 to +16‰). Sharp et al. (2010) speculated that the lighter δ^{37}Cl may reflect that the highly soluble Cl is contributed by a metal-salt condensed from vapor.

Mare basalts and pyroclastic glasses. Sharp et al. (2010b) analyzed a high-Ti orange pyroclastic glass sample (74220,862), "hand-picked" high-Ti orange pyroclastic glass beads (74002,36), a high-K, high-Ti mare basalt (10017,34), and two low-Ti mare basalts (12040,214 and 12052). The δ^{37}Cl values of these samples ranged from –1 to +9‰ and represent the smallest variation among lunar sample types analyzed in that study. Notably, all of the analyses in this group of samples consisted of leachable Cl with the exception of low-Ti pigeonite basalt 12052, which only consisted of non-leachable Cl and high-K, high-Ti mare basalt 10017,34, which consisted of both leachable and non-leachable Cl (Sharp et al. 2010b).

Apatites in lunar rocks. Chlorine isotopic data for apatites in lunar materials have been exclusively determined by various SIMS techniques. Thus far, δ^{37}Cl values of apatites have been determined for mare basalts (10044,12, 10044,644, 12039,42, 12040,46, 12040,211, 15555,207, 75055,55, and MIL 05035), KREEP basalts (NWA 2977, 72275,491, and 15386,45), regolith breccias [NWA 4472, NWA 773, Sayh al Uhaymir (SaU) 169, and Kalahari 009] (Tartèse et al. 2014a) and highlands samples including impact breccias, Mg-suite, and alkali-suite rocks (12013,148, 14305,94, 76535,56, 79215,51, Dhofar 458) (Boyce et al. 2013; McCubbin et al. 2012c; Sharp et al. 2010b; Wang et al. 2012; Fig. 8). Apatites from the mare basalts display a range in δ^{37}Cl values of approximately +2 to +18‰ (Fig. 8). The KREEP basalts span a range in δ^{37}Cl values of approximately +9 to +27‰ (Wang et al. 2012), although that entire range is represented by a single sample (NWA 2977), and the range of 15386 and 72275 is much more narrow (+21.8 to +24.5‰; McCubbin et al. 2012c). The apatites in brecciated portions of lunar samples span a range of +5 to +20‰ (Tartèse et al. 2014a). The highland samples span a wide range in δ^{37}Cl values that is consistently heavier than the basalts (δ^{37}Cl values of approximately +25 to +81‰), although the most extreme values are from a single sample (Dhofar 458; Wang et al. 2012), and the other samples display a range of δ^{37}Cl values from +25 to +33‰ (Boyce et al. 2013).

Discussion and unanswered questions

Distribution and abundances of volatiles in the lunar interior

The abundances of magmatic volatiles in the lunar interior have been poorly constrained, so one of the primary goals of this review is to determine the abundances and distribution of volatiles among the various geochemical reservoirs in the Moon. Before the abundances are discussed, we briefly summarize the thermal and magmatic evolution of the Moon and describe where volatiles are likely to be distributed within the Moon as a result of this process.

Thermal and magmatic evolution of the Moon and the distribution of volatiles. At the initial stages of lunar differentiation it is widely believed that much, if not all, of the silicate portion of the Moon was molten. This molten mass is referred to as the lunar magma ocean (LMO) (Smith et al. 1970; Wood et al. 1970). Most models of LMO crystallization predict that upon cooling, crystallization commences with early Mg-rich olivine followed by orthopyroxene, which sink to form a stratified lunar cumulate mantle (e.g., Elardo et al. 2011; Elkins-Tanton et al. 2002, 2003a; Snyder et al. 1992). By ~70% crystallization, when the remaining liquid is Fe-rich and dense, anorthitic feldspar begins to crystallize and float to the surface of the LMO, forming the primary anorthositic crust (Ringwood and Kesson 1976; Smith et al. 1970; Taylor and Jakes 1974; Wood et al. 1970). The residual LMO liquid continues to crystallize, eventually forming a cumulate layer with abundant Fe-Ti oxides. Continued crystallization of the LMO leads to the residual LMO liquid becoming highly enriched in incompatible lithophile elements, including potassium (K), rare earth elements (REEs), and phosphorous (P). The term urKREEP is used to identify the last 1–2% of residual LMO liquid (Warren 1988a, 1988b; Warren and Wasson 1979), and the volatile abundances and isotopic composition of this liquid are largely unconstrained. At this stage, the Moon consists of a primary anorthositic crust, a stratified cumulate mantle, and an urKREEP layer at the interface of the two lithologic domains.

urKREEP represents an important lunar volatile reservoir. The incompatible lithophile magmatic volatiles (H, F, and Cl) are likely to be highly enriched in the urKREEP liquid, and

TABLE 3. Compilation of volatile isotopic compositions of various lunar materials

Isotope	Method	Samples	Isotopic composition (‰)
$^{2}H/^{1}H$ (δD)	Stepped heating	Bulk-sample soils and regolith breccias	−1000 to −400‰ (H_2) −900 to −120‰ (H_2O)
	SIMS, combustion, and stepped heating	Minerals and agglutinates in soils and regolith breccias	−950 to +5500‰
	Combustion and stepped heating	Bulk-sample mare basalts	−100 to +340‰
	SIMS	Pyroclastic volcanic glasses	+187 to +4045‰
	SIMS	Apatite in mare basalts	−200 to +1100‰
	SIMS	Apatite in KREEP-rich lunar samples	−400 to +340‰
	SIMS	Apatite in lunar breccias	−243 to +904‰
$^{13}C/^{12}C$ ($\delta^{13}C$)	Combustion, pyrolysis, stepped heating	Soils/fines	−35.7 to +23.5‰
	Combustion, crushing	Agglutinates	+2.8 to +19.2‰
	Combustion, stepped heating	Dust	−24 to +9‰
	Combustion, pyrolysis, stepped heating	Basalts	−39.3 to 0 ‰
	Combustion, pyrolysis, stepped heating	Breccias	−35.7 to +15.5‰
	Stepped heating, combustion	Lunar meteorites (ALHA-81005 and Y-86032)	−26.7 to −23.9‰
	Pyrolysis, stepped heating	Drill core	−28.8 to +12.3‰
$^{15}N/^{14}N$ ($\delta^{15}N$)	Stepped heating	Mare basalts and breccias	~ +10‰
	Stepped heating	Black/orange glass spherules from various depths in Apollo 17 double-drive core 74001/74002	+13‰ (±1.5)
	Stepped heating	Clast W-1 in MAC88105 (lunar meteorite)	+16.9‰ (±3.4)
	Stepped heating	Mare basalt, breccia, anorthosite, glass spherules from Apollo 17 double-drive core 74001	+13‰ (±1.2)
	Crushing	Mare basalts	−0.25 to +22.40‰
$^{34}S/^{32}S$ ($\delta^{34}S$)	Combustion and acid hydrolysis	Igneous rocks	−0.5 to +2.0‰
	Combustion and acid hydrolysis	Soils	+4 to +17‰
	Combustion	Condensation coating on orange glass spherule	−2.62‰
	Acid hydrolysis	Brecciated olivine-bearing Anorthositic gabbro (77017)	−5.2‰
	Combustion	Sample 67015	−2.2 to +0.02‰
	SIMS	Vein and replacement troilite associated with lunar highlands clasts	−3.3 to −1.0‰
$^{37}Cl/^{35}Cl$ ($\delta^{37}Cl$)	Gas source mass spectrometry	Soils and regolith breccias	+5.6 to +14.1‰ (leachate) +14.3 to +16‰ (nonleachable)
	Gas source mass spectrometry	Mare basalts and pyroclastic volcanic glasses	−1 to +9‰
	SIMS	Apatite in mare basalts	+2 to +18‰
	SIMS	Apatite in KREEP basalts	+9 to +27‰
	SIMS	Apatite in KREEP-rich lunar samples	+25 to +81‰
	SIMS	Apatite in lunar breccias	+5.3 to +19.7‰

Notes: Data compiled from Barry et al. (2013); Becker et al. (1976); Boyce et al. (2013); Cadogan et al. (1971); Chang et al. (1971, 1974); Des Marais (1975, 1978); Ding et al. (1983); Epstein and Taylor (1970a , 1970b, 1971, 1972, 1973, 1975); Friedman et al. (1970a, 1971, 1974); Grady and Pillinger (1990); Greenwood et al. (2011); Kaplan and Smith (1970); Kaplan and Petrowski (1971); Kaplan et al. (1970, 1976); Kerridge et al. (1975a, 1975b, 1978, 1991); Mathew and Marti (2001); Merlivat et al. (1972, 1974, 1976); Moore et al. (1970); Murty and Goswami (1992); Petrowski et al. (1974); Saal et al. (2013); Sharp et al. (2010b); Shearer et al. (2012); Smith et al. (1973); Tartèse et al. (2013, 2014a); Wang et al. (2012).

hence this liquid may have hosted much of the Moon's initial inventory of F, Cl, and H (provided they did not degas or become preferentially stored in a volatile-bearing mineral phase prior to urKREEP formation). The key to understanding the initial relative and absolute volatile abundances of the Moon, at the time of the LMO is through knowing the volatile abundances of urKREEP.

The volatile abundances of the cumulate mantle would have been controlled by two primary factors, (1) the amount of residual liquid that remained trapped within the cumulate pile during LMO crystallization and (2) the partitioning behavior of volatiles between the LMO liquid and the nominally volatile-free (referred to henceforth as nominally anhydrous) phases that crystallized to form the cumulate mantle. Under both scenarios, the lunar mantle would have a heterogeneous distribution of volatiles, with volatile abundances generally decreasing with depth in the pre-cumulate overturn mantle stratigraphy. If the dominant control on the abundance of volatiles is trapped residual liquid in the cumulate lunar mantle, the mantle and urKREEP should have similar ratios of volatile incompatible lithophile elements (F, Cl, and H) with much lower abundances in the mantle compared to the urKREEP liquid. If the abundances of volatiles in the cumulate lunar mantle are primarily controlled by the partitioning behavior of nominally anhydrous phases, volatile abundances in the lunar mantle would not mirror the volatile abundances of urKREEP. Specifically, the volatile abundances would vary based on the primary mantle mineralogy where olivine-dominant portions of the mantle would have very low abundances of volatiles, given the incompatibility of F, Cl, and OH in olivine under LMO conditions (Beyer et al. 2012; Hauri et al. 2006; Tenner et al. 2009; Fig. 9). Furthermore, pyroxene-rich portions of the mantle would be highly depleted in Cl relative to F and H_2O given the similar pyroxene-melt partitioning relationships for F and OH and the exclusion of Cl in pyroxene due to the large ionic radius of Cl compared to F and OH (Aubaud et al. 2004; Beyer et al. 2012; Hauri et al. 2006; O'Leary et al. 2010). We will investigate both of these scenarios as we discuss the volatile abundances of urKREEP and the lunar mantle.

To complicate matters further, the expected volatile stratification in the cumulate pile after LMO crystallization is not preserved today due to the probable mixing and hybridization of mantle cumulates. Either contemporaneous with the end stages of LMO crystallization or soon after, the hot, buoyant, Mg-rich, olivine-dominated cumulates at the base of the

mantle rise toward the base of the anorthositic primary crust while the cooler, dense, Fe-rich cumulates sink deeper into the mantle. This event is known as the cumulate mantle overturn and occurs due to gravitational instability within the cumulate mantle (Elkins-Tanton et al. 2002; Hess and Parmentier 1995; Neal and Taylor 1992; Ryder 1991). This mantle overturn event triggered episodes of secondary crust production, primarily from two distinct processes. The first occurred subsequent to the emplacement of hot olivine-dominated Mg-rich cumulates with urKREEP and the anorthositic primary crust, which initiated an episode of partial melting responsible for the production of the highlands magnesian suite rocks (see Shearer et al. 2015 for an in-depth review). The second process of secondary crust production is related to partial melting within the overturned hybridized cumulate lunar mantle, which was responsible for the formation of mare volcanics, including mare basalts and the pyroclastic glasses (see Longhi 1992a for an in-depth review).

The abundances of volatiles in the lunar mantle reflect the distribution of volatiles in the lunar interior subsequent to differentiation, magma ocean crystallization, and gravitationally driven overturn. Furthermore, unless a sample has a geochemical KREEP component, its source is not likely to have incorporated volatiles from urKREEP. Consequently, the present-day abundances of volatiles in the lunar mantle represent an important mass balance constraint for any compositional model of the bulk silicate Moon (BSM), where the lunar mantle and crust (the crust being largely dominated by the urKREEP component) should add up to the initial inventory of volatiles in the LMO.

Abundances of F, Cl, and H_2O in urKREEP. Unfortunately, the lunar sample collection (Apollo and Luna returned samples and lunar meteorites) does not contain a sample of the original urKREEP material, and the composition of the KREEP component has only been inferred or estimated from KREEP-rich geochemical signatures in some lunar samples. Several methods have been employed to determine the absolute and relative abundances of F, Cl, and H_2O in urKREEP, and we summarize them here.

Relative abundances of F, Cl, and H_2O in urKREEP from highlands apatite. The highlands magnesian-suite rocks are KREEP-rich mafic-ultramafic igneous cumulates that contain apatite. The origin of the parental magmas that produced these cumulates involved the interaction of the earliest-formed Mg-rich olivine-dominated magma ocean cumulates with the primary anorthositic crust and urKREEP liquid (Elardo et al. 2011; Shearer et al. 2006, 2015; Shearer and Papike 2005). The earliest-formed Mg-rich olivine-dominated magma ocean cumulates would be very poor in volatiles compared to more evolved pyroxene-rich cumulates based on available silicate-melt partitioning data for volatiles in olivines and pyroxenes (Aubaud et al. 2004; Beyer et al. 2012; Hauri et al. 2006; O'Leary et al. 2010; Tenner et al. 2009; Fig. 9). Consequently, the volatile signature of any partial melt that formed from these materials, and hence the partial melts that formed the magnesian suite, would have been overprinted by the volatile signature of urKREEP (Fig. 10). Apatites that crystallized from the lunar highlands rocks then record the volatile signature of their parental liquids, providing a direct measurement of the relative abundances of volatiles in urKREEP (McCubbin et al. 2011). This method could not be used to quantify the abundances of volatiles in urKREEP without knowing how much urKREEP was present in the Mg-suite parent liquid or knowing the abundances of F, Cl, or H_2O in urKREEP, so only relative abundances were reported. The plot from McCubbin et al. (2011) has been updated using additional literature data (Barnes et al. 2014; Elardo et al. 2012; McCubbin et al. 2012c) as well as an updated version of the relative volatile abundance ternary diagram from McCubbin et al. (2013) (Fig. 11a). The apatite from highlands rocks indicate that the melts from which they formed had more Cl than H_2O and F, but it is unclear whether there was more H_2O or F (Fig. 11a). Consequently, we posit that the dominant volatile, by weight, in urKREEP was Cl.

Estimates of urKREEP F and Cl abundances from lunar soils. Treiman et al. (2014) estimated the absolute abundance of F in urKREEP to be ~660 ppm from the average of two independent measurements: the F/P ratios in several Luna 16 and 20 soil samples (Reed and Jovanovic 1973a) and the abundances of F, Be, and Li in KREEPy soil 14136 (Dreibus et al. 1977; Meyer 2010; Rose et al. 1972; Wänke et al. 1972, 1973). Both measures

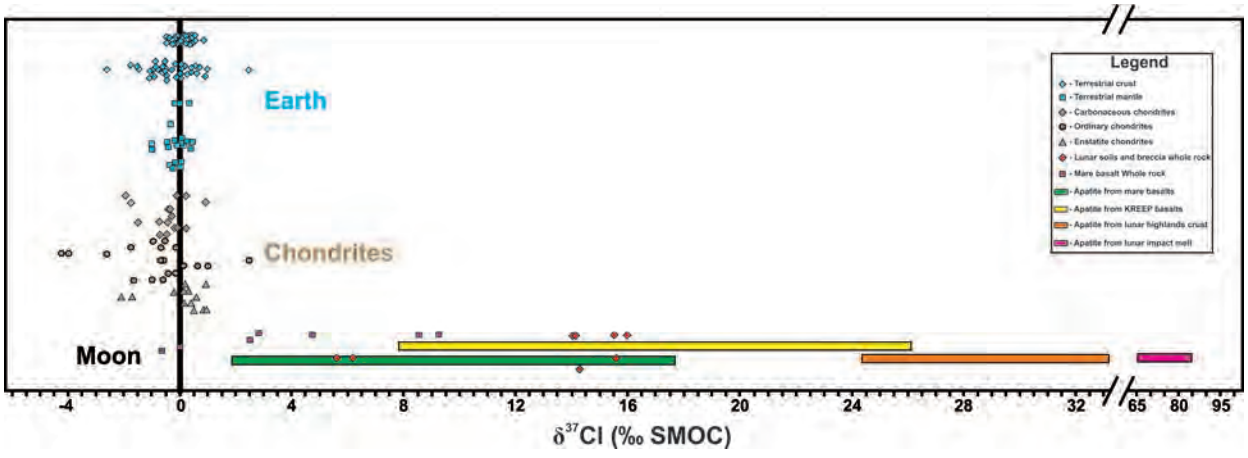

FIGURE 8. Chlorine isotope composition (reported as $\delta^{37}Cl$) of terrestrial, chondrite, and lunar samples. Data come from previously published studies (Boyce et al. 2013; McCubbin et al. 2012c; Sharp et al. 2010b, 2013b; Wang et al. 2012). Apatite data compiled for the present study is represented by a colored bar that indicates the full range of values for a given lunar rock type.

are consistent with a mass ratio F/La = ~1.0×10^{-2} × CI, or that urKREEP (using the bulk KREEP composition from Jolliff 1999; La at 1270 × CI) contains ~660 ppm F. Treiman et al. (2014) calculated the abundance of Cl in urKREEP to be ~150 ppm from the ratio of abundances of non-leachable Cl (Cl*) and P in KREEPy samples (Reed and Jovanovic 1981; Reed et al. 1972). These data imply that KREEP has a mass ratio Cl*/P = 0.018; for KREEP with 8850 ppm of P (Jolliff 1999), Cl* is ~150 ppm. Treiman et al. (2014) did not estimate H_2O abundances in urKREEP.

Estimates of urKREEP H_2O abundance from ferroan anorthosites. Hui et al. (2013) determined that the feldspar in FAN 60015 had 6 ppm H_2O, and reported that the melt from which the FAN formed had approximately 1600 ppm H_2O, using a mineral-melt partition coefficient for H_2O in plagioclase of 0.004. Hui et al. (2013) concluded that the initial LMO liquid would have had ~320 ppm H_2O and that the urKREEP liquid would have had up to 1.4 wt% H_2O, however we caution that these estimates are at the high end of all other estimates for the water content of the bulk Moon (Elkins-Tanton and Grove 2011; McCubbin et al. 2010b; Sharp et al. 2013a; Tartèse et al. 2013; Taylor et al. 2006a). Hui et al. (2013) did not estimate abundances of F or Cl.

Estimates of urKREEP F, Cl, and H_2O abundances from highlands apatite and lunar soil. Combining all three of these estimates, there is a discrepancy between the estimated abundances of F (660 ppm), Cl (150 ppm), and H_2O (1.4 wt%) in urKREEP and the relative abundances that were determined from highlands apatite (on average, Cl > H_2O ≈ F). Of the volatile elements F, Cl, and H, F is the least susceptible to volatilization (Aiuppa et al. 2009; Colson 1992; Ustunisik et al. 2011, 2015; Webster and Rebbert 1998) that would occur during the thermal processing of lunar megaregolith formation. Consequently, F is least likely to be redistributed in comparison to H and Cl. Furthermore, only the non-leachable Cl was used to estimate the Cl content of urKREEP by Treiman et al. (2014). Therefore, the F estimate in urKREEP by Treiman et al. (2014) is the most likely candidate to be a robust estimate for F abundance in urKREEP, whereas the estimate of Cl may be too low. The estimate of H_2O in urKREEP (1.4 wt% by Hui et al. 2013) has large uncertainties given (1) how little we know regarding an appropriate mineral-melt partition coefficient for H_2O in anorthitic plagioclase under lunar conditions, (2) the uncertainty in the point at which FAN sample 60015 crystallized from the LMO, and (3) the possibility of post-crystallization redistribution of H into or out of the anorthitic plagioclase over the last ~4.35 Ga.

Here we propose a refined estimate for the volatile abundance of urKREEP that combines the F estimate of Treiman et al. (2014) with the information on volatile abundances in highlands Mg-suite apatite (Barnes et al. 2014; Elardo et al. 2012; McCubbin et al. 2011, 2012c) using available apatite-melt partitioning data (Mathez and Webster 2005; McCubbin et al. 2015; Webster et al. 2009). From this combination of methods, we find that the urKREEP liquid would have had 660 ppm F, 1100–1350 ppm Cl, and 300–1250 ppm H_2O. The large range in H_2O abundance is related to the observed variability among H_2O abundances in Mg-suite apatites and the F value is adopted from Treiman et al. (2014). These values are substantially lower than the estimates from Hui et al. (2013), but they are consistent with other independent estimates for the water content of the Moon (Elkins-Tanton and Grove 2011; McCubbin et al. 2010b).

Volatile abundances of the lunar mantle. The volatile abundances of the lunar mantle have primarily been estimated from two sample types: the pyroclastic volcanic glasses and apatites within mare basalts. Both the glasses and mare basalts are believed to have been ultimately derived by partial melting of the over-turned hybridized cumulate lunar mantle, so the volatile abundances of those melts may tell us something about the magmatic source regions from which they melted, provided the abundances and ratios of the volatiles have not been affected by secondary processes.

Estimates of F, Cl, and H_2O in the lunar mantle from apatite in mare basalts. McCubbin et al. (2011) used the apatites from mare basalts to determine the relative abundances of H_2O, F, and Cl in the mare source regions using a relative volatile abundance diagram derived by experimental data on apatite-melt partitioning for F, Cl, and H_2O, which was later refined by McCubbin et al. (2013). We have updated this plot to include more recent mare basalt apatites from the literature (Elardo et al. 2014; McCubbin et al. 2010c; Tartèse et al. 2013) (Fig. 11b). Nearly all mare basalt apatites plot within the field indicating H_2O > F > Cl in mare basalt liquids, and McCubbin et al. (2011) argued that these relative abundances were inherited from the mare source region. Quantitative estimates of H_2O abundances of mare basalt parental magmas and their mantle source regions have also been attempted from the volatile contents of apatites in mare basalts (Boyce et al. 2010; McCubbin et al. 2010b; Tartèse et al. 2013, 2014b), although recent experimental data on the partitioning behavior of F, Cl, and OH between apatite and silicate melts have substantially changed the methods by which these calculations are conducted (McCubbin et al. 2015). Many previous studies have used estimates of Nernst-like mineral-melt partition coefficients for H_2O to determine the H_2O content of the silicate melt from which apatite formed and then back calculate to the parent melt by making some estimate of the degree of crystallization before phosphate saturation using the bulk rock P_2O_5 abundance (Barnes et al. 2014; McCubbin et al. 2010b, 2012c; Robinson et al. 2013; Tartèse et al. 2013, 2014a). However, Nernst-like partition coefficients do not adequately describe the partitioning behaviors of F, Cl, or OH between apatite and silicate melt because all three components are essential structural constituents in apatite and hence controlled by stoichiometric constraints. McCubbin et al. (2015) and Boyce et al. (2014) demonstrated that the partitioning of F, Cl, and OH between apatite and melt can be modeled as exchange equilibria, which indicate relatively constant ratios of D values for F, Cl, and OH. Using the example of F and OH (reported as the component H_2O), the exchange K_d equation takes the form

$$K_{d_{H_2O\text{-}F}}^{\text{Ap-Melt}} = \frac{X_F^{\text{Melt}} \div X_F^{\text{Ap}}}{X_{H_2O}^{\text{Melt}} \div X_{H_2O}^{\text{Ap}}} \quad (2)$$

where $K_{d_{H_2O\text{-}F}}^{\text{Ap-Melt}}$ is the OH-F apatite-melt exchange coefficient, X_F^{Melt} is the wt% F in the melt, X_F^{Ap} is the wt% F in the apatite, $X_{H_2O}^{\text{Ap}}$ is the amount of H_2O in apatite (wt%), and $X_{H_2O}^{\text{Melt}}$ is the wt% H_2O in the melt. These exchange coefficients may change as a function of melt composition, pressure, temperature, apatite composition, and oxygen fugacity, so further experimental work is

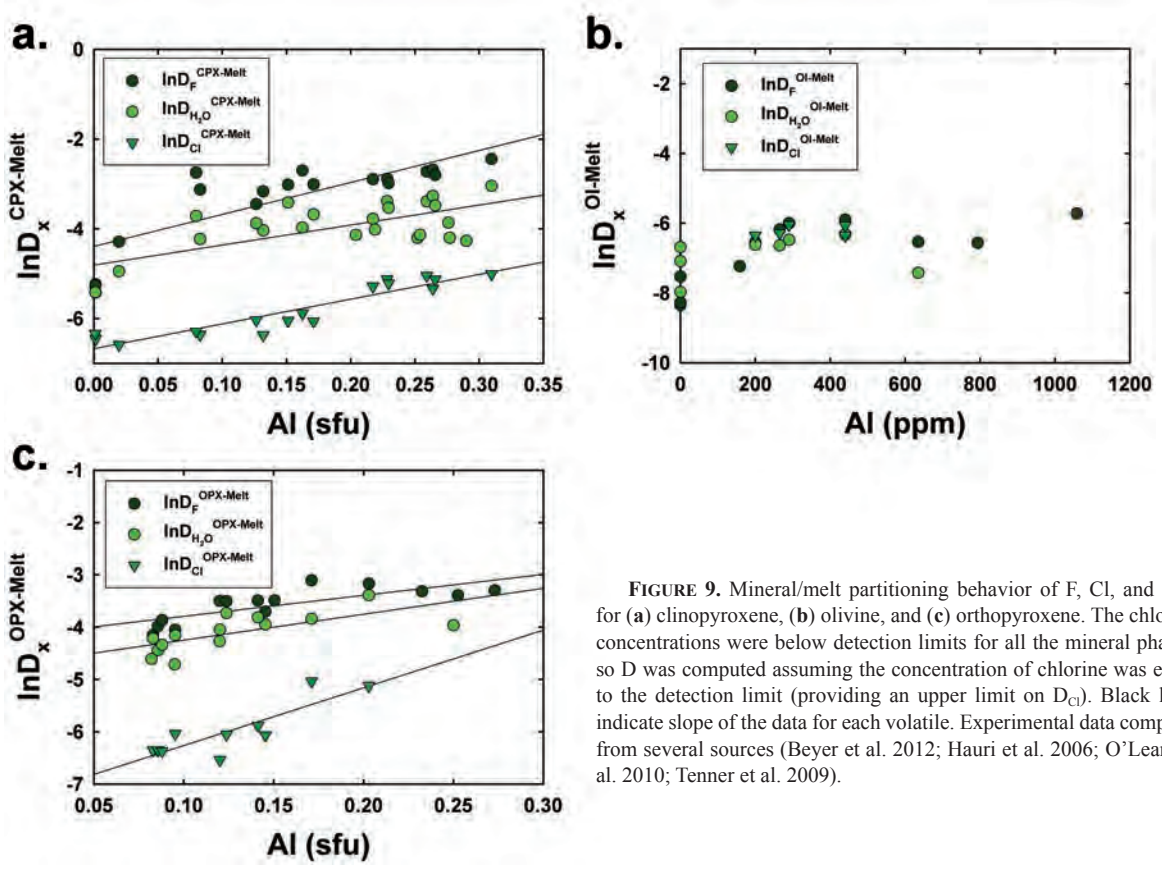

FIGURE 9. Mineral/melt partitioning behavior of F, Cl, and H_2O for (**a**) clinopyroxene, (**b**) olivine, and (**c**) orthopyroxene. The chlorine concentrations were below detection limits for all the mineral phases, so D was computed assuming the concentration of chlorine was equal to the detection limit (providing an upper limit on D_{Cl}). Black lines indicate slope of the data for each volatile. Experimental data compiled from several sources (Beyer et al. 2012; Hauri et al. 2006; O'Leary et al. 2010; Tenner et al. 2009).

needed to constrain these parameters. Furthermore, Pernet-Fisher et al. (2014) discussed additional complications related to the application of appropriate apatite-melt exchange coefficients in lunar samples that have experienced silicate-liquid immiscibility, which is yet another aspect of apatite-melt partitioning that requires additional experimental efforts.

Quantitative estimates of H_2O abundances of a mare basalt parental melt or mantle source region from apatite can be determined from the general batch melting equation, the appropriate exchange coefficient ($K_{d_{H_2O\text{-}F}}^{Ap\text{-}Melt} = 0.014$; McCubbin et al. 2015), the fluorine abundance of the bulk rock (18–78 ppm F; Haskin and Warren 1991), and the degree of partial melting that occurred in the source (assumed to be 3–10%), which are all non-trivial tasks that typically add a substantial amount of uncertainty to any quantitative estimate of volatile abundances in parental melts or source regions from apatite. Consequently, we have a fairly large range of F, Cl, and H_2O estimates for the lunar mantle from apatite (Table 4).

Estimates of volatiles in the lunar mantle from pyroclastic volcanic glasses. Given the uncertainties in the modeling of diffusive degassing in the degassed volcanic glass beads, we did not attempt to estimate the abundances of volatiles in the green glass source region. We also did not attempt to determine the volatile abundances for the red or yellow glasses because they have also experienced degassing (Hauri et al. 2015). However we have estimated the volatile abundances of the Apollo 17 orange glass source region from analyses of olivine-hosted melt inclusions within 74220 (Hauri et al. 2011). Assuming that the high-Ti melts formed by 3 to 10% partial melting, the orange glass source has 9–130 ppm H_2O, 2–11 ppm F, 57–250 ppm S, 0.034–0.24 ppm Cl, and 0.014–0.57 ppm C (Table 4). These values were estimated using the bulk distribution coefficients for H_2O, F, S, and Cl in Hauri et al. (2011). The C abundance was estimated using C solubility data in silicate liquids from Hirschmann and Withers (2008) and Ardia et al. (2013) as well as an estimated oxygen fugacity of the orange glass of –0.6ΔIW from Sato (1979), all of which point toward the orange glass being undersaturated with respect to graphite, and therefore graphite did not remain in the source after partial melting.

Summary of volatiles in the lunar mantle. Both apatites and volcanic glasses indicate that the relative abundance of volatiles in the lunar mantle is $H_2O > F > Cl$ (Hauri et al. 2011, 2015; Saal et al. 2008), indicating that this is an inherent geochemical characteristic of the lunar mantle. The lunar mantle also appears to be heterogeneous with respect to its abundances of volatiles, with H_2O varying from hundreds of parts per billion to approximately 100 ppm. Consequently, it is difficult to draw wide conclusions about the abundances of volatiles in the lunar interior from a single sample or set of analyses. An additional consistent observation between apatite and glass data sets is the depletion of Cl compared to F and H_2O in the lunar mantle, although the depletion in the glasses is more distinct. The Cl depletion in the lunar mantle is a potentially important observation that is consistent with the scenario in which the volatile abundances of the lunar mantle are primarily controlled by the F, Cl, and OH partitioning behavior between melt and nominally

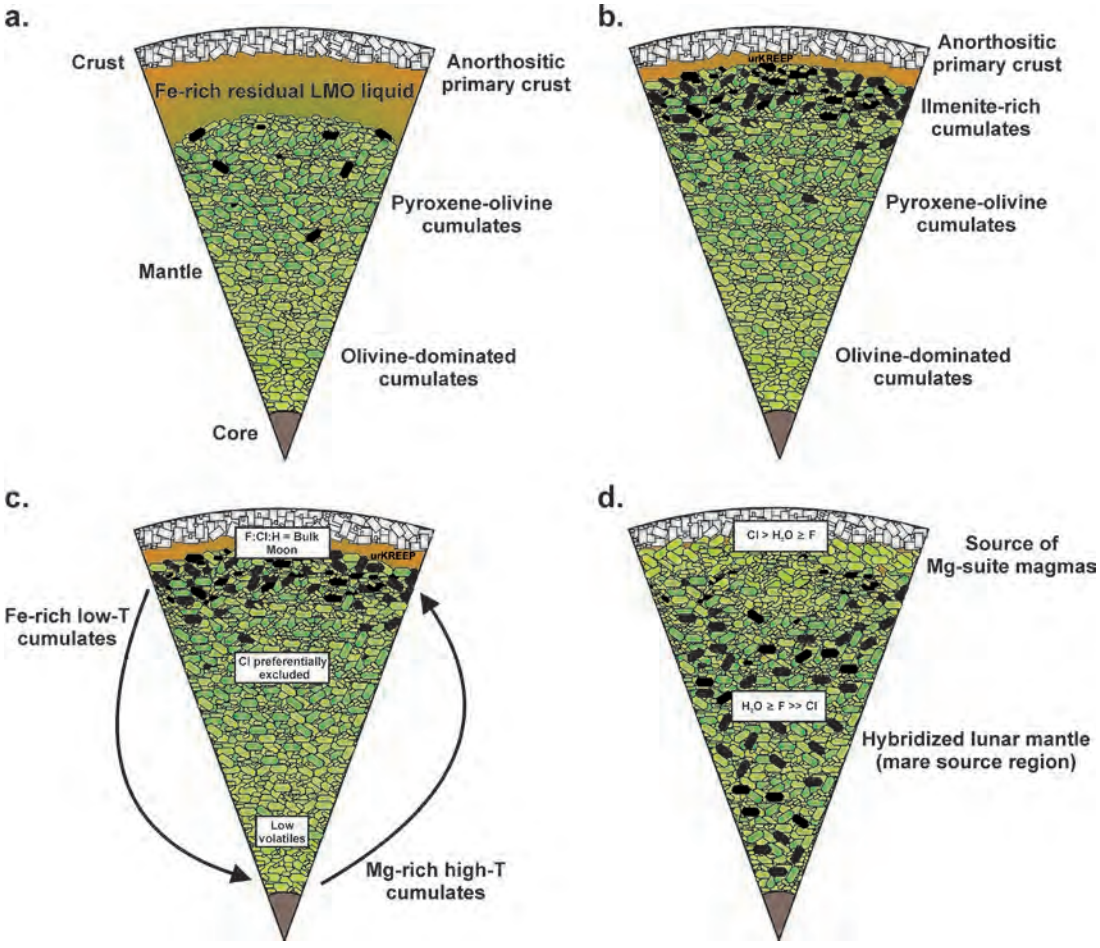

FIGURE 10. Cartoon illustrating the late stages of crystallization of the lunar magma ocean (LMO) and subsequent overturn to produce the source regions for the mare volcanics and the highlands magnesian suite. Relative abundances of F, Cl, and H are indicated pre- and post-overturn of the LMO cumulate pile: (**a**) formation of primary anorthositic floatation crust, (**b**) formation of the ilmenite-rich cumulate layer and urKREEP liquid, (**c**) density instability in the layered LMO cumulate pile with information concerning the distribution of lithophile magmatic volatile elements (F, Cl, H), and (**d**) final state of the lunar interior with the hybridized lunar mantle and the juxtaposition of Mg-rich olivine-dominant LMO cumulates with anorthositic crust and urKREEP that make up the source for the magnesian suite magmas. Relative abundances of F, Cl, and H indicated for the hybridized mantle and magnesian suite source.

anhydrous LMO phases. The S abundance of the lunar mantle has not been refined beyond the estimates from the bulk rock mare basalts (38–924 ppm) and the pyroclastic glasses (57–250 ppm). We do not estimate the abundance of C in the bulk lunar mantle due to a paucity of data, but the single sample for which data have been reported (Wetzel et al. 2014) indicates the lunar mantle has 0.014–0.57 ppm carbon (Table 4).

Abundances of F, Cl, and H_2O in the bulk silicate Moon. Estimates of the volatile abundances of urKREEP and the lunar mantle provide important constraints for determining the volatile abundances of the BSM. Most striking, is the difference in relative abundances of Cl, F, and H_2O between urKREEP and the lunar mantle. The lunar mantle seems to be consistently depleted in Cl compared to F and H_2O, whereas urKREEP is enriched in Cl compared to F and H_2O. This difference is exactly what was predicted from a scenario in which the cumulate lunar mantle volatile abundances were primarily controlled by the partitioning relationships of F, Cl, and H_2O between nominally anhydrous pyroxenes and LMO liquid. Consequently, the volatile abundances of the pyroxene-rich portions of the lunar mantle are not likely controlled by the amount of instantaneous trapped residual liquid in the cumulate, although quantitative limits on the amount of instantaneous trapped residual melt in the cumulate lunar mantle require additional modeling efforts, which we discuss below.

If the abundances of volatiles in the lunar mantle are controlled by nominally anhydrous mineral phases, one should be able to take the volatile content of urKREEP and reproduce the bulk lunar mantle using models of LMO crystallization and known partitioning relationships for F, Cl, and H_2O between nominally anhydrous LMO minerals and silicate melt. Consequently, we use the urKREEP composition from the present study that was derived from the F abundances in lunar soil and relative volatile abundances of highlands apatite (LSHA in Table 2) to estimate the bulk lunar mantle abundances of F, Cl, and H_2O, to compare with sample-based estimates.

Estimates for F, Cl, and H_2O in the lunar mantle were com-

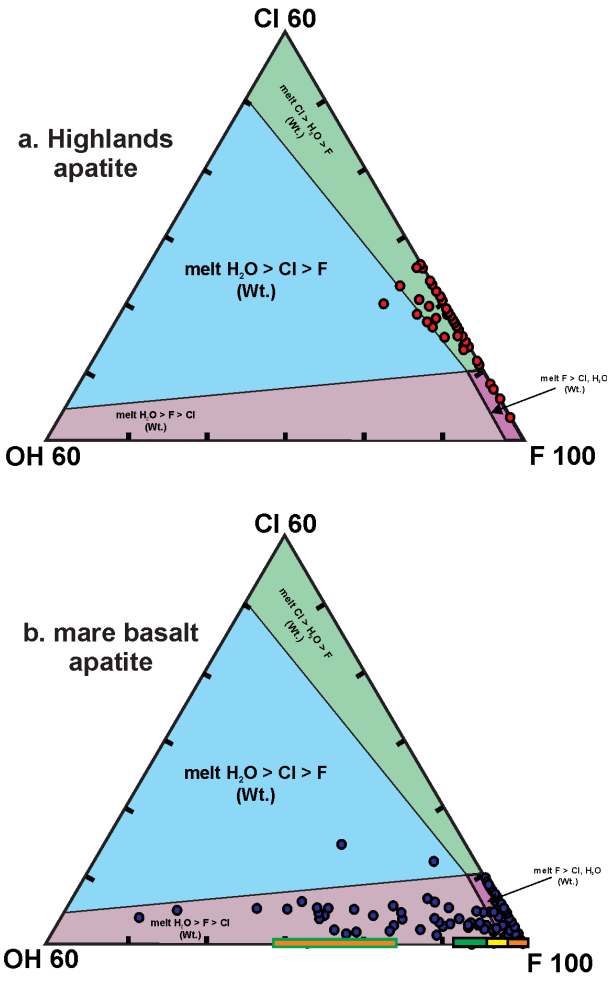

Figure 11. Truncated ternary plot of apatite X-site occupancy (mol%) from (**a**) highlands apatite. (**b**) Mare basalt apatite plotted on the relative volatile abundance diagram from McCubbin et al. (2013). In addition to apatite compositions from mare basalts, rectangular fields representing the apatite compositions that would be in equilibrium with the picritic glasses were also computed, using glass data from Hauri et al. (2015) and the apatite-melt partitioning model of McCubbin et al. (2015). The rectangular fields were color-coated based on the color of the picritic glass, and the olivine-hosted melt inclusions in the orange glass sample 74220 are represented by an orange field within a green rectangle. The solid black lines delineate fields of relative abundances of F, Cl, and H_2O (on a weight basis) in the melt from which the apatite crystallized. The diagram was constructed using available apatite/melt partitioning data for fluorine, chlorine, and hydroxyl (McCubbin et al. 2015).

puted based on LMO crystallization modeling results from Elardo et al. (2015). The LMO crystallization modeling from Elardo et al. (2015) was conducted using the FXMOTR program, which was used to simulate bottom-up fractional crystallization of an LMO, assuming that the entire silicate portion of the Moon participated in primordial differentiation. The FXMOTR program is based on the MAGFOX and MAGPOX programs designed by Longhi (1991, 1992b, 2006) that have been adapted for MATLAB by Davenport et al. (2014). The calculations simulated crystallization in 1% intervals of a 1060 km (4 GPa) LMO with a lunar primitive upper mantle (LPUM) bulk composition proposed by Longhi (2003, 2006), which likely represents the best estimate for the bulk composition of the Moon based on geochemical and crustal thickness constraints (Warren et al. 2005; Wieczorek et al. 2013). LMO mineral compositions and modal abundances within the LMO cumulate pile were obtained from the FXMOTR output files and are in general agreement with previous results of LMO crystallization products from modeling and experiments (e.g., Elardo et al. 2011; Elkins-Tanton et al. 2002, 2003a; Elkins-Tanton and Grove 2011; Snyder et al. 1992). These LMO mineral compositions were used to compute appropriate distribution coefficients for F and H_2O during LMO crystallization for each portion of the cumulate pile using the modal mineral abundances from the LMO crystallization modeling and available partition coefficients for H_2O and F between primary LMO minerals (mainly olivine, orthopyroxene, and clinopyroxene) and silicate melt (Aubaud et al. 2004; Beyer et al. 2012; Hauri et al. 2006; O'Leary et al. 2010; Tenner et al. 2009; Fig. 9). Equations for the partition coefficients used in the present study are available in the online supporting material (Supplementary Table 5[1]). Partition coefficients for Cl could not be determined because Cl was typically below detection in the nominally anhydrous minerals in the experimental studies from which F and H_2O data were obtained, so we used the upper bound of the bulk D value for Cl (0.00015) estimated by Hauri et al. (2015). There is a paucity of high-quality experimental data on the partitioning of F, Cl, and H_2O between oxide-melt and plagioclase-melt systems, so we did not include either of these minerals in the bulk distribution coefficients for F, Cl, and H_2O used in the LMO modeling. The amount of liquid trapped within the cumulate pile during LMO crystallization also plays an important role on the abundances of volatiles in the mantle source, so we conducted our calculations over a range (0, 0.1, 0.5, 1, 2, 2.5, 3, 4, and 5%) of values for the amount of instantaneous trapped residual liquid in the cumulate pile. Additional details of the calculations are provided in the online supporting material (Supplementary Tables 2–5[1]).

Using the LSHA urKREEP estimate (Table 4), the lunar mantle could have had at most 1% residual liquid trapped within the cumulate pile during LMO crystallization and still maintain the observed relative abundance differences between F, Cl, and H_2O between mare and urKREEP sources. This amount of trapped liquid implies very efficient removal of residual liquid during compaction of the cumulate lunar mantle, which has been seen on smaller scales in some terrestrial mafic intrusions (e.g., Holness et al. 2007; Schmidt et al. 2012) and is consistent with at least some estimates from LMO crystallization modeling (Elkins-Tanton et al. 2011; Elkins-Tanton and Grove 2011; Snyder et al. 1992). Assuming 0.5% trapped interstitial liquid in the cumulate pile, the LSHA urKREEP composition from Table 4 implies a cumulate lunar mantle with 0.54 ppm F, 0.15–0.61 ppm H_2O, and 0.26–0.32 ppm Cl and a bulk silicate Moon (BSM) composition with 7.1 ppm F, 3.1–13.1 ppm H_2O, and 11.3–13.8 ppm Cl. The S abundance of the BSM was recently estimated in a review paper by Hauri et al. (2015), using much of the same data discussed herein, and we adopt their value of 78.9 ppm S (Table 4). Furthermore, although there is very little reliable data on indigenous C in the lunar interior, we adopt the mantle estimates determined from the

analysis of C in olivine hosted melt inclusions from sample 74220 as the best range for the C content of the BSM (Table 4). These estimates highlight the importance of including the lunar crust within estimates of the volatile abundances of BSM because it is the primary host for incompatible lithophile elements, which are not mixed back into the mantle by processes like plate tectonics that operate on Earth. Hence estimates of incompatible lithophile volatiles in BSM that use only products of mare volcanism will be missing a substantial portion of the lunar volatile budget. In addition, the estimates for H_2O in the lunar mantle from this modeling are lower than most of the estimates for the lunar mantle abundances from mare basalts, apatites in mare basalts, and pyroclastic glasses (Table 4), indicating that the water abundance estimates from these materials may have been biased toward the "wettest" samples. However, the F abundances are also depleted relative to most of the mantle estimates in Table 4, indicating that the LSHA urKREEP composition may be underestimating the actual volatile abundances of urKREEP. The estimated abundances of F, Cl, and H_2O in LSHA urKREEP requires that F was not mobilized during thermal processing of the lunar soils, a tenuous assumption at best given that F is a demonstrably vapor-mobile element (e.g., Aiuppa et al. 2009; Ustunisik et al. 2011, 2015). Importantly, the discrepancy between the predicted abundances of F, Cl, and H_2O in the lunar mantle from LSHA urKREEP and the actual estimates from lunar samples indicates that additional work is required to determine the abundances of volatiles in the lunar interior. We discuss a potential upper limit to the volatile abundances of the lunar interior in the following section.

Upper limit estimates of F, Cl, and H_2O in BSM from highlands apatite and CI chondritic F abundances in BSM. One can place an upper bound on the Cl and H_2O abundances in BSM and the abundances of F, Cl, and H_2O in the lunar mantle and urKREEP by assuming a fluorine abundance in the primordial bulk Moon equivalent to that of CI carbonaceous chondrites, which is approximately 60 ppm (Lodders and Fegley 1998). Using an estimate of BSM F abundances derived from CI carbonaceous chondrite and relative F, Cl, and H_2O abundances from highlands apatite (CFHA), the BSM would have 60 ppm F, 27–114 ppm H_2O, and 100–123 ppm Cl, and we refer to this as the CFHA BSM (Table 4). Using the same LMO modeling methods and parameters described above for the LSHA urKREEP composition, we determined the abundances of F, Cl, and H_2O in the cumulate lunar mantle and urKREEP liquid using the CFHA BSM values for F, Cl, and H_2O. Using the CFHA BSM estimate (Table 4), the lunar mantle could have had up to 1% residual liquid trapped within the cumulate pile during LMO crystallization and still maintained the observed relative abundance differences between F, Cl, and H_2O between mare and urKREEP sources. This amount of trapped liquid is the same value estimated for the LSHA urKREEP estimate. Assuming 0.5% trapped interstitial liquid in the cumulate pile, the CFHA cumulate lunar mantle would have 4.5 ppm F, 1.2–5.3 ppm H_2O, and 2.3–2.9 ppm Cl (Table 4). Furthermore, the CFHA urKREEP liquid would have had 5548 ppm F, 0.26–1.09 wt% H_2O, and 0.98–1.20 wt% Cl.

Although low, the estimates for F, Cl, and H_2O in the lunar mantle using CFHA BSM are within the observed ranges of F, Cl, and H_2O abundances in the lunar mantle from mare basalts, apatites in mare basalts, and the pyroclastic glasses (Table 4). Importantly, these estimates should be considered reasonable upper limits for the abundances of volatiles in the lunar mantle, as the Moon is not likely to have superchondritic abundances of the moderately volatile element F. The estimates for F, Cl, and H_2O in the mantle are still much lower than many of the other estimates for the abundances of F, Cl, and H_2O in the bulk lunar mantle, lending further support to the idea that many of the estimates for H_2O abundances in the lunar mantle have been biased toward the "wettest" samples.

TABLE 4. Computed volatile abundances for various reservoirs/source regions within the lunar interior

Lunar reservoir	Basis of estimate	H_2O[a]	F[a]	Cl[a]	C[a]	S[a]
Mantle	74220: Olivine-hosted melt inclusion within orange glass	9–130	2–11	0.034–0.24	0.014–0.57	57–250
	Bulk rock mare basalts	0.3–11	1.1–12	0.009–2.8	–	38–924
	10058: Apatite	9–28	4–20	–	–	–
	12039: Apatite	16–51	4–10	–	–	–
	15058: Apatite	1–4	2–12	0.9–3	–	–
	15555: Apatite	10–30	2–10	–	–	–
	MIL 05035: Apatite	8–26	0.56–6	–	–	–
	LAP 04841: Apatite	53–166	4.5–19	2–6	–	–
	10044: Apatite	5–15	2–13	–	–	–
	75055: Apatite	4–13	3–9	–	–	–
	14053: Apatite	8–26	4.5–15	–	–	–
	12064: Apatite	2–7	1–6	–	–	–
	Bulk lunar mantle from CFHA & 0.5% ITL[c]	1.2–5.3	4.5	2.3–2.9	-	-
	Bulk lunar mantle from LSHA & 0.5% ITL[c]	0.15–0.61	0.54	0.26–0.32	-	-
urKREEP	Lunar soils[d]	–	660	150	–	–
	Lunar soils and highlands apatite (LSHA)	300–1250	660	1100–1350	–	–
	Ferroan anorthosite[e]	1.4 wt%	–	–	–	–
	Chondritic F and highlands apatite (CFHA)	0.26–1.09 wt%	5548	0.98–1.20 wt%	–	–
Bulk silicate Moon	Primordial bulk silicate moon[f] CFHA	27–114	60	100–123	0.014–0.57	78.9[b]
	Primordial bulk silicate moon[f] LSHA	3.1–13.1	7.1	11.3–13.8	0.014–0.57	78.9[b]

[a] Values presented in parts per million unless otherwise noted.
[b] Adopted from Hauri et al. (2015).
[c] ITL = Instantaneous trapped liquid within the cumulate pile.
[d] From Treiman et al. (2014).
[e] From Hui et al. (2013).
[f] Bulk silicate Moon as defined by the sum of the volatile abundances of the lunar mantle and crust (represented by urKREEP).

Alternatively, the estimates of H_2O in the mare source have been robust, but they are representative of individual source regions in a heterogeneous lunar mantle that are not representative of the drier bulk lunar mantle. This later scenario is not unreasonable, given that melting processes in the lunar interior were likely biased toward the wettest source regions given the depression of solidus temperatures of silicate systems that accompany the addition of H_2O. The CFHA estimates for urKREEP are similar to estimates of the H_2O content of urKREEP from Hui et al. (2013), but they are typically much higher than other quantitative estimates for F, Cl, and H_2O abundances in urKREEP (Elkins-Tanton and Grove 2011; McCubbin et al. 2010b; Treiman et al. 2014). These estimates are based on an improbable abundance of F, so additional work is required to determine the true depletion factor of F in the bulk Moon relative to chondrites. If a concerted effort is made to constrain the abundance of F in BSM, Cl and H_2O can be estimated using the techniques employed herein.

Isotopic compositions of H and Cl in the lunar interior. Much of the isotopic data for mare basalts and highlands rocks are from δD and $\delta^{37}Cl$ in bulk rocks, volcanic glasses, and apatites. The volatile isotopic composition of urKREEP comes exclusively from apatites in highlands rocks, whereas the mare volcanics include apatites, glasses, and whole rocks analyses. The origin of H isotopic compositions in volcanic lunar materials is currently a topic of much debate. Highlands rocks apatites that have water contents sufficiently high to prevent being dominated by spallogenic D generally have δD values between –200 and +400‰ (Fig. 6). Some have speculated that the lower end of this range (e.g., ~ –200 to +100‰) could correspond to the approximate δD value for urKREEP/the bulk Moon (Barnes et al. 2014; Saal et al. 2013; Tartèse and Anand 2013), but additional work is required to confirm this hypothesis. Mare basalt materials seem to span a wide range of δD from about –200 to >+1000‰ (Fig. 6), and some single samples exhibit several hundred per mil variations (Greenwood et al. 2011; Saal et al. 2013; Tartèse et al. 2013). This range in δD has either been attributed to degassing of H_2 (Saal et al. 2013; Sharp et al. 2013a; Tartèse and Anand 2013; Tartèse et al. 2013) or originating from mixing with a D-enriched reservoir in the lunar interior that originated from comets (Greenwood et al. 2011). Neither of these explanations can fully account for the range in measured δD values, and consideration of additional possibilities such as the role of solar-wind and cosmogenic spallation processes necessitates continued focused efforts to achieve greater insights into this problem. To illustrate a few complicating scenarios, it is known that there is a very light (–1000‰) SW reservoir in lunar surface materials, and this H could potentially interact with lunar lavas upon eruption. Furthermore, spallogenic D, especially from mature soils, is an additional potential source of contamination to lunar lava (Stephant and Robert 2014). Contamination from either of these sources could change the original δD value of a sample in either direction, which could complicate estimates of the indigenous δD signature of the lunar mantle. The best samples for assessing the D/H signature of the lunar mantle to date may be the olivine-hosted melt inclusions in the pyroclastic glasses such as those analyzed by Hauri et al. (2011) and Saal et al. (2013). Saal et al. (2013) showed that the lunar mantle was similar to CI carbonaceous chondrites and had a δD value similar to, but slightly heavier than, the bulk Earth (Halliday 2013; Lecuyer et al. 1998; Marty 2012). Olivines are not completely closed systems with respect to H, so the δD values from Saal et al. (2013) could have possibly been affected by degassing from or contamination into the melt inclusions. However, before a consensus can be reached regarding the true indigenous δD signature of the lunar mantle, further studies that focus on the textural context and timing of crystallization and closure of phases being analyzed for H isotopes are required.

Apatites from mare basalts display a wide range of $\delta^{37}Cl$ that start near terrestrial values (+2‰) and extend up to about +18‰. When the whole rock and volcanic glass analyses are also included, the mare materials extend down to –0.7‰ (Fig. 8), which Sharp et al. (2010b) argued reflects the Cl isotopic composition of the lunar mantle source, noting that it is indistinguishable from Earth and chondrites (Sharp et al. 2007, 2013b). All of the apatites in highlands rocks are highly fractionated with respect to $\delta^{37}Cl$ ($\delta^{37}Cl > +25$‰), indicating that urKREEP may constitute a heavy reservoir within the Moon. This seems to be further supported by Cl isotopic data on KREEP basalts that have an intermediate range in $\delta^{37}Cl$ values, consistent with them being a mixture of both mare and KREEP reservoirs (+9 to +27‰; Fig. 8). Speculation as to what could be responsible for this heavy urKREEP reservoir is premature, but it represents an important area of future research efforts.

Volcanic processes involving lunar volatiles

High-temperature alteration involving lunar volatiles. On Earth, hydrothermal alteration is the most common form of volatile-based alteration and it commonly results in the formation of a wide range of hydrothermal minerals and alteration products like phyllosilicates, serpentine, ferric oxide, sulfates, and more. Given the low oxygen fugacity on the Moon, and the paucity of liquid water or H_2O vapor, volatile-driven alteration is likely to have a completely different style than what we see on Earth.

Origin of volatiles in the "Rusty Rock" 66095. The Apollo 16 breccia 66095 (better known as the "Rusty Rock") has been the subject of much debate regarding the origin of its volatiles and oxidation. Taylor et al. (1973, 1974) concluded that the origin of the rust was oxidation and hydration of $FeCl_2$ (lawrencite) and that this alteration occurred in the Apollo crew cabin and/or on Earth. Taylor et al. (1973, 1974) provided very insightful arguments for terrestrial alteration that are still sagacious. They demonstrated in an experimental study that a mixture of $FeCl_2$ + Fe (initially 200 μm in diameter) would be converted to akaganéite over a two day period of time at a relative humidity of 60–70% and a temperature of 25 °C. Iron and lawrencite would be consumed via the reaction

$$FeCl_2 + Fe + 2H_2O + O_2 \leftrightarrow 2\beta FeO(OH) + 2H^+ + 2Cl \quad (3)$$

The higher amount of volatile-rich phases such as $FeCl_2$ would have contributed to the high degree of "rusty" alteration. Furthermore, Taylor and Burton (1976) illustrated that at particular lunar surface conditions (140 °C and 10^{-7} torr) akaganéite undergoes dehydration to an amorphous compound and crystallizes to maghemite (γFe_2O_3) with additional annealing. Epstein and Taylor (1971, 1974) observed that H and O isotopic compositions in water released from 66095 were similar to that of the Earth. Furthermore, water released from 66095 below 200 °C had an

isotopic composition overlapping atmospheric water vapor in Pasadena. However, Shearer et al. (2014) pointed out several observations that are not consistent with this oxidation-hydration being solely non-lunar: (1) the occurrence of stanfieldite in 66095 that was produced through the subsolidus oxidation of Fe-Ni-P metal + Ca-Fe-Mg-bearing silicates suggests that this rock was exposed to an oxidation process on the Moon; (2) the penetration of alteration into the interior of 66095 suggests that the alteration is not a result of simple and rapid terrestrial surface alteration; (3) there appears to be a systematic stratigraphy associated with this alteration; (4) the alteration of metal, akaganéite, and lawrencite to goethite + hematite display distinct morphological differences between akaganéite and the newly formed goethite + hematite, which suggests different episodes of FeOOH formation (Moon and Earth); (5) observations from numerous missions indicate that H-bearing species occur on or near the lunar surface (Clark 2009; Colaprete et al. 2010; Pieters et al. 2009; Sunshine et al. 2009); (6) recent studies of exchange of water vapor between goethite and the atmosphere illustrate the complexity of the exchange process and preserving original isotopic values in FeOOH phases. Therefore, the H/D of the akaganéite and its terrestrial alteration products may reflect exchange of H species with terrestrial environments and not the formation of terrestrial akaganéite.

Shearer et al. (2014) suggested that the lawrencite in 66095 may have formed within a fumarole system associated with an ejecta blanket. In this case, they suggested that the lawrencite may condense from distinctly different gas compositions and processes that dramatically influence metal transport on the Moon. In a gas that transports both chlorine and metals, lawrencite would condense through the reaction:

$$FeCl_2(g) \leftrightarrow FeCl_2(s) \quad (4)$$

The $FeCl_2(g)$ component occurs in terrestrial volcanic gases, but usually condenses to form iron sulfides via the reaction:

$$FeCl_2(g) + 2H_2S \leftrightarrow FeS_2(s) + 2HCl(g) + H_2(g) \quad (5)$$

(Symonds et al. 1987). With direct condensation of $FeCl_2(s)$ from lunar gases, Colson (1992) calculated that at temperatures between 650 and 570 °C over 90% of the $FeCl_2(g)$ would be removed from the gas. Alternatively, in the case that the gas in the fumarole system does not contain metal chlorides, but does contain other Cl-bearing species (e.g., HCl, PCl_3, $POCl_3$) (Symonds et al. 1987), the lawrencite forms through the reaction between Fe-Ni alloy or FeS and the gas:

$$Fe(s) + 2HCl(g) \leftrightarrow FeCl_2(s) + H_2(g) \quad (6)$$

This would account for the close spatial relationship between the lawrencite and Fe-Ni alloy and implies that this type of thermal system does not transport metal species in gas.

Origin of sulfide-rich veining in lunar samples. There are several documented occurrences in the Apollo collection of impact breccias or crustal samples that exhibit replacement textures and exotic mineral assemblages. Five such examples include 67016,294 and 67016,297, which are feldspathic fragmental breccias, 67915,150, which is a feldspathic polymict breccia, 76535, which is a highlands Mg-suite troctolite, and 76255, an Mg-suite gabbronorite (Elardo et al. 2012; Shearer et al. 2012, 2015). There have been numerous reports of sulfide replacement textures in these rocks, including troilite veining and sulfide-pyroxene intergrowths, which are wormy or vermicular in texture (Elardo et al. 2012; Lindstrom and Salpas 1983; Norman 1982; Norman et al. 1995; Shearer et al. 2012; Figs. 1e–1f). The replacement textures and assemblages are thought to have been formed by interaction of the rock with S-rich magmatic fluids (Norman et al. 1995), while impact-related exogenous S was added through circulation in ejecta blankets (Elardo et al. 2012; Haskin and Warren 1991).

Origin of volatile-rich coatings on volcanic glass beads. The general consensus as to the origin of these coatings is that they condensed to the surface of the glass droplets from a volcanic vapor phase present during lunar pyroclastic eruptions on the Moon. Morgan and Wandless (1979) suggested the enriched siderophile elements in the coatings on the lunar glasses came from an added meteorite component; however this theory was ruled out by Delano (1980) who showed the siderophile element signature from the lunar glasses is greater than that which could have been added by contamination of a IIB iron meteorite as proposed by Morgan and Wandless (1984). Several samples (as reported by McKay and Wentworth 1992) have lost some phases, have coarse mottled surfaces, and have had changes to the micromound textures due to their storage conditions since the return of the samples in the early 1970s. The majority of coatings are continuous, some with cracks and vesicles, typically a few micrometers or less in thickness, although micromounds on the sample surfaces can range from 3 to 5 nm thick (Clanton et al. 1978b; McKay and Wentworth 1993). The cracks and vesicles in the coatings have been attributed to shrinkage during cooling of the glass droplets, desiccation, or by evolution of the volatile species (Clanton et al. 1978b). McKay and Wentworth (1993) suggested the thicker the coating on a glass droplet, the longer time it spent in the plume after eruption or the higher the vapor-pressure experienced by the sample in the eruption cloud.

The chief propellant of the lunar fire-fountains. A substantial body of work has been produced with the aim of determining the volatile assistant that propelled the pyroclastic fire-fountain eruptions that produced an array of volcanic glass bead types. The presence and abundance of these volatiles as coatings on the lunar glass beads provides insight into the makeup of the vapor plume and gases associated with these pyroclastic eruptions. Of the volatiles discussed in the present study (H, C, N, F, S, Cl), only N has not yet been implicated as a probable propellant, and there is no evidence to suggest that it was N. Given the high amounts of S and Cl found on the surface of these glasses, Butler and Meyer (1976) suggest the volcanic vapors that drove the fire-fountaining eruptions most likely carried S_2 as well as chlorides or other elemental gases that could react on the surface of the beads to form sulfur-rich coatings. Meyer et al. (1975) suggested these volcanic vapors must have had Zn, Ga, Cd, Pb, and other elements found in the coatings that could be mobilized and also proposed an anhydrous sulfide, chloride, and fluoride rich vapor. Given most of the elements found on the surface are chalcophile in nature, Meyer et al. (1975) concluded

these elements may have originally been concentrated as sulfides during the formation of the source region. More recently, Elkins-Tanton et al. (2003b) have proposed that although most of the fire-fountain propellant was in a vapor phase, S cannot be the driving force in these eruptions from depth, despite it being the most abundant volatile in most mare basalts and mare volcanic glasses (Gibson et al. 1975, 1977; Hauri et al. 2011; Saal et al. 2008) because sulfur saturation increases with decreasing pressure. Alternatively, these authors favor, at least for the Apollo 15 glass beads, eruption driven by buoyancy and/or hydrostatic head, possibly with the aid of chlorine or fluorine degassing at depth. Based on the estimated abundances for Cl in mare source regions, it can be ruled out as the primary constituent, although its ubiquitous presence on glass bead coatings indicates it had to be present in the vapor. The affinity of F for the silicate melt likely rules it out as the primary propellant (Aiuppa et al. 2009), leaving H or C species as the prime targets. Many studies have implicated CO as the primary gas component, calling upon the oxidation of graphite at low pressure; however, graphite has never been found in lunar materials as an indigenous volcanic phase. It has been recently suggested that CO can dissolve directly into reducing magmas as iron-carbonyl [$Fe(CO)_5$, Wetzel et al. 2013], which removes the need for graphite in this argument, but there is no evidence to support elevated C abundances in mare magmas. Notably, the identification of iron-carbonyl in silicate liquids has recently come into question (Yoshioka et al. 2015). The olivine-hosted melt inclusions in the high-Ti pyroclastic glasses yielded 0.47–5.65 ppm C (Wetzel et al. 2014) (i.e., concentrations that are undersaturated with respect to graphite in the P-T-f_{O_2} conditions of the source; Ardia et al. 2013; Hirschmann and Withers 2008) despite being trapped in a melt inclusion, which prevented extensive degassing from occurring for H, F, S, and Cl (Hauri et al. 2011). Given all of the recent evidence for elevated H abundances in lunar magmas, a new effort has emerged to suggest H_2 as the primary propellant for the volcanic glasses (Sharp et al. 2013a; Vander Kaaden et al. 2015). H_2 has several advantages over the other candidate elements because its solubility is highly dependent on pressure and approaches insolubility at pressures of a few bars or less (Burnham 1994; Hirschmann et al. 2012; McMillan 1994; Stolper 1982a, 1982b). Furthermore, there is substantial evidence that H_2 was present in mare magmas, and that at least some magmas had over 1000 ppm H_2O (Hauri et al. 2011). Although not yet detected in volcanic glass coatings, the presence of H was required in the vapor phase to explain the precipitation of ZnS on some of the glass bead coatings (Bell et al. 2014; Colson 1992).

Post-crystallization diffusion of volatiles in apatite. Only one study investigated F-Cl-OH diffusive exchange in fluorapatite, and it was at 1 bar and 1 GPa (Brenan 1993). The data obtained by Brenan (1993) showed that volatile diffusion in apatite is (1) strongly anisotropic, being about three orders of magnitude faster parallel to the *c*-axis compared to diffusion along the *a*-axis at 1 bar; (2) about two orders of magnitude faster at 1 GPa than at 1 bar. From Brenan (1993), and considering a specific set of temperatures, initial cooling rate, and diffusion parameters, it is possible to explore the conditions for which apatite cores would be affected by re-equilibration of OH, F, and Cl by diffusion, according to the following relationship:

$$x = \sqrt{\frac{\mathrm{R} \cdot T_0^2 \cdot D(T_0)}{r_0 \cdot E_a}} \quad (7)$$

where x is the effective transport distance in m for a grain of spherical geometry, R is the gas constant, T_0 is the initial temperature in Kelvin, $D(T_0)$ is the diffusion coefficient at the initial temperature in m^2s^{-1}, r_0 is the initial cooling rate in Kelvin per second, and E_a is the activation energy (Brenan 1993). At 1 bar and for cooling rates typical of mare basalts, from 0.1 to 30 °C/h (Holness et al. 2012; Taylor et al. 1991), complete re-equilibration of volatiles in cores of apatite grains by diffusive exchange in mare basalts could only occur if grain radius is ≤10 μm and the magma experienced very slow cooling rates below 1 °C/h. It thus seems that mare basalt emplaced on the lunar surface cooled down too quickly to allow significant diffusive re-equilibration of the volatile elements OH, F, and Cl in apatites to have occurred.

In another study, Boyce and Hervig (2008) have shown that diffusion of halogens in apatite is an important process to consider before estimating magmatic OH, F, and Cl contents from apatite analysis, based on detailed measurements of OH, F, and Cl contents of apatite phenocrysts from the Cerro Galan ignimbrite (Argentina). Indeed, they showed that prolonged residence of apatite at high temperature around 800 °C induced diffusive mobility of volatiles in apatite. For mare basalts, eruption and emplacement of a new, hot, basaltic lava flow on top of an older, cold one would re-heat it, potentially initiating volatile diffusion in apatite grains. Numerical modeling carried out by Fagents et al. (2010) suggested that cooling of a 10 m thick basaltic flow emplaced at ~1200 °C on top of lunar regolith at ~ –50 °C takes about 5 to 15 yr, and that some of the heat is indeed transferred from the hot basaltic flow to the cold underlying unit over an order of a few meters. However, increase in temperature of the underlying unit does not exceed ~600 °C, which would probably be insufficient to cause substantial volatile diffusion from apatite grains that might be present in the underlying unit. Once the parent magma has crystallized and reached sub-solidus temperatures below ~800–900 °C, apatite appears to be closed to volatile diffusion. This observation is consistent with a study by Stormer and Carmichael (1971) that investigated the F-OH exchange between biotite and apatite in the altered Leucite Hills lavas. They observed that biotite exchanged F and OH with late-stage low-temperature aqueous fluids; however, apatite did not. Also, experiments carried out by Nadeau et al. (1999) on several specimens of F-rich apatites showed that ~80–90% of the water was released from apatite grains only after prolonged heating of ~10 to 50 h at a very high temperature of 1500 °C. The conditions required to devolatilize different apatite samples were correlated with grain size, suggesting that dehydration was controlled by a diffusive process, which thus appears to be very limited at low to moderate temperatures.

Possible effects of magmatic degassing on δD and δ^{37}Cl. For H isotopes, it is known that magmatic processes such as partial melting and crystallization have restricted effects on fractionation of H and D on the order of a few tens of permil (e.g., Bindeman et al. 2012). Another magmatic process at play during magma petrogenesis is degassing of volatile species. Whereas,

degassing of OH/H_2O results in very limited D/H fractionations (Kyser and O'Neil 1984; Newman et al. 1988; Taylor et al. 1983), the degassing of H-bearing species such as H_2, CH_4, or HCl, for example, strongly fractionates H from D (Richet et al. 1977; Sharp et al. 2013a; Tartèse and Anand 2013; Tartèse et al. 2013), leaving a D-enriched residual total H-component in the melt. Two important considerations arise when attempting to constrain the fractionation factor (α) involved in degassing calculations: (1) temperature-dependent H isotopic fractionation among gaseous molecules H_2O_t and H_2; (2) H isotopic fractionation due to pure kinetic degassing in a vacuum (i.e., Rayleigh fractionation). For the former, Richet et al. (1977) have calculated α as a function of temperature (α = 0.857–0.891 over the temperature range 900–1000 °C). For kinetic degassing in a vacuum, α is given by the square root of the ratio of the light and heavy isotopologs H_2 and HD (α = 0.866) and is independent of the temperature. Nevertheless, in both cases the values of α are similar and therefore either scenario is suitable for the purposes of this discussion. In the lunar case, degassing of 95–99% of H species (as H_2) in mare magmas under lunar f_{O_2} (~IW-1) would raise the δD value of the remaining H in the melt by +700 to +1000‰ (Sharp et al. 2013a; Tartèse and Anand 2013; Tartèse et al. 2013), which provides one possible explanation for some of the elevated δD values observed in lunar volcanic glasses and apatites.

Magmatic degassing has also been invoked to explain fractionation of Cl isotopes in lunar samples (Sharp et al. 2010b). These authors measured δ^{37}Cl values in a suite of lunar samples ranging from –1 to +24‰, which represents extreme variations compared to δ^{37}Cl values of terrestrial and of a vast majority of non-lunar extra-terrestrial materials that cluster around 0 ± 2‰ (Sharp et al. 2007, 2013b). Sharp et al. (2010b) speculated that the extreme enrichment in ^{37}Cl resulted from degassing of metal-chlorides in an anhydrous system. They argued that the presence of any water in the magmatic system would have caused degassing of HCl instead of metal chlorides, which would not fractionate heavy from light isotopes; however, Sharp et al. (2010a) did demonstrate Cl fractionation in H_2O-rich fumarolic systems experimentally. Sharp et al. (2013a) expanded their proposed δ^{37}Cl enrichment model and argued that the requirement for an anhydrous melt during Cl degassing did not preclude the possibility that significant H-bearing species existed in the melt before Cl loss ensued. This model was supported by experimental observations of differential degassing among H, F, S, and Cl where it was demonstrated that much of the H degassed before Cl (Ustunisik et al. 2011, 2015). Importantly, the attribution of enriched δ^{37}Cl values to degassing of metal chlorides is still an untested hypothesis that has yet to be demonstrated experimentally.

Volatiles in the lunar megaregolith

Origin of hydrogen in agglutinates. The measured D/H in 10084 agglutinates can be divided into two groups: one group with large D/H comparable to cometary values and high end of volcanic glasses, and the other shows depletion in D (up to –844‰) (Fig. 6). Three sources have been suggested for OH in the lunar soils, including redistribution of implanted SW hydrogen (Clark 2009; McCord et al. 2011; Pieters et al. 2009; Sunshine et al. 2009), trapped volcanic gas (Crotts 2008, 2009; Hauri et al. 2011) _ENREF_11, and redistribution of H introduced to the lunar surface through comet or meteorite impacts (Clark 2009; Colaprete et al. 2010; Feldman et al. 2001).

Experimental simulations have demonstrated that solar-wind implantation can produce OH in lunar soils and simulants (Ichimura et al. 2012; Poston et al. 2013a). However, the present-day solar wind is highly depleted in D ($D/H < 4 \times 10^{-7}$ or $\delta D \approx -1000$‰, Huss et al. 2012), which is much lower than all agglutinates analyzed in Liu et al. (2012a). Agglutinitic glasses represent melts of soils with implanted OH, so D in these glasses was likely elevated through Rayleigh distillation during impact melting, including spallation-generated D (Liu et al. 2012a). The higher than expected D can be explained by either kinetic fractionation during impact melting or assimilation of fine soil grains containing spallation induced D. The highly D-depleted agglutinates contain H that can be traced to solar-wind implantation. Because agglutinates make up a major proportion of lunar soils, often reaching 50 vol% of a mature soil (McKay et al. 1991), the detected OH in agglutinates represents an abundant reservoir of OH/H_2O in lunar soils.

Origin of hydrogen in lunar soils. The hydrogen isotope compositions of bulk soil samples are largely consistent with SW origin with highly depleted D/H values (e.g., Epstein and Taylor 1970b, 1971, 1972, 1973, 1974, 1975; Friedman et al. 1970a, 1970b, 1972; Merlivat et al. 1974; Stievenard et al. 1990). However, abundances of D in some samples are higher than expected from spallation D generated from solar- and galactic-cosmic ray bombardments (e.g., Epstein and Taylor 1970b, 1972; Friedman et al. 1972; Stephant and Robert 2014; Stievenard et al. 1990). These enriched D are generally ascribed to terrestrial contaminations (e.g., Epstein and Taylor 1972, 1975). However, there are suspicions that some of the D (and H_2O) in lunar soils and lunar rocks are indigenous lunar H or derived from cometary impacts (e.g., Epstein and Taylor 1970a; Friedman et al. 1972; Gibson and Moore 1973b; Stievenard et al. 1990).

The broad geographical distribution of the near-infrared hydroxyl/water signature observed on the lunar surface by near-infrared instruments has been interpreted as evidence for solar wind-induced hydroxylation (McCord et al. 2011; Pieters et al. 2009). The general lack of correlation with near-infrared hydroxyl absorptions with enhancements hydrogen as measured by Lunar Prospector provide further evidence that these deposits are present only as an exogenous thin (several monolayers) veneer (Clark 2009; Pieters et al. 2009; Sunshine et al. 2009). Hydroxyl and water absorptions are preferentially observed in association with highlands soils (Cheek et al. 2011; Pieters et al. 2009). This may be due to a weaker Si-O bond strength in anorthosite relative to mare minerals allowing protons to combine with exposed O on Si-O tetrahedra at grains boundaries and along crystal defects and dislocations (McCord et al. 2011). It may also be due to feldspathic minerals exhibiting a higher water desorption temperature than mare minerals and glasses (Hibbitts et al. 2011). Water from comets, chondritic materials, or native lunar water released during degassing, may, over the course of lunar history, have also adsorbed to lunar grains. However, water molecules begin to desorb from lunar analog materials by 225 K or colder (Hibbitts et al. 2011). Thus, water (as opposed to hydroxyl) would be expected to begin migrating across the lunar

surface along ballistic trajectories, in some cases escaping the Moon while at others ultimately condensing and accumulating within cold-traps (Crider and Vondrak 2000). Water produced by the solar wind would likely have the same fate, while solar wind-produced hydroxyl is more thermally stable than water and could persist even at equatorial latitudes (Hibbitts et al. 2011).

Some temporal variability of the strength of absorption bands near 3.0 μm has been reported based on EPOXI HRI-IR (Sunshine et al. 2009) and M^3 (Li and Milliken 2013) data analysis. In both cases, hydroxyl band strength below approximately 55° latitude is observed to begin at a maximum right after dawn (or nearest to the morning terminator), decrease to a minimum near lunar noon, and then begin to increase again during the lunar afternoon. Because hydroxyl is not directly released from the lunar surface, this process implies that surface OH^- molecules have either recombined with one another or excess protons to form H_2O or H_2, or that H has been broken off of the OH^- through photon stimulated desorption. In the laboratory, recombinative desorption of hydroxyl is observed at temperatures above 425 ± 25 K (Poston et al. 2013b), which is hotter than the maximum observed temperature on the lunar surface (Vasavada et al. 2012).

Origin of carbon in lunar soils. Interpretation of the wide range in $\delta^{13}C$ values for lunar samples varies among authors. An argument commonly used in the literature is a meteoritic carbon contribution, as well as a SW influence, mainly in the case of lunar soils (Anders et al. 1973; Epstein and Taylor 1970b; Kaplan and Petrowski 1971; Moore et al. 1970; Pillinger 1979). The general consensus is that the lunar soil contains ~1–2 wt% contributions from carbonaceous chondrite-type material, with an estimate of ~1.28 wt% in the lunar regolith (Anders et al. 1973). Based on calculations by Epstein and Taylor (1970b), meteoritic contribution of carbon to the lunar soil and breccias should therefore result in ~400 ppm carbon. As seen in Figure 7, the majority of samples have far less carbon than this. Therefore, Epstein and Taylor (1970b) have argued that a significant amount of carbon has been lost through vaporization, which takes place during impact of the meteorites onto the lunar surface. This theory is supported by Moore et al. (1970) who showed that about half of the material that makes up the lunar fines has been heated to temperatures high enough to expel volatile elements, including carbon. This contribution of meteoritic carbon to the lunar regolith followed by subsequent impacts resulting in heating and volatilization of carbon from the lunar surface will certainly mask the actual carbon content of indigenous lunar carbon. Additionally, a meteoritic source is consistent with the wide variation in carbon concentration and isotopic composition of lunar rocks and soils.

Although meteoritic contamination of lunar soils is a likely explanation for the diversity in carbon chemistry for lunar materials, numerous other explanations have been proposed as well. Epstein and Taylor (1970b) favored fractional evaporation during SW bombardment as well as the addition of a ^{13}C-rich material from other parts of the Moon in the igneous rocks analyzed. Kaplan and Smith (1970) suggested two processes to explain the variation in $\delta^{13}C$ values for lunar rocks and lunar fines: either preferential enrichment of the heavy isotope (^{13}C) to the fine material and some brecciated rocks, or preferential removal of the light isotope (^{12}C) from the unconsolidated/weakly consolidated rocks. Although the authors showed that there is no evidence to support the former, the latter could be accomplished by stripping of carbon by protons from the SW (Friedman et al. 1974; Kaplan and Smith 1970).

Mixing models and isotopic fractionation have also been suggested to explain the lunar carbon data set (Epstein and Taylor 1972; Kerridge et al. 1978; Pillinger 1979). Epstein and Taylor (1972) have invoked three different models to explain the scatter of the lunar carbon isotopic values seen in Figure 7. The first two models involve two-component mixing; fragmented lunar igneous rocks with SW carbon of variable $\delta^{13}C$ (+10 to +30‰) or lunar rocks with SW C or meteoritic C of variable $\delta^{13}C$ ($\delta^{13}C$ = –10 to +10‰). The latter model is accompanied by $\delta^{13}C$ enrichment and C loss due to particle bombardment. The third model from Epstein and Taylor (1972) is a three-component mixing model that involves lunar rocks, meteoritic debris, and SW C ($\delta^{13}C$ = +25 to +30‰). Kerridge et al. (1978) has also suggested a two-component mixing model with one end-member being lunar samples ($\delta^{13}C$ = 0 to +15‰) and the other being a terrestrial contamination component ($\delta^{13}C$ = –30‰). Furthermore, fractionation of carbon isotopes has been used to explain these differences. Pillinger (1979) has proposed various processes to fractionate carbon isotopes including thermal diffusion, hydrogen stripping, and preferential sputtering, mainly caused by a SW component. It is also possible that the variation in carbon isotopic compositions is a result of inhomogeneous samples that contain different amounts of CO, CO_2, elemental carbon, and carbides (Friedman et al. 1974).

Origin of nitrogen in lunar soils. An inverse correlation between soil grain diameter and N abundance revealed that the majority of N in lunar soils is surface-correlated (Goel et al. 1975), leading to the initial suggestion that it must be from a SW source (Kothari and Goel 1973; Muller 1974). However, $\delta^{15}N$ ($‰_{air}$) of lunar samples displays a huge variation from –100 to +330‰. Two main models have been proposed to attempt to explain this widely observed spread in $\delta^{15}N$ values in lunar soils, based on very different assumptions. The first model assumes that most of the N in soils comes from a SW source (Becker and Clayton 1975; Kerridge 1975), invoking a secular variation of around 30% (Assonov et al. 2002) in the solar wind $\delta^{15}N$ value over time to give rise to the spread of N isotopic compositions seen in the samples. However, this model does not take into account the much more limited variations recorded for noble gases (Kerridge 1989, 1993), nor the great excess of N in soils relative to solar-derived ^{36}Ar abundances (Frick et al. 1988; Wiens et al. 2004). The second hypothesis (Geiss and Bochsler 1982, 1991) suggests mixing of different sources of N: a solar N component of constant (isotopically heavy) composition, mixing with a non-solar N component (depleted in ^{15}N) indigenous to the Moon. It is only within the last few years that a direct measurement of the N isotopic composition of the SW has been made; data from the Genesis mission B/C array suggest that the SW is depleted in ^{15}N, with a $\delta^{15}N$ value of around –400‰ (Huss et al. 2012; Marty et al. 2011). In light of this new information, it appears neither model is fully correct, since a $\delta^{15}N$ value of –400‰ is significantly more $\delta^{15}N$-depleted than values recorded in lunar soils. This implies that, whatever the SW N contribution to lunar soil is, there is mixing occurring between the isotopically light solar component, and a non-solar component with a more $\delta^{15}N$-enriched isotopic composition. With the additional studies derived from single grains and bulk soils,

the favored explanation is mixing between SW and a second source (Hashizume et al. 2000; Ozima et al. 2005, 2008). Studies of individual mineral (metal, ilmenite, and pyroxene) grains from lunar soils were largely aimed to understand solar compositions (Furi et al. 2012; Hashizume et al. 2000). Single grain analyses display nitrogen isotope variation between SW and a planetary source (Hashizume et al. 2000). Based on the similar $^{15}N/^{14}N$ values between the planetary component in Hashizume et al. (2000) and Earth's atmosphere, Ozima et al. (2005, 2008) hypothesized the Earth's atmosphere was implanted on the Moon owing to an initially weak terrestrial magnetic field. More studies of N in other planetary materials indicated that the observed planetary component in young lunar soils can be readily explained by mixing of (micro)meteorite impactors enriched in ^{15}N (Furi et al. 2012).

Origin of fluorine, sulfur, and chlorine in lunar soils. Studies of F, S, and Cl in lunar soils have been somewhat limited compared to H, C, and N. In contrast to the volatile elements H, C, and N, much of the F, S, and Cl in lunar soils is likely to be indigenous to the Moon. This is in large part due to the fact that these elements are mainly absent in SW and only occur in trace abundances in meteoritic material (Lodders 2003; Lodders and Fegley 1998). Much of the inventory of these elements was likely brought to the surface by magmatic processes and subsequently redistributed by megaregolith formation. Consequently, lunar soils are likely a great resource for quantifying the abundances of F, S, and Cl in the lunar crust, as was recently shown by Treiman et al. (2014). As a cautionary note, S and Cl are both easily redistributed by thermal processes, so lunar soils are likely to be highly variable in these elements compared to F, which is less mobile (Aiuppa et al. 2009; Colson 1992; Ustunisik et al. 2011, 2015; Webster and Rebbert 1998).

Timing of volatile delivery to the Moon

Inferences and interpretations based on the wealth of new in situ data as well as fluid dynamic modeling seem to converge toward a consensus view that H_2O was present at the time of or shortly after the formation of the LMO (see Hauri et al. 2015 and references therein for an in-depth review). This inference is supported by the presence of H_2O in early products of lunar differentiation, including primary and secondary crust (Barnes et al. 2013; Boyce et al. 2013; Greenwood et al. 2011; Hui et al. 2013; McCubbin et al. 2010b, 2010c, 2011; Robinson et al. 2013). Although there is some evidence to suggest a similarity between Earth and Moon in terms of H isotopic composition and other elements (e.g., Si, Fe, Mg, O; Armytage et al. 2012; Chakrabarti and Jacobsen 2010; Fitoussi and Bourdon 2012; Poitrasson et al. 2004; Spicuzza et al. 2007; Wiechert et al. 2001; Zhang et al. 2012), it is unclear if the volatiles were delivered during or soon after the formation of the LMO (Hauri et al. 2015). Volatiles could have been equilibrated between the vapor-silicate portions of the proto-lunar disk and the molten portion of the Earth (e.g., Pahlevan and Stevenson 2007) or a lunar embryo made of largely solid/partially molten Earth material that cooled quickly in Earth orbit and later received additional disk material (Solomon and Chaiken 1976). However, there remains uncertainty over the mechanisms for retaining hydrogen in a vapor-silicate disk, including the role and effects of hydrodynamic escape on volatiles such as H (Pahlevan and Stevenson 2007). Recent modeling studies seem to indicate limited hydrodynamic escape of H_2/H_2O in oxidized vapor-silicate disk as long as the vapor phase is dominated by silicate (Hauri et al. 2015; Nakajima and Stevenson 2014; Visscher and Fegley 2013). However, the limited timescales of the proto-lunar disk (hundreds of years) likely prohibits the accretion of sufficient H_2O-rich materials to explain estimates for the H_2O content of the bulk silicate Moon (Hauri et al. 2015). The timescale of the LMO stage of lunar formation (~10^7 to 10^8 years; Elkins-Tanton et al. 2011) is more promising for the delivery of H_2O-rich material, and would require a mass of material that is consistent with the end of accretion, assuming the volatiles were being delivered by carbonaceous chondrites (Hauri et al. 2015). Recent analyses of carbonaceous chondrite-like δD values and $\delta^{15}N$ values in ancient eucrite meteorites demonstrate that a volatile component similar in composition to carbonaceous chondrites was present in the mantles of differentiated bodies of the inner Solar System within the first 8–20 million years after CAI formation (Sarafian et al. 2014), supporting the early existence of such a reservoir even within the inner Solar System.

There has also been some support for later delivery of volatiles to the Moon. Tartèse and Anand (2013) proposed the addition of carbonaceous chondrite-type material into the lunar interior following the crystallization of the LMO to explain the variable water contents of apatite grains in mare basalts, although the mechanism of its incorporation into the mare basalt source regions post-LMO is unclear and it does not explain the Cl depletion in the mare source relative to F. Additional evidence supporting an asteroidal input to the Moon's surface comes in the form of relics of chondrites in Apollo 16 regolith breccias (Joy et al. 2012) and graphite from sample 72275 (Steele et al. 2010). It is also interesting to note that the δD signatures recently acquired on lunar materials are not dissimilar to results published on select samples during the 1970s. At that time, the interpretation was that H_2 consisted of D-free hydrogen implanted on the lunar surface by the solar wind, whereas H_2O extracted from lunar soils and breccias was terrestrial water that had contaminated the samples (e.g., Epstein and Taylor 1973). Yet, if indigenous lunar water is characterized by an Earth-like H isotope composition, it is impossible to distinguish between indigenous lunar water and terrestrial water from H isotopes alone, making it difficult to interpret the origin of H in a sample without appropriate context.

Outstanding questions and future avenues of research

Volatile-bearing minerals on the Moon. Many of the volatile-bearing minerals that have been reported in lunar rocks remain "unverified" and a modern effort to reexamine some of these samples with modern techniques could yield additional important mineral systems through which one can try to understand lunar volatiles. A substantial effort has been put forth to understand the mineral apatite and what secrets it holds regarding volatiles in the lunar environment, but that wealth would be greatly enhanced by information about volatile abundances and isotopic compositions of coexisting amphiboles or biotite, which could potentially move the field forward much further than with apatite alone.

Lunar mantle heterogeneities in H_2O, F, and Cl. As discussed above, estimates of the abundances of H_2O, F, and Cl in

the lunar mantle vary substantially depending on the samples used, which either indicates a highly heterogeneous distribution of volatiles in the lunar interior (McCubbin et al. 2011; Robinson and Taylor 2014), or it represents an incomplete understanding of the origin and petrogenesis of the various lunar rock types. Consequently, this observation highlights the importance of using a diverse set of samples to try and estimate the volatile abundances of the lunar mantle, but it also highlights the importance of investigating the petrogenetic history of each sample beyond the information obtained directly for the magmatic volatiles.

The estimates of the volatile abundances of urKREEP, the lunar mantle, and BSM from the present study could be further refined with future experimental efforts that constrain the mineralogy and mineral composition of the entire LMO using appropriate BSM starting compositions as well as experimental work on mineral-melt partitioning of H_2O, F, and Cl between LMO minerals (olivine, pyroxene, Fe-Ti oxides, and anorthitic plagioclase) and silicate melt under reducing conditions relevant to lunar magmatism. Furthermore, the continued analysis of volcanic glasses, including the A-14 KREEP-rich glasses (Shearer et al. 1991) will help constrain the volatile abundances in the lunar mantle and in urKREEP. The continued analysis of apatite in mare basalts (including the KREEP basalts), with a specific focus on variations among petrologic types, will help one to understand the range in volatile compositions of the various lunar mare source regions and help to test the simple models put forth in this review.

H_2O abundance of the lunar mantle. All of the sample-based estimates for the H_2O content of the lunar mantle indicate a few to ~100 ppm H_2O (Table 4), however the upper limit determined from assuming a chondritic starting abundance of F in the context of LMO models is approximately 5 ppm H_2O (Table 4). This discrepancy either indicates that sample-based estimates of H_2O tend to overestimate the H_2O content of the lunar mantle or it requires an additional process to add H_2O to the lunar interior outside of the presently accepted model for the thermal and magmatic evolution of the Moon. Tartèse and Anand (2013) proposed that the addition of CI chondritic material to the mantle after LMO crystallization as one mechanism to explain the elevated H_2O abundances, which certainly solves the problem from a geochemical standpoint; however, the mechanism of its incorporation into the mare basalt source region post-LMO remains unclear (Hauri et al. 2015). Consequently, the question of the H_2O abundance of the lunar mantle is still an open one requiring additional research efforts.

Carbon contamination vs. indigenous carbon in lunar samples. It has long been recognized that contamination is a major issue affecting the carbon contents of lunar samples. Contamination of the Apollo samples could have occurred anywhere, including the time of sample collection, during transportation back to Earth (rocket fuel $\delta^{13}C = -35‰$) from exhaust gases emitted during Lunar Module [LM, later Lunar Excursion Module (LEM)] landing, astronaut activity, or subsequent laboratory handling (Moore et al. 1970). Commercial greases and oils typically used in laboratories have $\delta^{13}C \sim -30‰$, which can contaminate the samples during preparation and analysis. Terrestrial contamination values for $\delta^{13}C$ range from –90 to –5‰ when one considers contaminants such as methane, petroleum, land plants, and atmospheric CO_2 (Kaplan 1975; Pillinger 1979). Other possible contaminants include meteoritic or cometary material impacting the lunar surface ($\delta^{13}C \approx -20$ to –7‰) (Libby 1971; Smith and Kaplan 1970) as well as solar wind ($\delta^{13}C \approx -60 \pm 100‰$) (Hall 1973). Furthermore, cosmogenic carbon, which forms on the lunar surface as a result of spallation processes generated by cosmic rays acting on material in the upper few meters of the lunar surface, creates ^{13}C-enriched isotopic signatures released at high temperatures (Des Marais 1983). It is important to note that the majority of carbon contamination found in lunar samples is indistinguishable from the $\delta^{13}C$ values of possible terrestrial contaminants, making it very likely that lunar rocks with highly negative $\delta^{13}C$ values have been contaminated by one or more of these processes. It is also possible that the wide spread in isotopic data arises from either a heterogeneous distribution of carbon on the Moon or is due to mixing of any indigenous lunar carbon signature with that of one or more of these terrestrial or exogenous contaminants (Epstein and Taylor 1970b).

From the data discussed here, it is clear that the total carbon concentration and isotopic composition of lunar materials has yet to be accurately defined and most, if not all samples, have been exposed to some sort of contamination. Reanalysis of the Apollo samples using modern day, higher precision techniques such as SIMS (i.e., Hashizume et al. 2002) and higher resolution stepped combustion (i.e., Mortimer et al. 2015) should prove beneficial in distinguishing carbon contamination in these samples from indigenous lunar carbon. Des Marais (1978) has suggested that the loss of carbon (and nitrogen) was less extensive in rocks that crystallized at depth. Therefore, by analyzing such rocks, one would be able to get a more accurate estimate of the lunar inventories for carbon (Des Marais 1978; Grady and Pillinger 1990). Being able to correlate exposure ages of samples with carbon concentration and isotopic composition would also allow for better interpretation of analyses (Kerridge et al. 1975b, 1978). Only once these tasks are completed will it be possible to develop an accurate understanding of indigenous carbon on and in the Moon.

Geochemical signature of indigenous lunar nitrogen. Given the large contributions to N abundances from terrestrial contamination of lunar samples and the large isotopic contributions from cosmogenic N, the identification and isotopic characterization of very small amounts of indigenous lunar N has proven extremely challenging. It has only been in recent decades that more modern instrumentation and techniques, with much lower detection limits, have been able to address this issue. The $^{15}N/^{14}N$ ratio for the bulk Moon have been measured in lunar soils as summarized by Marty et al. (2003) and is characterized by $\delta^{15}N$ of ~+90 to –190‰. These values are within the range measured for carbonaceous chondrites, and are quite distinct from those in comets, strongly suggesting that the indigenous lunar N budget is characterized by a carbonaceous chondrite-like signature (Marty et al. 2003; Saal et al. 2013). These assertions seem to be reinforced by a pilot study involving step combustion experiments carried out on powdered chips of 6 mare basalts that yielded a $\delta^{15}N$ value of $0 \pm 9‰$, providing a much tighter constraint for the isotopic composition of indigenous lunar N (Mortimer et al. 2015). Their initial results suggest the indigenous lunar nitrogen fits within the range of carbonaceous chondrite

N, fitting best with CO chondrites. In addition they conclude that lunar indigenous N displays heterogeneous abundance and isotopic composition between different samples. Consequently, additional work is needed to fully determine the composition and origin of indigenous lunar nitrogen.

Origin of δD and δ^{37}Cl variations in volcanic lunar rocks and minerals. It is still very unclear whether or not the isotopic variations in H and Cl in volcanic lunar samples are being primarily driven by fractionation processes or mixing of various reservoirs. Given that almost the entire spread of δ^{37}Cl values observed in lunar samples is thus far observed only on the Moon, it is highly likely that Cl has been fractionated by some process on the Moon, but the process responsible has yet to be proven. Sharp et al. (2010b) provided evidence for Cl-isotope fractionation occurring as a result of degassing or vaporization of metal chlorides, but this process has yet to be demonstrated experimentally. In fact, experimental work on Cl-degassing from H-poor silicate melts under reducing conditions relevant to lunar magmatism is highlighted here as an important avenue of future research. Determining the fractionation process is a prerequisite to solving the question of the origin of the seemingly heavy Cl isotopic signature in urKREEP. Importantly, this process does not seem to have pervasively affected the lunar mantle in the same way it has affected the lunar crust.

H isotopes were likely affected by secondary processes and mixing of multiple reservoirs, which preclude straightforward interpretations of the existing data. From the plethora of data on lunar soils, it is clear that there is a very light (~−1000‰) reservoir of solar wind and a fairly heavy reservoir of spallogenic D at the lunar surface available for assimilation into erupted lava flows and impact melts. Furthermore, there has been substantial meteoritic and cometary infall to the Moon over the last ~4.35 Ga that could have produced distinct pockets of unique hydrogen isotopic reservoirs in and on the Moon. On account of low oxygen fugacity prevalent in the Moon, H_2 would dominate over H_2O in any degassing vapor, which would cause substantially higher isotopic fractionation of H compared to H_2O-dominated systems. Additional challenges involve identification of any terrestrial contamination in lunar samples and thin sections (e.g., thin section epoxy or terrestrial water in cracks). All of these possible sources could affect our ability to determine the indigenous H isotopic composition of the Moon, which many have recently argued is essentially the same as Earth and chondrites (Barnes et al. 2014; Saal et al. 2013; Tartèse et al. 2013, 2014b). This tantalizing possibility of a common source for water in the Earth-Moon system is gaining traction, but further support for this idea will require placing the isotopic data in the context of petrographic textures and timing of crystallization. For example, Tartèse et al. (2014b) report SIMS data for apatites in KREEP basalt 15386, for which apatite H_2O contents increase with decreasing δD values. Petrographic observations show that while most of the apatite grains in 15386 occur closely associated with late-stage mesostasis areas, one apatite analyzed is included within a pyroxene, suggesting it crystallized relatively early. Interestingly, this apatite grain is characterized by the lowest δD (~+90 ± 100‰) and highest OH content (~780 ppm H_2O), which is precisely what one would expect if the observed OH/δD relationship in apatites in 15386 resulted from crystallization during progressive magmatic degassing of H_2.

Acknowledgments

We thank CAPTEM and the Meteorite Working Group at NASA JSC for allocating us and many others samples for lunar volatile work. We thank Hanna Nekvasil, Donald Lindsley, James Greenwood, Erik Hauri, Alberto Saal, Jeff Taylor, Bradley Jolliff, Zach Sharp, Jim Papike, Juliane Gross, Alison Santos, Larry Taylor, and Katie Robinson for many helpful discussions concerning lunar volatiles. We also thank Noah Petro and an anonymous reviewer for helpful comments that have improved the quality of this work. We also thank Peter Isaacson for his work and comments as AE. This work was funded by NASA Lunar Advanced Science and Exploration Research (LASER) grant NNX13AK32G to F.M.M., NNX11AB30G to Carl Agee, and NNX13AJ58G to C.K.S., K.E.V.K. acknowledges support from NASA Cosmochemistry grant NNX11AG76G awarded to F.M.M. Y.L. acknowledges support from NASA Cosmochemistry grant NNX11AG58G to Larry Taylor, and internal support from JPL, which is managed by California Institute of Technology under a contract with NASA. M.A. acknowledges support from the U.K. Science and Technology Facilities Council grant (STFC/ST/I001298/1). S.M.E. was supported by Earth and Space Science Fellowship NNX12AO15H to S.M.E. and NASA Cosmochemistry grant NNX13AH85G to C.K.S. J.W.B. acknowledges support from a NASA Early Career Fellowship (NNX13AG40G). This research has made use of NASA's Astrophysics Data System.

References cited

Agrell, S.O., Bown, M.G., Gay, P., Long, J.V.P., and McConnell, J.D.C. (1971) "Goethite" on the Moon and the possible existence of other oxidized and hydroxyl-bearing phases in lunar impactites, p. 246–327. Proceedings of the 34th Annual Meeting of the Meteoritical Society, Tübingen, Germany.

Agrell, S.O., Scoon, J.H., Long, J.V.P., and Coles, J.N. (1972) The occurrence of goethite in a microbreccia from the Fra Mauro formation, p. 7–9. Proceedings of the Third Lunar Science Conference, Houston, Texas.

Aiuppa, A., Baker, D.R., and Webster, J.D. (2009) Halogens in volcanic systems. Chemical Geology, 263, 1–18.

Albarede, F. (2009) Volatile accretion history of the terrestrial planets and dynamic implications. Nature, 461, 1227–1233.

Alexander, C.M.O., Bowden, R., Fogel, M.L., Howard, K.T., Herd, C.D.K., and Nittler, L.R. (2012) The provenances of asteroids, and their contributions to the volatile inventories of the terrestrial planets. Science, 337, 721–723.

Anand, M. (2010) Lunar water: A brief review. Earth Moon and Planets, 107, 65–73.

Anand, M., Tartese, R., and Barnes, J.J. (2014) Understanding the origin and evolution of water in the Moon through lunar sample studies, p. 372. Philosophical Transactions of the Royal Society A—Mathematical Physical and Engineering Sciences.

Anders, E., Ganapathy, R., Krahenbuhl, U., and Morgan, J.W. (1973) Meteoritic material on the Moon. The Moon, 8, 3–24.

Ardia, P., Hirschmann, M.M., Withers, A.C., and Stanley, B.D. (2013) Solubility of CH_4 in a synthetic basaltic melt, with applications to atmosphere-magma ocean-core partitioning of volatiles and to the evolution of the Martian atmosphere. Geochimica et Cosmochimica Acta, 114, 52–71.

Armytage, R.M.G., Georg, R.B., Williams, H.M., and Halliday, A.N. (2012) Silicon isotopes in lunar rocks: Implications for the Moon's formation and the early history of the Earth. Geochimica et Cosmochimica Acta, 77, 504–514.

Arnold, J.R. (1979) Ice in the lunar polar regions. Journal of Geophysical Research, 84, 5659–5668.

Assonov, S.S., Franchi, I.A., Pillinger, C.T., Semenova, A.S., Shukolyukov, Y.A., Verchovsky, A.B., and Iassevitch, A.N. (2002) Nitrogen and argon release profiles in Luna 16 and Luna 24 regolith samples: The effects of regolith reworking. Meteoritics and Planetary Science, 37, 27–48.

Aubaud, C., Hauri, E.H., and Hirschmann, M.M. (2004) Hydrogen partition coefficients between nominally anhydrous minerals and basaltic melts. Geophysical Research Letters, 31, 1–4.

Barnes, J.J., Franchi, I.A., Anand, M., Tartèse, R., Starkey, N.A., Koike, M., Sano, Y., and Russell, S.S. (2013) Accurate and precise measurements of the D/H ratio and hydroxyl content in lunar apatites using NanoSIMS. Chemical Geology, 337, 48–55.

Barnes, J.J., Tartèse, R., Anand, M., McCubbin, F.M., Franchi, I.A., Starkey, N.A., and Russell, S.S. (2014) The origin of water in the primitive Moon as revealed by the lunar highlands samples. Earth and Planetary Science Letters, 390, 244–252.

Barry, P.H., Hilton, D.R., Marti, K., and Taylor, L.A. (2013) Indigenous lunar nitrogen. Proceedings of the 44th Lunar and Planetary Science Conference, The Woodlands, Texas, Abstract 2160.

Becker, R.H. (1980) Evidence for a secular variation in the $^{13}C/^{12}C$ ratio of carbon implanted in lunar soils Earth and Planetary Science Letters, 50, 189–196.

Becker, R.H., and Clayton, R.N. (1975) Nitrogen abundancesand isotopic composi-

tions in lunar samples. Proceedings of the Sixth Lunar Science Conference, Houston, Texas, 2131–2149.
——— (1978) Nitrogen isotope systematics of two Apollo 12 soils. Proceedings of the Ninth Lunar and Planetary Science Conference, Houston, Texas, 1619–1627.
Becker, R.H., Clayton, R.N., and Mayeda, T.K. (1976) Characterization of lunar nitrogen components. Proceedings of the Seventh Lunar Science Conference, Houston, Texas, 441–458.
Bell, A.S., de Moor, J.M., and Shearer, C.K. (2014) Thermodynamic and isotopic constraints on the gas composition and formation temperature of sulfide replacement assemblages in lunar breccias 67016, 294, 67016, 297, and 67915, 150. 45th Lunar and Planetary Science Conference, The Woodlands, Texas, 2187.
Bell, A.S., Shearer, C.K., deMoor, J.M., and Provencio, P. (2015) Using the sulfide replacement textures in lunar breccia 67915 to construct a thermodynamic model of H-S-O-C fluids in the lunar crust. Proceedings of the 46th Lunar and Planetary Science Conference, Woodlands, Texas, Abstract 2479.
Bell, D.R., and Rossman, G.R. (1992) Water in the Earth's mantle: The role of nominally anhydrous minerals. Science, 255, 1391–1397.
Benkert, J.P., Baur, H., Signer, P., and Wieler, R. (1993) He, Ne, and Ar from the solar-wind and solar energetic particles in lunar ilmenites and pyroxenes. Journal of Geophysical Research: Planets, 98, 13,147–13,162.
Beyer, C., Klemme, S., Wiedenbeck, M., Stracke, A., and Vollmer, C. (2012) Fluorine in nominally fluorine-free mantle minerals: Experimental partitioning of F between olivine, orthopyroxene and silicate melts with implications for magmatic processes. Earth and Planetary Science Letters, 337, 1–9.
Bhattacharya, S., Saran, S., Dagar, A., Chauhan, P., Chauhan, M., Ajai, A., and Kiran Kumar, S. (2013) Endogenic water on the Moon associated with non-mare silicic volcanism: Implications for hydrated lunar interior. Current Science, 105, 685–691.
Bindeman, I.N., Kamenetsky, V., Palandri, J., and Vennemann, T. (2012) Hydrogen and oxygen isotope behaviors during variable degrees of upper mantle melting: Example from the basaltic glasses from Macquarie Island. Chemical Geology, 310, 126–136.
Boardman, J.W., Pieters, C.M., Green, R.O., Lundeen, S.R., Varanasi, P., Nettles, J., Petro, N.E., Besse, S., and Taylor, L.A. (2011) Measuring moonlight: An overview of the spatial properties, lunar coverage, selenolocation and related Level 1B products of the Moon Mineralogy Mapper. Journal of Geophysical Research: Planets, 116, E00G14, http://dx.doi.org/10.1029/2010JE003730.
Boyce, J.W., and Hervig, R.L. (2008) Magmatic degassing histories from apatite volatile stratigraphy. Geology, 36, 63–66.
Boyce, J.W., Liu, Y., Rossman, G.R., Guan, Y.B., Eiler, J.M., Stolper, E.M., and Taylor, L.A. (2010) Lunar apatite with terrestrial volatile abundances. Nature, 466, 466–469.
Boyce, J.W., Guan, Y., Treiman, A.H., Greenwood, J.P., Eiler, J.M., and Ma, C. (2013) Volatile components in the moon: Abundances and isotope ratios of Cl and H in lunar apatites Proceedings of the 44th Lunar and Planetary Science Conference, The Woodlands, Texas. Abstract 2851.
Boyce, J.W., Tomlinson, McCubbin, F.M., Treiman, A.H., and Greenwood, J.P. (2014) The lunar apatite paradox. Science, 344, 400–402.
Brenan, J. (1993) Kinetics of fluorine, chlorine, and hydroxl exchange in fluorapatite. Chemical Geology, 110, 195–210.
Brilliant, D.R., Franchi, I.A., and Pillinger, C.T. (1994) Nitrogen components in lunar soil-12023: Complex grains are not the carrier of isotopically light nitrogen. Meteoritics, 29, 718–723.
Bucholz, C.E., Gaetani, G.A., Behn, M.D., and Shimizu, N. (2013) Post-entrapment modification of volatiles and oxygen fugacity in olivine-hosted melt inclusions. Earth and Planetary Science Letters, 374, 145–155.
Bul'Bak, T.A., and Shvedenkov, G.Y. (2005) Experimental study on incorporation of C-H-O-N fluid components in Mg-cordierite. European Journal of Mineralogy, 17, 829–838.
Burger, P.V., Shearer, C.K., Sharp, Z.D., McCubbin, F.M., Provencio, P.P., and Steele, A. (2013) Driving fumarole activity on the Moon 1. Chlorine distribution and its isotope composition in "Rusty Rock" 66095. Implications for the petrogenesis of "Rusty Rock," origin of "rusty" alteration, and volatile element behavior on the Moon. Proceedings of the 44th Lunar and Planetary Science Conference, The Woodlands, Texas, Abstract 2812.
Burnham, C.W. (1994) Development of the Burnham model for prediction of H_2O solubility in magmas. Volatiles in Magmas, 30, 123–129.
Butler, P. (1971) Lunar Sample Catalog, Apollo 15. Curators office, MSC 03209, Houston, Texas.
———(1972) Lunar Sample Information Catalog Apollo 16, 370. Lunar Receiving Laboratory. MSC 03210 Curator's Catalog.
——— (1978) Recognition of Lunar Glass Droplets Produced Directly from Endogenous Melts: the Evidence from S-Zn Coatings. Proceedings of the Ninth Lunar and Planetary Science Conference, Houston, Texas, 143–145.
Butler, P. Jr., and Meyer, C. Jr. (1976) Sulfur prevails in coatings on glass droplets: Apollo 15 green and brown glasses and Apollo 17 orange and black (devitrified) glasses. Proceedings of the Seventh Lunar Science Conference, 1561–1581.
Cadogan, P.H., Eglinton, G., Maxwell, J.R., and Pillinger, C.T. (1971) Carbon chemistry of the lunar surface. Nature, 231, 29–31.
Carter, J.L., and Padovani, E. (1973) Genetic implications of some unusual particles in Apollo 16 less than 1 mm fines 68841,11 and 69941,13. Proceedings of the 4th Lunar Science Conference, 323–332.
Carter, J.L., Clanton, U.S., Fuhrman, R., Laughton, R.B., McKay, D.S., and Usselman, T.M. (1975) Morphology and composition of chalcopyrite, chromite, Cu, Ni-Fe, pentandite, and troilite in vugs of 76015 and 76215. Proceedings of the 6th Lunar Science Conference, 719–728.
Chakrabarti, R., and Jacobsen, S.B. (2010) The isotopic composition of magnesium in the inner Solar System. Earth and Planetary Science Letters, 293, 349–358.
Chang, S., Kvenvolden, K., Lawless, J., Ponnamperuma, C., and Kaplan, I.R. (1971) Carbon, carbides, and methane in an Apollo 12 sample. Science, 171, 474–477.
Chang, S., Lawless, J., Romiez, M., Kaplan, I.R., Petrowski, C., Sakai, H., and Smith, J.W. (1974) Carbon, nitrogen and sulfur in lunar fines 15012 and 15013: Abundances, distributions and isotopic compositions. Geochimica et Cosmochimica Acta, 38, 853–872.
Cheek, L.C., Pieters, C.M., Boardman, J.W., Clark, R.N., Combe, J.P., Head, J.W., Isaacson, P.J., McCord, T.B., Moriarty, D., Nettles, J.W., and others. (2011) Goldschmidt crater and the Moon's north polar region: Results from the Moon Mineralogy Mapper (M^3). Journal of Geophysical Research: Planets, 116, E00G02.
Chou, C.-L., Boynton, W.V., Sundberg, L.L., and Wasson, J.T. (1975) Volatiles on the surface of Apollo 15 green glass and trace-element distributions among Apollo 15 soils. Proceedings of the Sixth Lunar Science Conference, Houston, Texas, 1701–1727.
Cirlin, E.H., and Housley, R.M. (1977) An Atomic Absorption Study of Volatile Trace Metals in Lunar Samples. Proceedings of the Eighth Lunar and Planetary Science Conference, Houston, Texas, 184–186.
Cirlin, E.H., Housley, R.M., and Grant, R.W. (1978) Studies of volatiles in Apollo 17 samples and their implications to vaport transport processes. Proceedings of the Ninth Lunar and Planetary Science Conference, Houston, Texas, 2049–2063.
Clanton, U.S., McKay, D.S., Waits, G., and Fuhrman, R. (1978a) Sublimate morphology on 74001 and 74002 orange and black glassy droplets. Proceedings of the Ninth Lunar and Planetary Science Conference, Houston, Texas, 1945–1957.
——— (1978b) Unusual Surface Features on Volcanic Droplets from 74001 and 74002. Proceedings of the Ninth Lunar and Planetary Science Conference, Houston, Texas, 172–174.
Clark, R.N. (2009) Detection of adsorbed water and hydroxyl on the Moon. Science, 326, 562–564.
Colaprete, A., Schultz, P., Heldmann, J., Wooden, D., Shirley, M., Ennico, K., Hermalyn, B., Marshall, W., Ricco, A., Elphic, R.C., and others. (2010) Detection of water in the LCROSS ejecta plume. Science, 330, 463–468.
Colson, R.O. (1992) Mineralization on the Moon? Theoretical consideration of Apollo 16 "Rusty Rocks", sulfide replacement in 67016 and surface-correlated volatiles on lunar volcanic glasses. Proceedings 22th Lunar and Planetary Science Conference, Houston, Texas, 427–436.
Coplen, T.B. (1994) Reporting of stable hydrogen, carbon, and oxygen isotopic abundances. Pure and Applied Chemistry, 66, 273–276.
Crider, D.H., and Vondrak, R.R. (2000) The solar wind as a possible source of lunar polar hydrogen deposits. Journal of Geophysical Research: Planets, 105, 26773–26782.
Crotts, A.P.S. (2008) Lunar outgassing, transient phenomena, and the return to the Moon. Part 1: Existing data. Astrophysical Journal, 687, 692–705.
——— (2009) Transient lunar phenomena. Part 2: Regularity and reality. Astrophysical Journal, 697, 1–15.
Dasgupta, R., and Dixon, J.E. (2009) Volatiles and volatile-bearing melts in the Earth's interior. Chemical Geology, 262, 1–3.
Dasgupta, R., Hirschmann, M.M., and Smith, N.D. (2007) Water follows carbon: CO_2 incites deep silicate melting and dehydration beneath mid-ocean ridges. Geology, 35, 135–138.
Davenport, J.D., Longhi, J., Neal, C.R., Jolliff, B.J., and Bolster, D. (2014) Simulating planetary igneous crystallization environments (SPICES): A suite of igneous crystallization programs. Proceedings of the 45th Lunar and Planetary Science Conference, Woodlands, Texas, Abstract 1111.
Day, J.M.D., and Moynier, F. (2014) Evaporative fractionation of volatile stable isotopes and their bearing on the origin of the Moon. Philosophical Transactions of the Royal Society A—Mathematical Physical and Engineering Sciences, 372.
Delano, J.W. (1980) Chemistry and liquidus phase relations of Apollo 15 red glass: Implications for the deep lunar interior. Proceedings of the 11th Lunar and Planetary Science Conference, Houston, Texas, 251–288.
Delano, J.W., and Livi, K. (1981) Lunar volcanic glasses and their constraints on mare petrogenesis. Geochimica et Cosmochimica Acta, 45, 2137–2149.
Delano, J.W., Hanson, B.Z., and Watson, E.B. (1994) Abundance and diffusivity of sulfur in lunar picritic magmas. Proceedings of the 25th Lunar and Planetary Science Conference, Houston, Texas, p. 325–326.
Des Marais, D.J. (1978) Carbon, nitrogen and sulfur in Apollo 15, 16, and 17 rocks. Proceedings of the Ninth Lunar and Planetary Science Conference, Houston, Texas, 2451–2467.
——— (1983) Light element geochemistry and spallogenesis in lunar rocks.

Geochimica et Cosmochimica Acta, 47, 1769–1781.
Des Marais, D.J., Hayes, J.M., and Meinschein, W.G. (1974) The distribution in lunar soil of hydrogen released by pyrolysis. Proceedings of the Fifth Lunar Conference, Houston, Texas, 1811–1822.
Des Marais, D.J., Basu, A., Hayes, J.M., and Meinschein, W.G. (1975) Evolution of carbon isotopes, agglutinates, and the lunar regolith. Proceedings of the Sixth Lunar Science Conference, Houston, Texas, 2353–2373.
Ding, T.P., Thode, H.G., and Rees, C.E. (1983) Sulfur content and sulfur isotope composition of orange and black glasses in Apollo 17 drive tube—74002/1. Geochimica et Cosmochimica Acta, 47, 491–496.
Ding, T., Valkiers, S., Kipphardt, H., De Bievre, P., Taylor, P.D.P., Gonfiantini, R., and Krouse, R. (2001) Calibrated sulfur isotope abundance ratios of three IAEA sulfur isotope reference materials and V-CDT with a reassessment of the atomic weight of sulfur. Geochimica et Cosmochimica Acta, 65, 2433–2437.
Dreibus, G., Spettel, B., and Wänke, H. (1977) Lithium and halogens in lunar samples. Philosophical Transactions Royal Society London A, 285, 49–54.
Duncan, A.R., Erlank, A.J., Willis, J.P., and Ahrens, L.H. (1973) Composition and inter-relationships of some Apollo 16 samples. Proceedings of the Fourth Lunar Science Conference, Houston, Texas, 1097–1113.
Dymek, R.F., Albee, A.L., and Chodos, A.A. (1976) Petrology and origin of Boulders #2 and #3, Apollo 17 station 2. Proceedings of the Seventh Lunar Science Conference, Houston, Texas, 2335–2378.
Ebihara, M., Wolf, R., and Anders, E. (1981) Siderophile, volatile, and incompatible trace elements in Apollo Breccia 66095. Proceedings of the 12th Lunar and Planetary Science Conference, Houston, Texas, 249–250.
Eck, R.V., Lippinco. Er, Dayhoff, M.O., and Pratt, Y.T. (1966) Thermodynamic equilibrium and inorganic origin of organic compounds. Science, 153, 628–633.
Eke, V.R., Teodoro, L.F.A., and Elphic, R.C. (2009) The spatial distribution of polar hydrogen deposits on the Moon. Icarus, 200, 12–18.
El Goresy, A., Ramdohr, P., and Medenbach, O. (1973a) Lunar samples from Descartes site: Opaque mineralogy and geochemistry. Proceedings of the Fourth Lunar Science Conference, Houston, Texas, 733–750.
El Goresy, A., Ramdohr, P., Pavicevic, M., Medenbach, O., Muller, O., and Gentner, W. (1973b) Zinc, lead, chlorine and FeOOH-bearing assemblages in the Apollo 16 sample 66095: Origin by impact of a comet or a carbonaceous chondrite? Earth and Planetary Science Letters, 18, 411–419.
Elardo, S.M., Draper, D.S., and Shearer, C.K. (2011) Lunar Magma Ocean crystallization revisited: Bulk composition, early cumulate mineralogy, and the source regions of the highlands Mg-suite. Geochimica et Cosmochimica Acta, 75, 3024–3045.
Elardo, S.M., McCubbin, F.M., and Shearer, C.K. (2012) Chromite symplectites in Mg-suite troctolite 76535 as evidence for infiltration metasomatism of a lunar layered intrusion. Geochimica et Cosmochimica Acta, 87, 154–177.
Elardo, S.M., Shearer Jr., C.K., Fagan, A.L., Borg, L.E., Gaffney, A.M., Burger, P.V., Neal, C.R., Fernandes, V.A., and McCubbin, F.M. (2014) The origin of young mare basalts inferred from lunar meteorites Northwest Africa 4734, 032, and LaPaz Icefield 02205. Meteoritics and Planetary Science, 19, 261–291.
Elardo, S.M., Shearer, C.K., Vander Kaaden, K.E., McCubbin, F.M., and Bell, A.S. (2015) Petrogenesis of primitive and evolved basalts in a cooling Moon: Experimental constraints from the youngest known lunar magmas. Earth and Planetary Science Letters, in press.
Elkins-Tanton, L.T., and Grove, T.L. (2011) Water (hydrogen) in the lunar mantle: Results from petrology and magma ocean modeling. Earth and Planetary Science Letters, 307, 173–179.
Elkins-Tanton, L.T., Van Orman, J.A., Hager, B.H., and Grove, T.L. (2002) Re-examination of the lunar magma ocean cumulate overturn hypothesis: Melting or mixing is required. Earth and Planetary Science Letters, 196, 239–249.
Elkins-Tanton, L.T., Chatterjee, N., and Grove, T.L. (2003a) Experimental and petrological constraints on lunar differentiation from the Apollo 15 green picritic glasses. Meteoritics and Planetary Science, 38, 515–527.
——— (2003b) Magmatic processes that produced lunar fire fountains. Geophysical Research Letters, 30, 1–4.
Elkins-Tanton, L.T., Burgess, S., and Yin, Q.-Z. (2011) The lunar magma ocean: Reconciling the solidification process with lunar petrology and geochronology. Earth and Planetary Science Letters, 304, 326–336.
Elphic, R.C., Eke, V.R., Teodoro, L.F.A., Lawrence, D.J., and Bussey, D.B.J. (2007) Models of the distribution and abundance of hydrogen at the lunar south pole. Geophysical Research Letters, 34, 1–4.
Epstein, S., and Taylor, H.P. Jr. (1970a) $^{18}O/^{16}O$, $^{30}Si/^{28}Si$, D/H, and $^{13}C/^{12}C$ studies of lunar rock and minerals. Science, 167, 533–535.
——— (1970b) The concentration and isotopic composition of hydrogen, carbon and silicon in Apollo 11 lunar rocks and minerals Proceedings of the Apollo 11 Lunar Science Conference, 1085–1096.
——— (1971) O^{18}/O^{16}, Si^{30}/Si^{28}, D/H, and C^{13}/C^{12} ratios in lunar samples. Proceedings of the Second Lunar Science Conference, Houston, Texas, 1421–1441.
——— (1972) O^{18}/O^{16}, Si^{30}/Si^{28}, C^{13}/C^{12}, and D/H studies of Apollo 14 and 15 samples. Proceedings of the Third Lunar Science Conference, Houston, Texas, 1429–1454.
——— (1973) The isotopic composition and concentration of water, hydrogen, and carbon in some Apollo 15 and 16 soils and in the Apollo 17 orange soil. Proceedings of the Fourth Lunar Science Conference, Houston, Texas, 1559–1575.
——— (1974) D/H and $^{18}O/^{16}O$ ratios of H_2O in the "rusty" breccia 66095 and the origin of "lunar water". Proceedings of the Fifth Lunar Conference, Houston, Texas, 1839–1854.
——— (1975) Investigation of the carbon, hydrogen, oxygen, and silicon isotope and concentration relationships on the grain surfaces of various lunar soils and in some Apollo 15 and 16 cores samples. Proceedings of the Sixth Lunar Science Conference, Houston, Texas, 1771–1798.
Fagents, S.A., Rumpf, M.E., Crawford, I.A., and Joy, K.H. (2010) Preservation potential of implanted solar wind volatiles in lunar palaeoregolith deposits buried by lava flows. Icarus, 207, 595–604.
Farquhar, J., and Wing, B.A. (2005) Sulfur multiple isotopes of the Moon: ^{33}S and ^{36}S abundances relative to Canyon Diablo Troilite. Proceedings of the 36th Lunar and Planetary Science Conference, Houston, Texas, 2380.
Fegley, B. Jr., and Swindle, T.D. (1993) Lunar volatiles: Implications for lunar resource utilization. In J.S. Lewis, M.S. Mathews, and L. Guerrieri, Eds., Resources of Near-earth Space, p. 367–426. University of Arizona Press, Tucson.
Feldman, W.C., Lawrence, D.J., Elphic, R.C., Barraclough, B.L., Maurice, S., Genetay, I., and Binder, A.B. (2000) Polar hydrogen deposits on the Moon. Journal of Geophysical Research: Planets, 105, 4175–4195.
Feldman, W.C., Maurice, S., Binder, A.B., Barraclough, B.L., Elphic, R.C., and Lawrence, D.J. (1998) Fluxes of fast and epithermal neutrons from lunar prospector: Evidence for water ice at the lunar poles. Science, 281, 1496–1500.
Feldman, W.C., Maurice, S., Lawrence, D.J., Little, R.C., Lawson, S.L., Gasnault, O., Wiens, R.C., Barraclough, B.L., Elphic, R.C., Prettyman, T.H., and others. (2001) Evidence for water ice near the lunar poles. Journal of Geophysical Research: Planets, 106, 23231–23251.
Fitoussi, C., and Bourdon, B. (2012) Silicon isotope evidence against an enstatite chondrite earth. Science, 335, 1477–1480.
Fogel, R.A., and Rutherford, M.J. (1995) Magmatic volatiles in primitive lunar glasses: I. FTIR and EPMA analyses of Apollo 15 green and yellow glasses and revision of the volatile-assisted fire-fountain theory. Geochimica et Cosmochimica Acta, 59, 201–215.
Frick, U., Becker, R.H., and Pepin, R.O. (1988) Solar wind record in the lunar regolilh: Nitrogen and noble gases. Proceedings of the 18th Lunar and Planetary Science Conference, Houston, Texas, 87–120.
Friedman, I., Gleason, J.D., and Hardcastle, K.G. (1970a) Water, hydrogen, deuterium, carbon and C^{13} content of selected lunar material. Proceedings of the Apollo 11 Lunar Science Conference, 1103–1109.
Friedman, I., O'Neil, J.R., Adami, L.H., Gleason, J.D., and Hardcast. K. (1970b) Water, hydrogen, deuterium, carbon, carbon-13, and oxygen-18 content of selected lunar material. Science, 167, 538–540.
Friedman, I., O'Neil, J.R., Gleason, J.D., and Hardcastle, K.G. (1971) The carbon and hydrogen content and isotopic composition of some Apollo 12 materials. Proceedings of the Second Lunar Science Conference, Houston, Texas, 1407–1415.
Friedman, I., Hardcastle, K.G., and Gleason, J.D. (1972) Isotopic composition of carbon and hydrogen in some Apollo 14 and 15 samples. In J.W. Chamberlain and C.Watkins, Eds., The Apollo 15 Lunar Samples, p. 302–306. The Lunar Science Institute, Houston.
Friedman, I., Hardcastle, K.G., and Gleason, J.D. (1974) Isotopic composition of carbon and hydrogen in some Apollo 14 and 15 lunar samples. Journal of Research of the U.S. Geological Survey, 2, 7–12.
Frondel, C., Klein, C., Ito, J., and Drake, J.C. (1970) Mineralogical and chemical studies of Apollo 11 lunar fines and selected rocks. Proceedings of the Apollo 11 Lunar Science Conference, 1, 445–474.
Frondel, J.W. (1975) Lunar Mineralogy, 323 p. Wiley, New York.
Furi, E., Marty, B., and Assonov, S.S. (2012) Constraints on the flux of meteoritic and cometary water on the Moon from volatile element (N-Ar) analyses of single lunar soil grains, Luna 24 core. Icarus, 218, 220–229.
Gaetani, G.A., O'Leary, J.A., Shimizu, N., Bucholz, C.E., and Newville, M. (2012) Rapid reequilibration of H_2O and oxygen fugacity in olivine-hosted melt inclusions. Geology, 40, 915–918.
Gardiner, L.R., Jull, A.J.T., and Pillinger, C.T. (1978) Progress towards the direct measurement of $^{13}C/^{12}C$ ratios for hydrolysable carbon in lunar soil by static mass spectrometry. Proceedings of the Ninth Lunar Science Conference, 2149–2165.
Garrison, J.R. Jr., and Taylor, L.A. (1980) Genesis of highlands basalt breccias: A view from 66095. Proceedings of the Conference on the Lunar Highlands Crust, Houston, Texas, 395–417.
Gay, P., Bown, M.G., and Rickson, K.O. (1970) Mineralogical studies of lunar rock 12013,10. Earth and Planetary Science Letters, 9, 124–126.
Geiss, J., and Bochsler, P. (1982) Nitrogen isotopes in the solar system. Geochimica et Cosmochimica Acta, 46, 529–548.
——— (1991) Long time variations in solar wind properties: Possible causes versus observations. In C.P. Sonnett, M.S. Gianipapa, and M.S. Mathews, Eds., The Sun in Time, p. 98–117. University of Arizona Press, Tucson.
Gibson, E.K. Jr. (1977) Volatile elements, carbon, nitrogen, sulfur, sodium, potassium and rubidium in the lunar regolith. Physics and Chemistry of the Earth, 10, 57–62.

Gibson, E.K. Jr., and Andrawes, F.F. (1978a) Sulfur abundances in the 74001/74002 drive tube core from Shorty Crater, Apollo 17. Proceedings of the Ninth Lunar and Planetary Science Conference, Houston, Texas, 2011–2017.

——— (1978b) Nature of the gases released from lunar rocks and soils upon crushing. Proceedings of the Ninth Lunar and Planetary Science Conference, Houston, Texas, 2433–2450.

Gibson, E.K. Jr., and Moore, C.B. (1973a) Variable carbon contents of lunar soil 74220. Earth and Planetary Science Letters, 20, 404–408.

Gibson, E.K. Jr., and Moore, G.W. (1973b) Volatile-rich lunar soil: Evidence of possible cometary impact. Science, 179, 69–71.

——— (1974) Sulfur abundances and distributions in the valley of Taurus-Littrow. Proceedings of the Fifth Lunar Science Conference, 2, 1823–1837.

Gibson, E.K. Jr., Chang, S., Lennon, K., Moore, G.W., and Pearce, G.W. (1975) Sulfur abundances and distributions in mare basalts and their source magmas. Proceedings of the Sixth Lunar Science Conference, Houston, Texas, 1287–1301.

Gibson, E.K., Brett, R., and Andrawes, F. (1977) Sulfur in lunar mare basalts as a function of bulk composition. Proceedings of the Eighth Lunar Science Conference, 1417–1428.

Gladstone, G.R., Hurley, D.M., Retherford, K.D., Feldman, P.D., Pryor, W.R., Chaufray, J.-Y., Versteeg, M., Greathouse, T.K., Steffl, A.J., Throop, H., and others. (2010) LRO-LAMP Observations of the LCROSS Impact Plume. Science, 330, 472–476.

Goel, P.S., Shukla, P.N., Kothari, B.K., and Garg, A.N. (1975) Total nitrogen in lunar soils, breccias, and rocks. Geochimica et Cosmochimica Acta, 39, 1347–1352.

Goldberg, R.H., Burnett, D.S., and Tombrello, T.A. (1975) Fluorine surface films on lunar samples: Evidence for both lunar and terrestrial origin Proceedings of the Sixth Lunar Science Conference, Houston, Texas. 2189–2200.

Goldberg, R.H., Tombrello, T.A., and Burnett, D.S. (1976) Fluorine as a consituent in lunar magmatic gases. Proceedings of the Seventh Lunar Science Conference, 1597–1613.

Goldstein, J.I., and Axon, H.J. (1973) Composition, structure, and thermal history of metallic particles from 3 Apollo 16 soils, 65701, 68501, and 63501. Proceedings of the Fourth Lunar Science Conference, 751–775.

Goldstein, J.I., Axon, H.J., and Yen, C.F. (1972) Metallic particles in the Apollo 14 lunar soil. Proceedings of the Third Lunar Science Conference, 1037–1064.

Goldstein, J.I., Hewins, R.H., and Romig, A.D. (1976) Carbides in lunar soils and rocks. Proceedings of the Seventh Lunar Science Conference, 807–818.

Grady, M.M., and Pillinger, C.T. (1990) The carbon and nitrogen stable isotope geochemistry of two lunar meteorites: ALHA-81005 and Y-86032. Proceedings of the NIPR Symposium on Antarctic Meteorites, 3, 27–39.

Green, R.O., Pieters, C., Mouroulis, P., Eastwood, M., Boardman, J., Glavich, T., Isaacson, P., Annadurai, M., Besse, S., Barr, D., and others. (2011) The Moon Mineralogy Mapper (M^3) imaging spectrometer for lunar science: Instrument description, calibration, on-orbit measurements, science data calibration and on-orbit validation. Journal of Geophysical Research: Planets, 116, E00G19, http://dx.doi.org/10.1029/2011JE003797.

Greenwood, J.P., Itoh, S., Sakamoto, N., Warren, P., Taylor, L., and Yurimoto, H. (2011) Hydrogen isotope ratios in lunar rocks indicate delivery of cometary water to the Moon. Nature Geoscience, 4, 79–82.

Gross, J., and Treiman, A.H. (2011) Unique spinel-rich lithology in lunar meteorite ALHA 81005: Origin and possible connection to M^3 observations of the far-side highlands. Journal of Geophysical Research: Planets, 116 http://dx.doi.org/10.1029/2011JE003858.

Gross, J., Isaacson, P., Treiman, A.H., Le, L., and Gorman, J. (2014) Spinel-rich lithologies in the lunar highland crust: Linking lunar samples with crystallization experiments and remote sensing. American Mineralogist, 99 1849–1859.

Hall, D.N.B. (1973) Detection of the ^{13}C, ^{17}O, and ^{18}O isotope bands of CO in the infrared solar spectrum. Astrophysical Journal, 182, 977–982.

Halliday, A.N. (2013) The origins of volatiles in the terrestrial planets. Geochimica et Cosmochimica Acta, 105, 146–171.

Harley, S.L., and Carrington, D.P. (2001) The distribution of H_2O between cordierite and granitic melt: H_2O incorporation in cordierite and its application to high-grade metamorphism and crustal anatexis. Journal of Petrology, 42, 1595–1620.

Harley, S.L., Thompson, P., Hensen, B.J., and Buick, I.S. (2002) Cordierite as a sensor of fluid conditions in high-grade metamorphism and crustal anatexis. Journal of Metamorphic Geology, 20, 71–86.

Hashizume, K., and Chaussidon, M. (2005) A non-terrestrial ^{16}O-rich isotopic composition for the protosolar nebula. Nature, 434, 619–622.

Hashizume, K., Chaussidon, M., Marty, B., and Robert, F. (2000) Solar wind record on the Moon: Deciphering presolar from planetary nitrogen. Science, 290, 1142–1145.

Hashizume, K., Chaussidon, M., Marty, B., and Terada, K. (2002) Micro-analyses of carbon isotopic composition in lunar soil samples. Proceedings of the 33rd Lunar and Planetary Science Conference, 1465.

Haskin, L.A., and Warren, P.H. (1991) Lunar Chemistry. In G. Heiken, D.T. Vaniman, and B.M. French, Eds., Lunar Sourcebook: A user's guide to the Moon, 357–474. Cambridge University Press, U.K.

Hauri, E.H., Gaetani, G.A., and Green, T.H. (2006) Partitioning of water during melting of the Earth's upper mantle at H_2O-undersaturated conditions. Earth and Planetary Science Letters, 248, 715–734.

Hauri, E.H., Weinreich, T., Saal, A.E., Rutherford, M.C., and Van Orman, J.A. (2011) High pre-eruptive water contents preserved in lunar melt inclusions. Science, 333, 213–215.

Hauri, E.H., Saal, A.E., Rutherford, M.C., and Van Orman, J.A. (2015) Water in the Moon's interior: Truth and consequences. Earth and Planetary Science Letters, 409, 252–264.

Heber, V.S., Baur, H., and Wieler, R. (2003) Helium in lunar samples analyzed by high-resolution stepwise etching: Implications for the temporal constancy of solar wind isotopic composition. Astrophysical Journal, 597, 602–614.

Heiken, G.H., and McKay, D.S. (1974) Lunar deposits of possible pyroclastic origin. Geochimica et Cosmochimica Acta, 38, 1703–1718.

Hendrix, A.R., Retherford, K.D., Gladstone, G.R., Hurley, D.M., Feldman, P.D., Egan, A.F., Kaufmann, D.E., Miles, P.F., Parker, J.W., Horvath, D., and others. (2012) The lunar far-UV albedo: Indicator of hydration and weathering. Journal of Geophysical Research, 117, E12001.

Herzberg, C.T. (1983) The reaction forsterite + cordierite = aluminous orthopyroxene + spinel in the system MgO-Al_2O_3-SiO_2. Contributions to Mineralogy and Petrology, 84, 84–90.

Herzberg, C.T., and Baker, M.B. (1980) The cordierite- to spinel-cataclasite transition: Structure and formation of the lunar crust. Proceedings of the Conference on the Lunar Highlands. Houston, Texas, 113–132.

Hess, P.C., and Parmentier, E.M. (1995) A model for the thermal and chemical evolution of the Moons interior: Implications for the onset of mare volcanism. Earth and Planetary Science Letters, 134, 501–514.

Hibbitts, C.A., Grieves, G.A., Poston, M.J., Dyar, M.D., Alexandrov, A.B., Johnson, M.A., and Orlando, T.M. (2011) Thermal stability of water and hydroxyl on the surface of the Moon from temperature-programmed desorption measurements of lunar analog materials. Icarus, 213, 64–72.

Hirschmann, M.M., and Withers, A.C. (2008) Ventilation of CO_2 from a reduced mantle and consequences for the early Martian greenhouse. Earth and Planetary Science Letters, 270, 147–155.

Hirschmann, M.M., Withers, A.C., Ardia, P., and Foley, N.T. (2012) Solubility of molecular hydrogen in silicate melts and consequences for volatile evolution of terrestrial planets. Earth and Planetary Science Letters, 345, 38–48.

Holloway, J.R. (1998) Graphite-melt equilibria during mantle melting: constraints on CO_2 in MORB magmas and the carbon content of the mantle. Chemical Geology, 147, 89–97.

Holloway, J.R., and Jakobsson, S. (1986) Volatile solubilities in magmas: Transport of volatiles from mantles to planet surfaces. Journal of Geophysical Research-Solid Earth and Planets, 91, D505–D508.

Holness, M.B., Tegner, C., Nielsen, T.F.D., Stripp, G., and Morse, S.A. (2007) A textural record of solidification and cooling in the Skaergaard intrusion, East Greenland. Journal of Petrology, 48, 2359–2377.

Holness, M.B., Richardson, C., and Anand, M. (2012) A new proxy for dolerite crystallisation times in planetary samples. Proceedings of the 43rd Lunar and Planetary Science Conference, The Woodlands, Texas, Abstract 1589.

Housley, R.M., Grant, R.W., and Paton, N.E. (1973) Origin and characteristics of excess Fe metal in lunar glass welded aggregates. Proceedings of the Fourth Lunar Science Conference, 2737–2749.

Hughes, J.M., Jolliff, B.L., and Gunter, M.E. (2006) The atomic arrangement of merrillite from the Fra Mauro Formation, Apollo 14 lunar mission: The first structure of merrillite from the Moon. American Mineralogist, 91, 1547–1552.

Hui, H.J., Peslier, A.H., Zhang, Y.X., and Neal, C.R. (2013) Water in lunar anorthosites and evidence for a wet early Moon. Nature Geoscience, 6, 177–180.

Humayun, M., and Clayton, R.N. (1995) Potassium isotope cosmochemistry: Genetic implications of volatile element depletion. Geochimica et Cosmochimica Acta, 59, 2131–2148.

Hurley, D.M., Gladstone, G.R., Stern, S.A., Retherford, K.D., Feldman, P.D., Pryor, W., Egan, A.F., Greathouse, T.K., Kaufmann, D.E., Steffl, A.J., and others. (2012) Modeling of the vapor release from the LCROSS impact: 2. Observations from LAMP. Journal of Geophysical Research: Planets, 117, E00H07.

Huss, G.R., Nagashima, K., Jurewicz, A.J.G., Burnett, D.S., and Olinger, C.T. (2012) The isotopic composition and fluence of solar-wind nitrogen in a genesis B/C array collector. Meteoritics and Planetary Science, 47, 1436–1448.

Ichimura, A.S., Zent, A.P., Quinn, R.C., Sanchez, M.R., and Taylor, L.A. (2012) Hydroxyl (OH) production on airless planetary bodies: Evidence from H^+/D^+ ion-beam experiments. Earth and Planetary Science Letters, 345, 90–94.

Ireland, T.R., Holden, P., Norman, M.D., and Clarke, J. (2006) Isotopic enhancements of O^{17} and O^{18} from solar wind particles in the lunar regolith. Nature, 440, 776–778.

Irwin, H., Curtis, C., and Coleman, M. (1977) Isotopic evidence for source of diagenetic carbonates formed during burial of organic-rich sediments. Nature, 269, 209–213.

Jadweb, J. (1973) Rare micron-size minerals in lunar fines. Proceedings of the Fourth Lunar Science Conference, 861–874.

Jambon, A. (1994) Earth degassing and large-scale geochemical cycling of volatile elements. Reviews in Mineralogy, 30, 479–517.

Jolliff, B.L. (1999) Large-scale separation of K-frac and REEP-frac in the source regions of Apollo impact-melt breccias, and a revised estimate of the KREEP

composition. In G.A. Snyder, C.R. Neal, and W.G. Ernst, Eds., Planetary Petrology and Geochemistry, p. 135–154. Bellweather Publishing for Geological Society of America, Washington D.C.
Jolliff, B.L., Haskin, L.A., Colson, R.O., and Wadhwa, M. (1993) Partitioning in REE-saturating minerals: Theory, experiment, and modeling of whitlockite, apatite, and evolution of lunar residual magmas. Geochimica et Cosmochimica Acta, 57, 4069–4094.
Jolliff, B.L., Gillis, J.J., Haskin, L.A., Korotev, R.L., and Wieczorek, M.A. (2000) Major lunar crustal terranes: Surface expressions and crust-mantle origins. Journal of Geophysical Research: Planets, 105, 4197–4216.
Jolliff, B.L., Hughes, J.M., Freeman, J.J., and Zeigler, R.A. (2006) Crystal chemistry of lunar merrillite and comparison to other meteoritic and planetary suites of whitlockite and merrillite. American Mineralogist, 91, 1583–1595.
Jolliff, B.L., Wiseman, S.A., Lawrence, S.J., Tran, T.N., Robinson, M.S., Sato, H., Hawke, B.R., Scholten, F., Oberst, J., Hiesinger, H., and others. (2011) Non-mare silicic volcanism on the lunar farside at Compton-Belkovich. Nature Geoscience, 4, 566–571.
Jovanovic, S., and Reed, G.W. Jr. (1973) Trace element studies in Apollo 16 samples. Proceedings of the Third Lunar Science Conference, 418.
——— (1975) Cl and P_2O_5 systematics: Clues to early lunar magmas. Proceedings of the Sixth Lunar Science Conference, Houston, Texas, 1737–1751.
Jovanovic, S., Jensen, K., and Reed, G.W. Jr. (1976) Trace elements and the evolution of lunar rocks. Proceedings of the Seventh Lunar Science Conference, Houston, Texas, 437–439.
Joy, K.H., Zolensky, M.E., Nagashima, K., Huss, G.R., Ross, D.K., McKay, D.S., and Kring, D.A. (2012) Direct detection of projectile relics from the end of the Lunar Basin-Forming Epoch. Science, 336, 1426–1429.
Kaplan, I.R. (1975) Stable isotopes as a guide to biogeochemical processes. Proceedings of the Royal Society B, 189, 183–211.
Kaplan, I.R., and Petrowski, C. (1971) Carbon and sulfur isotope studies on Apollo 12 lunar samples. Proceedings of the Second Lunar Science Conference, Houston, Texas, 1397–1406.
Kaplan, I.R., and Smith, J.W. (1970) Concentration and isotopic composition of carbon and sulfur in Apollo 11 lunar samples Science, New Series, 167, 541–543.
Kaplan, I.R., Smith, J.W., and Ruth, E. (1970) Carbon and sulfur concentration and isotopic composition in Apollo 11 lunar samples. Proceedings of the Apollo 11 Lunar Science Conference, 1317–1329.
Kaplan, I.R., Kerridge, J.F., and Petrowski, C. (1976) Light element geochemistry of the Apollo 15 site Proceedings of the Seventh Lunar Science Conference, Houston, Texas, 481–492.
Kaufmann, R., Long, A., Bentley, H., and Davis, S. (1984) Natural chlorine isotope variations. Nature, 309, 338–340.
Kerber, L., Head, J.W., Solomon, S.C., Murchie, S.L., Blewett, D.T., and Wilson, L. (2009) Explosive volcanic eruptions on Mercury: Eruption conditions, magma volatile content, and implications for interior volatile abundances. Earth and Planetary Science Letters, 285, 263–271.
Kerridge, J.F. (1975) Solar nitrogen: Evidence for a secular increase in ratio of nitrogen-15 to nitrogen-14. Science, 188, 162–164.
——— (1989) What has caused the secular increase in solar N^{15}? Science, 245, 480–486.
——— (1993) Long-term compositional variation in solar corpuscular radiation: Evidence from nitrogen isotopes in the lunar regolith. Reviews of Geophysics, 31, 423–437.
Kerridge, J.F., Kaplan, I.R., and Lesley, F.D. (1974) Accumulation and isotopic evolution of carbon on the lunar surface. Proceedings of the Fifth Lunar Conference, 2, 1855–1868.
Kerridge, J.F., Kaplan, I.R., and Petrowski, C. (1975a) Evidence for meteoritic sulfur in the lunar regolith. Proceedings of the Sixth Lunar Science Conference, Houston, Texas, 2151–2162.
Kerridge, J.F., Kaplan, I.R., Petrowski, C., and Chang, S. (1975b) Light element geochemistry of the Apollo 16 site Geochimica et Cosmochimica Acta, 39, 137–162.
Kerridge, J.F., Kaplan, I.R., Kung, C.C., Winter, D.A., and Friedman, D.L. (1978) Light element geochemistry of the Apollo 12 site Geochimica et Cosmochimica Acta, 42, 391–402,
Kerridge, J.F., Eugster, O., Kim, J.S., and Marti, K. (1991) Nitrogen isotopes in the 74001/74002 double-drive tube from Shorty Crater, Apollo 17. Proceedings of the 21st Lunar and Planetary Science Conference, Houston, Texas, 291–299.
Killen, R.M., Potter, A.E., Hurley, D.M., Plymate, C., and Naidu, S. (2010) Observations of the lunar impact plume from the LCROSS event. Geophysical Research Letters, 37, L23201.
Klein, N., and Rutherford, M.J. (1998) Volcanic gas formed during eruption of Apollo 17 orange glass magma; Evidence from glassy melt inclusions and experiments. Proceedings of the 29th Lunar and Planetary Science Conference, Houston, Texas, Abstract 1448.
Klima, R., Cahill, J., Hagerty, J., and Lawrence, D. (2013) Remote detection of magmatic water in Bullialdus Crater on the Moon. Nature Geoscience, 6, 737–741.
Kothari, B.K., and Goel, P.S. (1973) Nitrogen in lunar samples. Proceedings of the Fourth Lunar Science Conference, Houston, Texas, 1587–1596.
Krahenbuhl, U., Ganapathy, R., Morgan, J.W., and Anders, E. (1973) Volatile elements in Apollo 16 samples: Implications for highland volcanism and accretion history of the moon. Proceedings of the Fourth Lunar Science Conference, Houston, Texas, 1325–1348.
Krahenbuhl, U., Grutter, A., von Gunten, H.R., Meyer, G., Wegmuller, F., and Wyttenbach, A. (1977) Distribution of volatile and non-volatile elements in grain-size fractions of Apollo 17 Lunar Soils. Abstracts of the Lunar and Planetary Science Conference, 8, 561–563.
Kyser, T.K., and O'Neil, J.R. (1984) Hydrogen isotope systematics of submarine basalts. Geochimica et Cosmochimica Acta, 48, 2123–2133.
Lawrence, D.J., Feldman, W.C., Barraclough, B.L., Binder, A.B., Elphic, R.C., Maurice, S., Miller, M.C., and Prettyman, T.H. (1999) High resolution measurements of absolute thorium abundances on the lunar surface. Geophysical Research Letters, 26, 2681–2684.
Lawrence, D.J., Elphic, R.C., Feldman, W.C., Prettyman, T.H., Gasnault, O., and Maurice, S. (2003) Small-area thorium features on the lunar surface. Journal of Geophysical Research: Planets, 108, 5102.
Lawrence, D.J., Feldman, W.C., Elphic, R.C., Hagerty, J.J., Maurice, S., McKinney, G.W., and Prettyman, T.H. (2006) Improved modeling of Lunar Prospector neutron spectrometer data: Implications for hydrogen deposits at the lunar poles. Journal of Geophysical Research: Planets, 111, 1–19.
Lawrence, D.J., Puetter, R.C., Elphic, R.C., Feldman, W.C., Hagerty, J.J., Prettyman, T.H., and Spudis, P.D. (2007) Global spatial deconvolution of Lunar Prospector Th abundances. Geophysical Research Letters, 34, L03201.
Lecuyer, C., Gillet, P., and Robert, F. (1998) The hydrogen isotope composition of seawater and the global water cycle. Chemical Geology, 145, 249–261.
Li, S., and Milliken, R.E. (2013) Quantitative mapping of lunar surface hydration with Moon Mineralogy Mapper (M^3) data. Proceedings of the 44th Lunar and Planetary Science Conference, Woodlands, Texas, Abstract 1337.
—— (2014) Quantitative mapping of hydration in lunar pyroclastic deposits: Insights into water from the lunar interior. Proceedings of the 45th Lunar and Planetary Science Conference. Woodlands, Texas, Abstract 2012.
Libby, W.F. (1971) Terrestrial and meteorite carbon appear to have the same isotopic composition. Proceedings of the National Academy of Sciences, 68, 377.
Libowitzky, E., and Beran, A. (2006) The structure of hydrous species in nominally anhydrous minerals: Information from polarized IR spectroscopy. Reviews in Mineralogy and Geochemistry, 62, 29–52.
Liebscher, A., and Heinrich, C.A. (2007) Fluid-fluid interactions in the Earth's lithosphere. Reviews in Mineralogy and Geochemistry, 65, 1–13.
Lindstrom, M.M., and Salpas, P.A. (1983) Geochemical studies of feldspathic fragmental breccias and the nature of North Ray crater ejecta. Proceedings 13th Lunar and Planetary Science Conference, A671–A683.
Liu, Y., and Taylor, L.A. (2011) Characterization of lunar dust and a synopsis of available lunar simulants. Planetary and Space Science, 59, 1769–1783.
Liu, Y., Guan, Y.B., Zhang, Y.X., Rossman, G.R., Eiler, J.M., and Taylor, L.A. (2012a) Direct measurement of hydroxyl in the lunar regolith and the origin of lunar surface water. Nature Geoscience, 5, 779–782.
Liu, Y., Mosenfelder, J.L., Guan, Y., Rossman, G.R., Eiler, J.M., and Taylor, L.A. (2012b) SIMS analysis of water abundances in nominally anhydrous minerals in lunar basalts. Proceedings of the 43rd Lunar and Planetary Science Conference, Woodlands, Texas, 1866.
Liu, Y., Guan, Y., Chen, Y., Zhang, Y., Eiler, J.M., Rossman, G.R., and Taylor, L.A. (2013) Hydroxyl in lunar regolith: Dependence on soil composition and maturity. Proceedings of the 44th Lunar and Planetary Science Conference, The Woodlands, Texas, Abstract 2203.
Lodders, K. (2003) Solar system abundances and condensation temperatures of the elements. Astrophysical Journal, 591, 1220–1247.
Lodders, K., and Fegley, B. (1998) The Planetary Scientist's Companion. Oxford University Press, New York.
Longhi, J. (1991) Comparative liquidus equilibria of hypersthene-normative basalts at low pressure. American Mineralogist, 76, 785–800.
——— (1992a) Experimental petrology and petrogenesis of mare volcanics. Geochimica et Cosmochimica Acta, 56, 2235–2251.
——— (1992b) Origin of picritic green glass magmas by polybaric fractional fusion. Proceedings of Lunar and Planetary Science, 22, 343–353.
——— (2003) A new view of lunar ferroan anorthosites: Postmagma ocean petrogenesis. Journal of Geophysical Research: Planets, 108, 5083.
——— (2006) Petrogenesis of picritic mare magmas: Constraints on the extent of early lunar differentiation. Geochimica et Cosmochimica Acta, 70, 5919–5934.
Lucey, P., Korotev, R.L., Gillis, J.J., Taylor, L.A., Lawrence, D., Campbell, B.A., Elphic, R., Feldman, B., Hood, L.L., Hunten, D., and others. (2006) Understanding the lunar surface and space-moon interactions. Reviews in Mineralogy and Geochemistry, 60, p. 83–219.
Marty, B. (2012) The origins and concentrations of water, carbon, nitrogen and noble gases on Earth. Earth and Planetary Science Letters, 313, 56–66.
Marty, B., Hashizume, K., Chaussidon, M., and Wieler, R. (2003) Nitrogen isotopes on the Moon: Archives of the solar and planetary contributions to the inner solar system. Space Science Reviews, 106, 175–196.
Marty, B., Chaussidon, M., Wiens, R.C., Jurewicz, A.J.G., and Burnett, D.S. (2011) A N^{15}-poor isotopic composition for the solar system as shown by Genesis solar wind samples. Science, 332, 1533–1536.

Marvin, U.B., Carey, J.W., and Lindstrom, M.M. (1989) Cordierite-spinel troctolite, a new Mg-rich lithology from the lunar highlands. Science, 243, 925–928.
Mathew, K.J., and Marti, K. (2001) Lunar nitrogen: indigenous signature and cosmic-ray production rate. Earth and Planetary Science Letters, 184, 659–669.
Mathez, E.A., and Webster, J.D. (2005) Partitioning behavior of chlorine and fluorine in the system apatite-silicate melt-fluid. Geochimica et Cosmochimica Acta, 69, 1275–1286.
McCallum, I.S., and Schwartz, J.M. (2001) Lunar Mg suite: Thermobarometry and petrogenesis of parental magmas. Journal of Geophysical Research: Planets, 106, 27969–27983.
McCord, T.B., Taylor, L.A., Combe, J.P., Kramer, G., Pieters, C.M., Sunshine, J.M., and Clark, R.N. (2011) Sources and physical processes responsible for OH/H_2O in the lunar soil as revealed by the Moon Mineralogy Mapper (M-3). Journal of Geophysical Research: Planets, 116, E00G05.
McCubbin, F.M., Smirnov, A., Nekvasil, H., Wang, J., Hauri, E., and Lindsley, D.H. (2010a) Hydrous magmatism on Mars: A source of water for the surface and subsurface during the Amazonian. Earth and Planetary Science Letters, 292, 132–138.
McCubbin, F.M., Steele, A., Hauri, E.H., Nekvasil, H., Yamashita, S., and Hemley, R.J. (2010b) Nominally hydrous magmatism on the Moon. Proceedings of the National Academy of Sciences, 107, 11223–11228.
McCubbin, F.M., Steele, A., Nekvasil, H., Schnieders, A., Rose, T., Fries, M., Carpenter, P.K., and Jolliff, B.L. (2010c) Detection of structurally bound hydroxyl in fluorapatite from Apollo Mare basalt 15058,128 using TOF-SIMS. American Mineralogist, 95, 1141–1150.
McCubbin, F.M., Jolliff, B.L., Nekvasil, H., Carpenter, P.K., Zeigler, R.A., Steele, A., Elardo, S.M., and Lindsley, D.H. (2011) Fluorine and chlorine abundances in lunar apatite: Implications for heterogeneous distributions of magmatic volatiles in the lunar interior. Geochimica et Cosmochimica Acta, 75, 5073–5093.
McCubbin, F.M., Hauri, E.H., Elardo, S.M., Vander Kaaden, K.E., Wang, J., and Shearer, C.K. Jr. (2012a) Hydrous melting of the martian mantle produced both depleted and enriched shergottites. Geology, 40, 683–686.
McCubbin, F.M., Riner, M.A., Vander Kaaden, K.E., and Burkemper, L.K. (2012b) Is Mercury a volatile-rich planet? Geophysical Research Letters, 39, L09202.
McCubbin, F.M., Shearer, C.K., and Sharp, Z.D. (2012c) Magmatic volatile reservoirs on the moon and the chemical signatures of urKREEP. Proceedings of the Second Conference on the Lunar Highlands Crust. Houston, Texas, Abstract 9035.
McCubbin, F.M., Elardo, S.M., Shearer, C.K., Smirnov, A., Hauri, E.H., and Draper, D.S. (2013) A petrogenetic model for the comagmatic origin of chassignites and nakhlites: Inferences from chlorine-rich minerals, petrology, and geochemistry. Meteoritics and Planetary Science, 48, 819–853.
McCubbin, F.M., Vander Kaaden, K.E., Tartèse, R., Boyce, J.W., Mikhail, S., Whitson, E.S., Bell, A.S., Anand, M., Franchi, I.A., Wang, J., and Hauri, E.H. (2015) Experimental investigation of F, Cl, and OH partitioning between apatite and Fe-rich basaltic melt at 1.0–1.2 GPa and 950–1000 °C. American Mineralogist, 100, 1790–1802.
McEwing, C.E., Thode, H.G., and Rees, C.E. (1980) Sulfur isotope effects in the dissociation and evaporation of troilite: A possible mechanism for S^{34} enrichment in lunar soils. Geochimica et Cosmochimica Acta, 44, 565–571.
McKay, D.S., and Wentworth, S.J. (1992) Morphology and composition of condensates on Apollo 17 orange and black glass. In Lunar Science Institution, Workshop on Geology of the Apollo 17 Landing Site, 31–36.
——— (1993) Grain surface features of Apollo 17 orange and black glass. In Lunar and Planetary Institution, 24th Lunar and Planetary Science Conference, Part 2: G-M961–962.
McKay, D.S., Clanton, U.S., and Ladle, G. (1973a) Scanning electron microscope study of Apollo 15 green glass. Proceedings of the Fourth Lunar Science Conference, Houston, Texas, 225–238.
——— (1973b) Surface morphology of Apollo 15 green glass spheres. Proceedings of the Fourth Lunar Science Conference, Houston, Texas, 484–486.
McKay, D.S., Clanton, U.S., Morrison, D.A., and Ladle, G.H. (1972) Vapor phase crystallization in Apollo 14 breccia. Proceedings of the Third Lunar Science Conference, Houston, Texas, 739–752.
McKay, D.S., Heiken, G., Basu, A., Blanford, G., Simon, S., Reedy, R., French, B.M., and Papike, J.J. (1991) The Lunar Regolith. In G. Heiken, D.T. Vaniman, and B.M. French, EdsLunar Sourcebook: A User's Guide to the Moon, p. 285–356. Cambridge University Press, U.K.
McMillan, P.F. (1994) Water solubility and speciation models. Reviews in Mineralogy, 30, 131–156.
Merlivat, L., Nief, G., and Roth, E. (1972) Deuterium content of lunar material. Proceedings of the Third Lunar Science Conference, Houston, Texas, 1473–1477.
Merlivat, L., Lelu, M., Nief, G., and Roth, E. (1974) Deuterium, hydrogen, and water content of lunar material. Proceedings of the Fifth Lunar Conference, Houston, Texas, 1885–1895.
——— (1976) Spallation deuterium in rock 70215. Proceedings of the Seventh Lunar Science Conference, Houston, Texas, 649–658.
Meyer, C. (1990) A brief literature review of observations pertaining to condensed volatile coatings on lunar volcanic glasses. Workshop on Lunar Volcanic Glasses: Scientific and Resource Potential, p. 50–51.
——— (2010) Lunar sample compendium. Proceedings of the 41st Lunar and Planetary Science Conference, Woodlands, Texas, Abstract 1016.
Meyer, C. Jr., McKay, D.S., Anderson, D.H., and Butler, P. Jr. (1975) The source of sublimates on the Apollo 15 green and Apollo 17 orange glass samples. Proceedings of the Sixth Lunar Science Conference, 1673–1699.
Miller, R.S., Nerurkar, G., and Lawrence, D.J. (2012) Enhanced hydrogen at the lunar poles: New insights from the detection of epithermal and fast neutron signatures. Journal of Geophysical Research, 117, E11007.
Mills, R.D., Simon, J.I., Alexander, C.M.O., Wang, J., Christoffersen, R., and Rahman, Z. (2014) Chemical zoning of feldspars in lunar granitoids: Implications for the origins of lunar silicic magmas. 45th Lunar and Planetary Science Conference, The Woodlands, Texas, 1547.
Mitrofanov, I.G., Sanin, A.B., Boynton, W.V., Chin, G., Garvin, J.B., Golovin, D., Evans, L.G., Harshman, K., Kozyrev, A.S., Litvak, M.L., and others. (2010) Hydrogen mapping of the lunar South Pole using the LRO neutron detector experiment LEND. Science, 330, 483–486.
Mitrofanov, I., Litvak, M., Sanin, A., Malakhov, A., Golovin, D., Boynton, W., Droege, G., Chin, G., Evans, L., Harshman, K., and others. (2012) Testing polar spots of water-rich permafrost on the Moon: LEND observations onboard LRO. Journal of Geophysical Research, 117, E00H27.
Moore, C.B., Gibson, E.K., Larimer, J.W., Lewis, C.F., and Nichiporuk, W. (1970) Total carbon and nitrogen abundances in Apollo 11 lunar samples and selected achondrites and basalts Proceedings of the Apollo 11 Lunar Science Conference, 1375–1382.
Morgan, J.W., and Wandless, G.A. (1979) 74001 drive tube: Siderophile elements match IIB iron meteorite pattern. Proceedings of the 10th Lunar and Planetary Science Conference, 327–340.
——— (1984) Surface-correlated trace elements in 15426 lunar glasses. Proceedings of the 15th Lunar and Planetary Science Conference 562–563.
Mortimer, J., Verchovsky, A.B., Anand, M., Gilmour, I., and Pillinger, C.T. (2015) Simultaneous analysis of abundance and isotopic composition of nitrogen, carbon, and noble gases in lunar basalts: Insights into interior and surface processes on the Moon. Icarus, in press, http://dx.doi.org/10.1016/j.icarus.2014.10.006.
Mosenfelder, J.L., and Rossman, G.R. (2013a) Analysis of hydrogen and fluorine in pyroxenes: I. Orthopyroxene. American Mineralogist, 98, 1026–1041.
——— (2013b) Analysis of hydrogen and fluorine in pyroxenes: II. Clinopyroxene. American Mineralogist, 98, 1042–1054.
Mosenfelder, J.L., Le Voyer, M., Rossman, G.R., Guan, Y., Bell, D.R., Asimow, P.D., and Eiler, J.M. (2011) Analysis of hydrogen in olivine by SIMS: Evaluation of standards and protocol. American Mineralogist, 96, 1725–1741.
Muller, O. (1974) Solar wind nitrogen and indigenous nitrogen in Apollo 17 lunar samples. Proceedings of the Fifth Lunar Conference, Houston, Texas, 1907–1918.
Murty, S.V.S., and Goswami, J.N. (1992) Nitrogen, noble gases, and nuclear tracks in lunar meteorites MAC88104/105. Proceedings of the 22nd Lunar and Planetary Science Conference, Houston, Texas, 225–237.
Nadeau, S.L., Epstein, S., and Stolper, E. (1999) Hydrogen and carbon abundances and isotopic ratios in apatite from alkaline intrusive complexes, with a focus on carbonatites. Geochimica et Cosmochimica Acta, 63, 1837–1851.
Nakajima, M., and Stevenson, D.J. (2014) Investigation of the initial state of the Moon-forming disk: Bridging SPH simulations and hydrostatic models. Icarus, 233, 259–267.
Naughton, J.J., Hammond, D.A., Margolis, S.V., and Muenow, D.W. (1972) The nature and effect of the volatile cloud produced by volcanic and impact events on the Moon as derived from a terrestrial volcanic model. Proceedings of the Third Lunar Science Conference, 2015–2024.
Neal, C.R., and Taylor, L.A. (1992) Petrogenesis of mare basalts: A record of lunar volcanism. Geochimica et Cosmochimica Acta, 56, 2177–2211.
Newman, S., Epstein, S., and Stolper, E. (1988) Water, carbon dioxide, and hydrogen isotopes in glasses from the CA 1340 AD eruption of the Mono craters, California: Constraints on degassing phenomina and initial volatile content. Journal of Volcanology and Geothermal Research, 35, 75–96.
Nicholis, M.G., and Rutherford, M.J. (2009) Graphite oxidation in the Apollo 17 orange glass magma: Implications for the generation of a lunar volcanic gas phase. Geochimica et Cosmochimica Acta, 73, 5905–5917.
Nier, A.O., and Schlutter, D.J. (1994) Helium and neon in lunar ilmenites of different antiquities. Meteoritics, 29, 662–672.
Norman, M.D. (1982) Petrology of lunar suevitic breccia 67016. Proceedings 12th Lunar and Planetary Science Conference, 235–252.
Norman, M.D., Keil, K., Griffin, W.L., and Ryan, C.G. (1995) Fragments of ancient lunar crust: Petrology and geochemistry of ferroan noritic anorthosites from the Descartes Region of the Moon. Geochimica et Cosmochimica Acta, 59, 831–847.
Norris, S.J., Swart, P.K., Wright, I.P., and Pillinger, C.T. (1983) Is carbon in the ancient solar wind isotopically light? Proceedings of the 14th Lunar and Planetary Science Conference, 566–567.
Nozette, S., Lichtenberg, C.L., Spudis, P., Bonner, R., Ort, W., Malaret, E., Robinson, M., and Shoemaker, E.M. (1996) The Clementine bistatic radar experiment. Science, 274, 1495–1498.
Nunes, P.D., and Tatsumot, M. (1973) Excess lead in Rusty Rock 66095 and im-

plications for an early lunar differentiation. Science, 182, 919–920.
O'Leary, J.A., Gaetani, G.A., and Hauri, E.H. (2010) The effect of tetrahedral Al(3+) on the partitioning of water between clinopyroxene and silicate melt. Earth and Planetary Science Letters, 297, 111–120.
Ozima, M., Seki, K., Terada, N., Miura, Y.N., Podosek, F.A., and Shinagawa, H. (2005) Terrestrial nitrogen and noble gases in lunar soils. Nature, 436, 655–659.
Ozima, M., Yin, Q.Z., Podosek, F., and Miura, Y. (2008) Toward understanding early Earth evolution: Prescription for approach from terrestrial noble gases and light elements records in lunar soils. Geochimica et Cosmochimica Acta, 72, A714–A714.
Pahlevan, K., and Stevenson, D.J. (2007) Equilibration in the aftermath of the lunar-forming giant impact. Earth and Planetary Science Letters, 262, 438–449.
Paniello, R.C., Day, J.M.D., and Moynier, F. (2012) Zinc isotopic evidence for the origin of the Moon. Nature, 490, 376–379.
Papike, J.J., Simon, S.B., and Laul, J.C. (1982) The lunar regolith: Chemistry, mineralogy, and petrology. Reviews of Geophysics, 20, 761–826.
Papike, J.J., Simon, S.B., White, C., and Laul, J.C. (1981) The relationship of the lunar regolith <10 μm fraction and agglutinates. Part I: A model for agglutinate formation and some indirect supportive evidence. Proceedings of the 12th Lunar and Planetary Science Conference, Houston, Texas, 409–420.
Papike, J.J., Taylor, L.A., and Simon, S. (1991) Lunar minerals. In G. Heiken, D.T. Vaniman, and B.M. French, Eds., Lunar Sourcebook: A User's Guide to the Moon, p. 121–181. Cambridge University Press, U.K.
Papike, J.J., Ryder, G., and Shearer, C.K. (1998) Lunar samples. Reviews in Mineralogy, 36, 5-1–5-234.
Patino-Douce, A.E., and Roden, M. (2006) Apatite as a probe of halogen and water fugacities in the terrestrial planets. Geochimica et Cosmochimica Acta, 70, 3173–3196.
Patino-Douce, A.E., Roden, M.F., Chaumba, J., Fleisher, C., and Yogodzinski, G. (2011) Compositional variability of terrestrial mantle apatites, thermodynamic modeling of apatite volatile contents, and the halogen and water budgets of planetary mantles. Chemical Geology, 288, 14–31.
Pernet-Fisher, J.F., Howarth, G.H., Liu, Y., Chen, Y., and Taylor, L.A. (2014) Estimating the lunar mantle water budget from phosphates: Complications associated with silicate-liquid-immiscibility. Geochimica et Cosmochimica Acta, 144, 326–341.
Petro, N.E., Isaacson, P.J., Pieters, C.M., Jolliff, B.L., Carter, L.M., and Klima, R.L. (2013) Presence of OH/H_20 Associated with the Lunar Compton-Belkovich volcanic complex identified by the Moon Mineralogy Mapper (M^3). Proceedings of the 44th Lunar and Planetary Science Conference, Woodlands, Texas, Abstract 2668.
Petrowski, C., Kerridge, J. F., and Kaplan, I.R. (1974) Light element geochemistry of the Apollo 17 site. Proceedings of the Fifth Lunar Science Conference, Houston, Texas, 1939–4948.
Pieters, C.M., and Taylor, L.A. (2003) Systematic global mixing and melting in lunar soil evolution. Geophysical Research Letters, 30, 2048.
Pieters, C.M., Goswami, J.N., Clark, R.N., Annadurai, M., Boardman, J., Buratti, B., Combe, J.P., Dyar, M.D., Green, R., Head, J.W., and others. (2009) Character and spatial distribution of OH/H_2O on the surface of the Moon seen by M-3 on Chandrayaan-1. Science, 326, 568–572.
Pillinger, C.T. (1979) Solar-wind exposure effects in the lunar soil. Reports on Progress in Physics, 42, 897–960.
Poitrasson, F., Halliday, A.N., Lee, D.C., Levasseur, S., and Teutsch, N. (2004) Iron isotope differences between Earth, Moon, Mars and Vesta as possible records of contrasted accretion mechanisms. Earth and Planetary Science Letters, 223, 253–266.
Poston, M.J., Aleksandrov, A.B., Grieves, G.A., Hibbitts, C.A., Dyar, M.D., and Orlando, T.M. (2013a) Thermal stability of adsorbed water molecules on lunar materials. Proceedings of the 44th Lunar and Planetary Science Conference, 2177.
Poston, M.J., Grieves, G.A., Aleksandrov, A.B., Hibbitts, C.A., Dyar, M.D., and Orlando, T.M. (2013b) Water interactions with micronized lunar surrogates JSC-1A and albite under ultra-high vacuum with application to lunar observations. Journal of Geophysical Research: Planets, 105–115, http://dx.doi.org/10.1029/2012JE004283.
Prissel, T.C., Parman, S.W., Jackson, C.R.M., Dhingra, D., Ganskow, G., Cheek, L., and Rutherford, M.J. (2012) Melt-wallrock reactions on the Moon: Experimental constraints on the formation of newly discovered Mg-spinel anorthosites. Proceedings of the 43rd Lunar and Planetary Science Conference, The Woodlands, Texas, Abstract 2743.
Provencio, P.P., Shearer, C.K., and Brearley, A.J. (2013) Driving fumarole activity on the Moon 2.Nano-Scale textural and chemical analysis of alteration in "Rusty Rock" 66095. Proceedings of the 44th Lunar and Planetary Science Conference, The Woodlands, Texas, Abstract 1664.
Ramdohr, P. (1972) Lunar pentlandite and sulfidization reactions in microbreccia 14315,9. Earth and Planetary Science Letters, 15, 113–115.
Reed, G.W., and Jovanovic, S. (1973a) Halogens in LUNA 16 and LUNA 20 soils. Geochimica et Cosmochimica Acta, 37, 1007–1009.
Reed, G.W. Jr., and Jovanovic, S. (1973b) Fluorine in lunar samples: implications concerning lunar fluorapatite. Geochimica et Cosmochimica Acta, 37, 1457–1462.
——— (1981) The significance of Cl/P_2O_5 ratios from lunar samples—A response. Proceedings of the 12th Lunar and Planetary Science Conference, 333–336.
Reed, G.W., Jovanovi. S, and Fuchs, L.H. (1971) Fluorine and other trace elements in lunar plagioclase concentrates. Earth and Planetary Science Letters, 11, 354–358.
Reed, G.W. Jr., Jovanovic, S., and Fuchs, L.H. (1972) Trace element relations between Apollo 14 and 15 and other lunar samples, and the implications of a moon-wide CI-KREEP coherence and Pt-metal noncoherence. Proceedings of the Third Lunar Science Conference, 1989–2001.
Reed, G.W. Jr., Jovanovic, S., and Allen, R.O. Jr. (1977) Volatile metal deposits on lunar soils—Relation to volcanism. Proceedings of the Eighth Lunar Science Conference, 3, 3917–3930.
Reedy, R.C. (1981) Cosmic-ray-produced stable nuclides: Various production rates and their implications. Proceedings of the 12th Lunar and Planetary Science Conference, Houston, Texas, 871–873.
Richet, P., Bottinga, Y., and Janoy, M. (1977) A review of hydrogen, carbon, nitrogen, oxygen, sulphur, and chlorine stable isotope fractionation among gaseous molecules. Annual Review Earth and Planetary Science, 5, 65–110.
Rigby, M.J., and Droop, G.T.R. (2008) The cordierite fluid monitor: case studies for and against its potential application. European Journal of Mineralogy, 20, 693–712.
Rigby, M.J., Droop, G.T.R., and Bromiley, G.D. (2008) Variations in fluid activity across the Etive thermal aureole, Scotland: Evidence from cordierite volatile contents. Journal of Metamorphic Geology, 26, 331–346.
Righter, K., Yang, H., Costin, G., and Downs, R.T. (2008) Oxygen fugacity in the Martian mantle controlled by carbon: New constraints from the nakhlite MIL 03346. Meteoritics and Planetary Science, 43, 1709–1723.
Ringwood, A.E., and Kesson, S.E. (1976) A dynamic model for mare basalt petrogenesis. Proceedings of the Seventh Lunar Science Conference, Houston, Texas, 1697–1722.
Robert, F., Gautier, D., and Dubrulle, B. (2000) The solar system D/H ratio: Observations and theories. Space Science Reviews, 92, 201–224.
Robinson, K.L., and Taylor, G.J. (2014) Heterogeneous distriubtion of water in the Moon. Nature Geoscience, 7, 401–408.
Robinson, K.L., Nagashima, K., and Taylor, G.J. (2013) D/H of intrusive moon rocks: Implications for lunar origin. Proceedings of the 44th Lunar and Planetary Science Conference, The Woodlands, Texas, Abstract 1327.
Rose, H.J., Cuttitta, F., Annell, C.S., Carron, M.K., Christian, R.P., Dwornik, E.J., Greenland, L.P., and Ligon, D.T. (1972) Compositional data for twenty one Fra Mauro materials. Proceedings of the 3rd Lunar Science Conference, 1215–1229.
Rossman, G.R. (1996) Studies of OH in nominally anhydrous minerals. Physics and Chemistry of Minerals, 23, 299–304.
Rutherford, M.J., and Papale, P. (2009) Origin of basalt fire-fountain eruptions on Earth versus the Moon. Geology, 37, 219–222.
Ryder, G. (1991) Lunar ferroan anorthosites and mare basalt sources: The mixed connection. Geophysical Research Letters, 18, 2065–2068.
Ryder, G., and Schuraytz, B.C. (2001) Chemical variation of the large Apollo 15 olivine-normative mare basalt rock samples. Journal of Geophysical Research: Planets, 106, 1435–1451.
Saal, A.E., Hauri, E.H., Lo Cascio, M., Van Orman, J.A., Rutherford, M.C., and Cooper, R.F. (2008) Volatile content of lunar volcanic glasses and the presence of water in the Moon's interior. Nature, 454, 192–195.
Saal, A.E., Hauri, E.H., Van Orman, J.A., and Rutherford, M.J. (2013) Hydrogen isotopes in lunar volcanic glasses and melt inclusions reveal a carbonaceous chondrite heritage. Science, 340, 1317–1320.
Sarafian, A.R., Roden, M.F., and Patino-Douce, A.E. (2013) The volatile content of Vesta: Clues from apatite in eucrites. Meteoritics and Planetary Science, 48, 2135–2154.
Sarafian, A.R., Nielsen, S.G., Marschall, H.R., McCubbin, F.M., and Monteleone, B.D. (2014) Early accretion of water in the inner solar system from a carbonaceous chondrite-like source. Science, 346, 623–626.
Sato, M. (1979) The driving mechanism of lunar pyroclastic eruptions inferred from the oxygen fugacity behavior of Apollo 17 orange glass. Proceedings of the 10th Lunar and Planetary Science Conference, Houston, Texas, 311–325.
Schmidt, M.W., Forien, M., Solferino, G., and Bagdassarov, N. (2012) Settling and compaction of olivin in basaltic magmas: an experimental study on the timescales of cumulate formation. Contributions to Mineralogy and Petrology, 164, 959–976.
Schultz, P.H., Hermalyn, B., Colaprete, A., Ennico, K., Shirley, M., and Marshall, W.S. (2010) The LCROSS cratering experiment. Science, 330, 468–472.
Sharp, Z.D., Barnes, J.D., Brearley, A.J., Chaussidon, M., Fischer, T.P., and Kamenetsky, V.S. (2007) Chlorine isotope homogeneity of the mantle, crust and carbonaceous chondrites. Nature, 446, 1062–1065.
Sharp, Z.D., Barnes, J.D., Fischer, T.P., and Halick, M. (2010a) An experimental determination of chlorine isotope fractionation in acid systems and applications to volcanic fumaroles. Geochimica et Cosmochimica Acta, 74, 264–273.
Sharp, Z.D., Shearer, C.K., McKeegan, K.D., Barnes, J.D., and Wang, Y.Q. (2010b) The chlorine isotope composition of the Moon and implications for an anhy-

drous mantle. Science, 329, 1050–1053.
Sharp, Z.D., McCubbin, F.M., and Shearer, C.K. (2013a) A hydrogen-based oxidation mechanism relevant to planetary formation. Earth and Planetary Science Letters, 380, 88–97.
Sharp, Z.D., Mercer, J.A., Jones, R.H., Brearley, A.J., Selverstone, J., Bekker, A., and Stachel, T. (2013b) The chlorine isotope composition of chondrites and Earth. Geochimica et Cosmochimica Acta, 107, 189–204.
Shearer, C.K., and Papike, J. (2005) Early crustal building processes on the moon: Models for the petrogenesis of the magnesian suite. Geochimica et Cosmochimica Acta, 69, 3445–3461.
Shearer, C.K., Papike, J.J., Galbreath, K.C., and Shimizu, N. (1991) Exploring the lunar mantle with secondary ion mass spectrometry: A comparison of lunar picritic glass beads from the Apollo 14 and Apollo 17 sites. Earth and Planetary Science Letters, 102, 134–147.
Shearer, C.K., Hess, P.C., Wieczorek, M.A., Pritchard, M.E., Parmentier, E.M., Borg, L.E., Longhi, J., Elkins-Tanton, L.T., Neal, C.R., Antonenko, I., and others. (2006) Thermal and magmatic evolution of the moon. Reviews in Mineralogy and Geochemistry, 60, 365–518.
Shearer, C.K., Burger, P.V., Guan, Y., Papike, J.J., Sutton, S.R., and Atudorei, N.V. (2012) Origin of sulfide replacement textures in lunar breccias. Implications for vapor element transport in the lunar crust. Geochimica et Cosmochimica Acta, 83, 138–158.
Shearer, C.K., Sharp, Z.D., Burger, P.V., McCubbin, F.M., Provencio, P.P., Brearley, A.J., and Steele, A. (2014) Chlorine distribution and its isotopic composition in "Rusty Rock" 66095. Implications for volatile element enrichments of "Rusty Rock" and lunar soils, origin of "rusty" alteration, and volatile element behavior on the Moon. Geochimica et Cosmochimica Acta, 83, 138–158.
Shearer, C.K., Elardo, S.M., Petro, N.E., Borg, L.E., and McCubbin, F.M. (2015) Origin of the lunar highlands Mg-suite plutonic rocks. An integrated petrology, geochemistry, chronology, and remote sensing perspective. American Mineralogist, 100, 294–325.
Silver, L.T. (1975) Volatile lead components in lunar regolith at the Apollo Mare Sites. Abstracts of the Lunar and Planetary Science Conference, 6, 738.
Simpson, R.A., and Tyler, G.L. (1999) Reanalysis of Clementine bistatic radar data from the lunar South Pole. Journal of Geophysical Research, 104, 3845–3862.
Skinner, B.J. (1970) High crystallization temperatures indicated for igneous rocks from Tranquillity-Base. Science, 167, 652–654.
Smith, J.V., Anderson, A.T., Newton, R.C., Olsen, E.J., Wyllie, P.J., Crewe, A.V., Isaacson, M.S., and Johnson, D. (1970) Petrologic history of the moon inferred from petrography, mineralogy, and petrogenesis of Apollo 11 rocks. Proceedings of the Apollo 11 Lunar Science Conference, 897–925.
Smith, J.W., and Kaplan, I.R. (1970) Endogenous carbon in carbonaceous meteorites. Science, 167, 1367–1370.
Smith, J.W., Kaplan, I.R., and Petrowski, C. (1973) Carbon, nitrogen, sulfur, helium, hydrogen, and metallic iron in Apollo 15 drill stem fines. Proceedings of the Fourth Lunar Science Conference, Houston, Texas, 1651–1656.
Smyth, J.R. (2006) Hydrogen in high pressure silicate and oxide mineral structures. Reviews in Mineralogy and Geochemistry, 62, 85–115.
Snyder, G.A., Taylor, L.A., and Neal, C.R. (1992) A chemical-model for generating the sources of mare basalts—combined equilibrium and fractional crystallization of the lunar magmasphere. Geochimica et Cosmochimica Acta, 56, 3809–3823.
Solomon, S.C., and Chaiken, J. (1976) Thermal expansion and thermal stress in the Moon and terrestrial planets: Clues to early thermal history. Proceedings of the Seventh Lunar Science Conference, Houston, Texas, 3229–3243.
Spicuzza, M.J., Day, J.M.D., Taylor, L.A., and Valley, J.W. (2007) Oxygen isotope constraints on the origin and differentiation of the Moon. Earth and Planetary Science Letters, 253, 254–265.
Spudis, P.D., Bussey, D.B.J., Baloga, S.M., Butler, B.J., Carl, D., Carter, L.M., Chakraborty, M., Elphic, R.C., Gillis-Davis, J.J., Goswami, J.N., and others. (2010) Initial results for the north pole of the Moon from Mini-SAR Chandrayaan-1 mission. Geophysical Research Letters, 37, L06204.
Spudis, P.D., Bussey, D.B.J., Baloga, S.M., Cahill, J.T.S., Glaze, L.S., Patterson, G.W., Raney, R.K., Thompson, T.W., Thomson, B.J., and Ustinov, E.A. (2013) Evidence for water ice on the moon: Results for anomalous polar craters from the LRO Mini-RF imaging radar. Journal of Geophysical Research: Planets, 118, 1–14.
Steele, A., McCubbin, F.M., Fries, M., Glamoclija, M., Kater, L., and Nekvasil, H. (2010) Graphite in an Apollo 17 impact melt breccia. Science, 329, 51.
Steele, A., McCubbin, F.M., Fries, M., Kater, L., Boctor, N.Z., Fogel, M.L., Conrad, P.G., Glamoclija, M., Spencer, M., Morrow, A.L., and others. (2012) A reduced organic carbon component in martian basalts. Science, 337, 212–215.
Stephant, A., and Robert, F. (2014) The negligible chondritic contribution in the lunar soils water. Proceedings of the National Academy of Sciences, 111, 15007–15012.
Stievenard, M., Jouzel, J., and Robert, F. (1990) The isotopic signature of hydrogen in lunar basalts. Proceedings of the 21st Lunar and Planetary Science Conference, 21, 1204–1205.
Stolper, E. (1982a) The speciation of water in silicate melts. Geochimica et Cosmochimica Acta, 46, 2609–2620.
——— (1982b) Water in silicate glasses: An infrared spectroscopic study. Contributions to Mineralogy and Petrology, 81, 1–17.
Stormer, J.C., and Carmichael, I.S.E. (1971) Fluorine-hydroxyl exchange in apatite and biotite: Potential igneous geothermometer. Contributions to Mineralogy and Petrology, 31, 121–131.
Sunshine, J.M., Farnham, T.L., Feaga, L.M., Groussin, O., Merlin, F., Milliken, R.E., and A'Hearn, M.F. (2009) Temporal and spatial variability of lunar hydration as observed by the Deep Impact Spacecraft. Science, 326, 565–568.
Symonds, R.B., Rose, W.I., Reed, M.H., Lichte, F.E., and Finnegan, D.L. (1987) Volatilization, transport and sublimation of metallic and nonmetallic elements in high-temperature gases at Merapi-volcano, Indonesia. Geochimica et Cosmochimica Acta, 51, 2083–2101.
Tarasov, L.S., Nasarov, M.A., Shevaleevsky, I.D., Makarov, E.S., and Ivanov, V.I. (1973) Mineralogy of anorthositic rocks from the region of the crater Apollonius C (Luna-20). Proceedings of the Fourth Lunar Science Conference, 4, 333–349.
Tartèse, R., and Anand, M. (2013) Late delivery of chondritic hydrogen into the lunar mantle: Insights from mare basalts. Earth and Planetary Science Letters, 361, 480–486.
Tartèse, R., Anand, M., Barnes, J.J., Starkey, N.A., Franchi, I.A., and Sano, Y. (2013) The abundance, distribution, and isotopic composition of hydrogen in the Moon as revealed by basaltic lunar samples: Implications for the volatile inventory of the Moon. Geochimica et Cosmochimica Acta, 122, 58–74.
Tartèse, R., Anand, M., Joy, K.H., and Franchi, I.A. (2014a) H and Cl isotope systematics of apatite in brecciated lunar meteorites Northwest Africa 4472, Northwest Africa 773, Sayh al Uhaymir 169, and Kalahari 009. Meteoritics and Planetary Science, 49, 2266–2289.
Tartèse, R., Anand, M., McCubbin, F.M., Elardo, S.M., Shearer, C.K. Jr., and Franchi, I.A. (2014b) Apatites in lunar KREEP basalts: The missing link to understanding the H isotope systematics of the Moon. Geology, 42, 363–366.
Tatsumoto, M., Premo, W.R., and Unruh, D.M. (1987) Origin of lead from green glass of Apollo 15426: A Search for primitive lunar lead. Proceedings of the 17th Lunar and Planetary Science Conference, Part 2, Journal of Geophysical Research, 92, E361–E371.
Taylor, B.E., Eichelberger, J.C., and Westrich, H.R. (1983) Hydrogen isotopic evidence of rhyolitic magma degassing during shallow intrusion and eruption. Nature, 306, 541–545.
Taylor, G.J., Warren, P., Ryder, G., Delano, J., Pieters, C., and Lofgren, G. (1991) Lunar Rocks. In G.H. Heiken, D.T. Vaniman, and D.M. French, Eds., The Lunar Source Book, p. 183–284. Cambridge University Press, U.K.
Taylor, L.A., and Burton, J.C. (1976) Experiments on the stability of FeOOH on the surface of the Moon. Meteoritics, 11, 225–230.
Taylor, L.A., and Williams, K.L. (1973) Cu-Fe-S Phases in Lunar Rocks. American Mineralogist, 58, 952–954.
Taylor, L.A., Mao, H.K., and Bell, P.M. (1973) "Rust" in the Apollo 16 rocks. Proceedings Fourth Lunar Science Conference, 829–839.
——— (1974) Identification of the hydrated iron oxide mineral akaganéite in Apollo 16 lunar rocks. Geology, 2, 429–432.
Taylor, L.A., Rossman, G.R., and Qu, Q. (1995) Where has all the lunar water gone? Proceedings of the 26th Lunar and Planetary Science Conference, 26, 1399.
Taylor, L.A., Pieters, C., Keller, L.P., Morris, R.V., McKay, D.S., Patchen, A., and Wentworth, S. (2001) The effects of space weathering on Apollo 17 mare soils: Petrographic and chemical characterization. Meteoritics and Planetary Science, 36, 285–299.
Taylor, L.A., Patchen, A., Mayne, R.G., and Taylor, D.H. (2004) The most reduced rock from the moon, Apollo 14 basalt 14053: Its unique features and their origin. American Mineralogist, 89, 1617–1624.
Taylor, L.A., Pieters, C., Patchen, A., Taylor, D.-H.S., Morris, R.V., Keller, L.P., and McKay, D.S. (2010) Mineralogical and chemical characterization of lunar highland soils: Insights into the space weathering of soils on airless bodies. Journal of Geophysical Research: Planets, 115, E02002.
Taylor, S.R. (2001) Solar System Evolution: A New Perspective, 460 p. Cambridge University Press, U.K.
Taylor, S.R., and Jakes, P. (1974) The geochemical evolution of the moon. Proceedings of the Fifth Lunar Science Conference, Houston, Texas, 1287–1305.
Taylor, S.R., Pieters, C.M., and MacPherson, G.J. (2006a) Earth-moon system, planetary science, and lessons learned. Reviews in Mineralogy and Geochemistry, 60, 657–704.
Taylor, S.R., Taylor, G.J., and Taylor, L.A. (2006b) The Moon: A Taylor perspective. Geochimica et Cosmochimica Acta, 70, 5904–5918.
Tenner, T.J., Hirschmann, M.M., Withers, A.C., and Hervig, R.L. (2009) Hydrogen partitioning between nominally anhydrous upper mantle minerals and melt between 3 and 5 GPa and applications to hydrous peridotite partial melting. Chemical Geology, 262, 42–56.
Teodoro, L.F.A., Eke, V.R., and Elphic, R.C. (2010) Spatial distribution of lunar polar hydrogen deposits after KAGUYA (SELENE). Geophysical Research Letters, 37, 1–5.
Thiemens, M.H., and Clayton, R.N. (1980) Solar and cosmogenic nitrogen in the Apollo 17 deep drill core. Proceedings of the 11th Lunar and Planetary Science Conference, Houston, Texas, 1435–1451.

Thomas-Keprta, K.L., Clemett, S.J., Messenger, S., Ross, D.K., Le, L., Rahman, Z., McKay, D.S., Gibson, E.K., Gonzalez, C., and Peabody, W. (2014) Organic matter on the Earth's Moon. Geochimica et Cosmochimica Acta, 134, 1–15.

Treiman, A.H. (1991) Thermobarometry of lunar cordierite-troctolite in 15295,101: Metamorphic temperature and a potential barometer. Proceedings of the 22nd Lunar and Planetary Science Conference, Houston, Texas, 1407–1408.

Treiman, A.H., and Gross, J. (2012) Lunar cordierite-spinel troctolite: Igneous history and volatiles. Proceedings of the 43rd Lunar and Planetary Science Conference, The Woodlands, Texas, Abstract 1196.

Treiman, A.H., Boyce, J.W., Gross, J., Guan, Y., Eiler, J., and Stolper, E.M. (2014) Phosphate-halogen metasomatism of granulite 79215: Impact-induced fractionation of lunar volatiles and incompatible elements. American Mineralogist, 99, 1860–1870.

Ustunisik, G., Nekvasil, H., and Lindsley, D. (2011) Differential degassing of H_2O, Cl, F, and S: Potential effects on lunar apatite. American Mineralogist, 96, 1650–1653.

Ustunisik, G., Nekvasil, H., Lindsley, D.H., and McCubbin, F.M. (2015) Degassing pathways of Cl-, F-, H-, and S-bearing magmas near the lunar surface: Implications for the composition and Cl isotopic values of lunar apatite. American Mineralogist, 100, 1717–1727.

Vander Kaaden, K.E., Agee, C.B., and McCubbin, F.M. (2015) Density and compressibility of the molten lunar picritic glasses: Implications for the roles of Ti and Fe in the structures of silicate melts. Geochimica et Cosmochimica Acta, 149, 1–20.

Vasavada, A.R., Bandfield, J.L., Greenhagen, B.T., Hayne, P.O., Siegler, M.A., Williams, J.-P., and Paige, D.A. (2012) Lunar equatorial surface temperatures and regolith properties from the Diviner Lunar Radiometer Experiment. Journal of Geophysical Research: Planets, 117, E00H18.

Vaughan, W.M., Head, J.W., Wilson, L., and Hess, P.C. (2013) Geology and petrology of enormous volumes of impact melt on the Moon: A case study of the Orientale basin impact melt sea. Icarus, 223, 749–765.

Visscher, C., and Fegley, B. Jr. (2013) Chemistry of impact-generated silicate melt-vapor debris disks. Astrophysical Journal Letters, 767.

Vry, J.K., Brown, P.E., and Valley, J.W. (1990) Cordierite volatile content and the role of CO_2 in high-grade metamorphism. American Mineralogist, 75, 71–88.

Wang, Y., Guan, Y., Hsu, W., and Eiler, J.M. (2012) Water content, chlorine and hydrogen isotope compositions of lunar apatite. Proceedings of the 75th Annual Meteoritical Society Meeting, Cairns, Australia, Abstract 5170.

Wänke, H., Baddenhausen, H., Balacescu, A., Teschke, F., Spettel, B., Dreibus, G., Palme, H., Quijano-Rico, M., Kruse, H., Wlotzka, F., and Begemann, F. (1972) Multielement analyses of lunar samples and some implications of the results. Proceedings of the Third Lunar Science Conference, 1251–1268.

Wänke, H., Baddenhausen, H., Dreibus, G., Jagoutz, E., Palme, H., Spettel, B., and Teschke, F. (1973) Multielement analyses of Apollo 15, 16, and 17 samples and the bulk composition of the Moon. Proceedings of the Fourth Lunar Science Conference, 1461–1481.

Wänke, H., Palme, H., Kruse, H., Baddenhausen, H., Cendales, M., Dreibus, G., Hofmeister, H., Jagoutz, E., Palme, C., and Spettel, B. (1976) Chemistry of lunar highland rocks-A refined evaluation of the composition of the primary matter. Proceedings of the Seventh Lunar Science Conference, Houston, Texas, 3479–3499.

Warren, P.H. (1988a) KREEP: Major-element diversity, trace-element uniformity (almost). In G.J. Taylor and P.H. Warren, Eds., Workshop on Moon in transition: Apollo 14, KREEP, and evolved lunar rocks, p. 149–153. Lunar and Planetary Institute, Houston, Texas.

——— (1988b) The origin of pristine KREEP: Effects of mixing between urKREEP and the magmas parental to the Mg-rich cumulates. Proceedings of Lunar and Planetary Science, 18, 233–241.

Warren, P.H., and Wasson, J.T. (1979) The origin of KREEP. Reviews of Geophysics and Space Physics, 17, 73–88.

Warren, P.H., Ulff-Moller, F., and Kallemeyn, G.W. (2005) "New" lunar meteorites: Impact melt and regolith breccias and large-scale heterogeneities of the upper lunar crust. Meteoritics and Planetary Science, 40, 989–1014.

Wasson, J.T., Boynton, W.V., Kallemeyn, G.W., Sundberg, L.L., and Wai, C.M. (1976) Volatile compounds released during lunar lava fountaining. Proceedings of the Seventh Lunar Science Conference, 2, 1583–1595.

Watson, K., Murray, B., and Brown, H. (1961) On the possible presence of ice on the Moon. Journal of Geophysical Research, 66, 1598–1600.

Webster, J.D., and Mandeville, C.W. (2007) Fluid immiscibility in volcanic environments. Reviews in Mineralogy and Geochemistry, 65, 313–362.

Webster, J.D., and Rebbert, C.R. (1998) Experimental investigation of H_2O and Cl^- solubilities in F-enriched silicate liquids; implications for volatile saturation of topaz rhyolite magmas. Contributions to Mineralogy and Petrology, 132, 198–207.

Webster, J.D., Tappen, C.M., and Mandeville, C.W. (2009) Partitioning behavior of chlorine and fluorine in the system apatite-melt-fluid. II: Felsic silicate systems at 200 MPa. Geochimica et Cosmochimica Acta, 73, 559–581.

Wetzel, D.T., Rutherford, M.J., Jacobsen, S.D., Hauri, E.H., and Saal, A.E. (2013) Degassing of reduced carbon from planetary basalts. Proceedings of the National Academy of Sciences, 110, 8010–8013, www.pnas.org/cgi/doi/10.1073/pnas.1219266110.

Wetzel, D.T., Hauri, E.H., Saal, A.E., and Rutherford, M.J. (2014) Dissolved carbon content of the lunar volcanic glass beads and melt inclusions: Carbon from the lunar interior. 45th Lunar and Planetary Science Conference, The Woodlands, Texas, 2238.

Wiechert, U., Halliday, A.N., Lee, D.C., Snyder, G.A., Taylor, L.A., and Rumble, D. (2001) Oxygen isotopes and the moon-forming giant impact. Science, 294, 345–348.

Wieczorek, M.A., Neumann, G.A., Nimmo, F., Kiefer, W.S., Taylor, G.J., Melosh, H.J., Phillips, R.J., Solomon, S.C., Andrews-Hanna, J.C., Asmar, S.W., and others. (2013) The Crust of the Moon as Seen by GRAIL. Science, 339, 671–675.

Wieler, R., Humbert, F., and Marty, B. (1999) Evidence for a predominantly non-solar origin of nitrogen in the lunar regolith revealed by single grain analyses. Earth and Planetary Science Letters, 167, 47–60.

Wiens, R.C., Bochsler, P., Burnett, D.S., and Wimmer-Schweingruber, R.F. (2004) Solar and solar-wind isotopic compositions. Earth and Planetary Science Letters, 222, 697–712.

Wing, B.A., and Farquhar, J. (2015) Sulfur isotope homogeneity of lunar mare basalts. Geochimica et Cosmochimica Acta, in press.

Wood, J.A., Dickey, J.S. Jr., Marvin, U.B., and Powell, B.N. (1970) Lunar anorthosites and a geophysical model of the moon. Proceedings of the Apollo 11 Lunar Science Conference, 965–988.

Wright, K. (2006) Atomistic models of OH defects in nominally anhydrous minerals. Reviews in Mineralogy and Geochemistry, 62, 67–83.

Yoshioka, T., McCammon, C., Shcheka, S., and Keppler, H. (2015) The speciation of carbon monoxide in silicate melts and glasses. American Mineralogist, 100, 1641–1644.

Zhang, J.J., Dauphas, N., Davis, A.M., Leya, I., and Fedkin, A. (2012) The proto-Earth as a significant source of lunar material. Nature Geoscience, 5, 251–255.

Manuscript received February 13, 2014
Manuscript accepted February 3, 2015
Manuscript handled by Peter Isaacson